

Title	Erebus Volcanic Province: petrology
Authors	Martin, Adam P.;Cooper, Alan F.;Price, Richard C.;Kyle, Philip R.;Gamble, John A.
Publication date	2021-02-09
Original Citation	Martin, A. P., Cooper, A. F., Price, R. C., Kyle, P. R. and Gamble, J. A. (2021) 'Erebus Volcanic Province: petrology', Geological Society, London, Memoirs, 55, pp. 447-489. doi: 10.1144/M55-2018-80
Type of publication	Article (peer-reviewed)
Link to publisher's version	<a href="https://doi.org/10.6084/m9.figshare.c.5199416">https://doi.org/10.6084/m9.figshare.c.5199416</a> - 10.1144/M55-2018-80
Rights	© 2021, the Authors. Published by The Geological Society of London. All rights reserved.
Download date	2025-07-04 12:31:45
Item downloaded from	<a href="https://hdl.handle.net/10468/11409">https://hdl.handle.net/10468/11409</a>



# UCC

**University College Cork, Ireland**  
Coláiste na hOllscoile Corcaigh



## Erebus Volcanic Province: petrology

Adam P. Martin<sup>1\*</sup>, Alan F. Cooper<sup>2</sup>, Richard C. Price<sup>3</sup>, Philip R. Kyle<sup>4</sup> and John A. Gamble<sup>5,6</sup>

<sup>1</sup>GNS Science, Private Bag 1930, Dunedin, New Zealand

<sup>2</sup>Department of Geology, University of Otago, PO Box 56, Dunedin, New Zealand

<sup>3</sup>Science and Engineering, University of Waikato, Hamilton, New Zealand

<sup>4</sup>Department of Earth and Environmental Science, New Mexico Institute of Mining and Technology, Socorro, NM 87801, USA

<sup>5</sup>School of Geography, Environment and Earth Sciences, Victoria University of Wellington, Wellington, New Zealand

<sup>6</sup>School of Biological, Earth and Environmental Science, University College Cork, Distillery Fields, North Mall, Cork, Ireland

APM, 0000-0002-4676-8344; PRK, 0000-0001-6598-8062

\*Correspondence: [A.Martin@gns.cri.nz](mailto:A.Martin@gns.cri.nz)

**Abstract:** Igneous rocks of the Erebus Volcanic Province have been investigated for more than a century but many aspects of petrogenesis remain problematic. Current interpretations are assessed and summarized using a comprehensive dataset of previously published and new geochemical and geochronological data. Igneous rocks, ranging in age from 25 Ma to the present day, are mainly nepheline normative. Compositional variation is largely controlled by fractionation of olivine + clinopyroxene + magnetite/ilmenite + titanite ± kaersutite ± feldspar, with relatively undifferentiated melts being generated by <10% partial melting of a mixed spinel + garnet lherzolite source. Equilibration of radiogenic Sr, Nd, Pb and Hf is consistent with a high time-integrated HIMU *sensu stricto* source component and this is unlikely to be related to subduction of the palaeo-Pacific Plate around 0.5 Ga. Relatively undifferentiated whole-rock chemistry can be modelled to infer complex sources comprising depleted and enriched peridotite, HIMU, eclogite-like and carbonatite-like components. Spatial (west–east) variations in Sr, Nd and Pb isotopic compositions and Ba/Rb and Nb/Ta ratios can be interpreted to indicate increasing involvement of an eclogitic crustal component eastwards. Melting in the region is related to decompression, possibly from edge-driven mantle convection or a mantle plume.

**Supplementary material:** Whole-rock, clinopyroxene, englacial tephra and marine drill-core volcanic rock and glass chemistry ± isotopes ± chronology from published sources (referenced) and new data (ESM1) are available at <https://doi.org/10.6084/m9.figshare.c.5199416>

Volcanoes, volcanology and geology were the subjects of the earliest scientific observations in the Ross Sea (Ross 1847), and they formed part of the justification for scientific exploration during the heroic era (c. 1900–20). The samples collected in these early studies are still of value and they are part of the dataset used in this chapter (e.g. Prior 1899, 1902, 1907; Thomson 1916; Smith 1954). Igneous rocks were extensively studied as part of the International Geophysical Year programme (the third Polar Year) of 1957–58, and a significant outcome was published descriptions of the petrography of McMurdo Sound igneous rocks (e.g. Harrington 1958b, 1965; McCraw 1962). Since the International Geophysical Year, numerous workers have contributed to understanding the petrogenesis of igneous rocks in the McMurdo Sound region, using techniques such as geochronology (e.g. Armstrong 1978; Kelly *et al.* 2008; Martin *et al.* 2010), chemistry and petrology (e.g. Wright-Grassham 1987; Cooper *et al.* 2007), and isotopes (Sun and Hanson 1975; Phillips *et al.* 2018). The most advanced petrological techniques have been applied to igneous rocks from Ross Island (e.g. Kyle *et al.* 1992; Kelly *et al.* 2008; Sims *et al.* 2013; Iacovino *et al.* 2016) and the actively convecting, phonolite lake of Mount Erebus (Kyle *et al.* 1992; Moussallam *et al.* 2013, 2015). Drilling, onshore but mainly offshore, has also contributed considerably to the understanding of McMurdo Sound igneous volcanism, with significant programmes including drilling by the Dry Valley Drilling Project (DVDP), the Cape Roberts Drilling Project (CRP: Cape Roberts Science Team 1999) and the Antarctic Drilling Project (ANDRILL: Pompilio *et al.* 2007; Panter *et al.* 2008; Naish *et al.* 2009). A record of McMurdo Sound volcanic activity is also found in geophysical studies and studies of englacial tephra. This chapter builds on the seminal work presented in the Antarctic Research Series on Antarctic volcanism (Kyle 1990b).

The definition of the Erebus Volcanic Province used here closely follows Kyle (1990b) as modified by Smellie and Martin (2021; see Fig. 1). It includes Cenozoic-aged igneous rocks erupted and emplaced between Franklin Island and Mason Spur, volcanic islands in the Ross Sea, occurrences in the foothills of the Transantarctic Mountains, tephra in rock, ice core and in sediments, and volcanic rocks from the seafloor (Fig. 1). This chapter will provide a thorough overview of more than 1000 whole-rock and glass analyses, more than 100 isotope analyses on whole rocks and crystals, and more than 100 radiometric dates (Table 1) from the Erebus Volcanic Province. This includes both published (78% of the data) and unpublished analyses. An extensive list of references is provided. Chronology and physical volcanology of the Erebus Volcanic Province are described in Smellie and Martin (2021), and radiometric ages are only used in this chapter to investigate petrogenetic trends. A marine record of Antarctic volcanism from drill cores is also discussed by Di Roberto *et al.* (2021), and only drill cores from the Erebus Volcanic Province (onshore and offshore) are summarized in this chapter. Clinopyroxene chemistry of relatively undifferentiated compositions will be provided where available; ‘relatively undifferentiated’ is defined here as whole-rock compositions with SiO<sub>2</sub> <55 wt% and MgO >6 wt% (definition after Sprung *et al.* 2007). These analyses are included in the Supplementary material (ESM1), with each analysis linked to a bibliographical reference. An overview of the geological setting is presented, followed by a presentation of a refined subdivision of the province. A petrological review of major volcanic islands and other occurrences in the Transantarctic Mountain foothills, drill core and elsewhere is given along with a review of historical work undertaken in each area. Current lithological maps are provided for many of the major volcanic centres. The whole-rock geochemistry and geothermobarometry of the

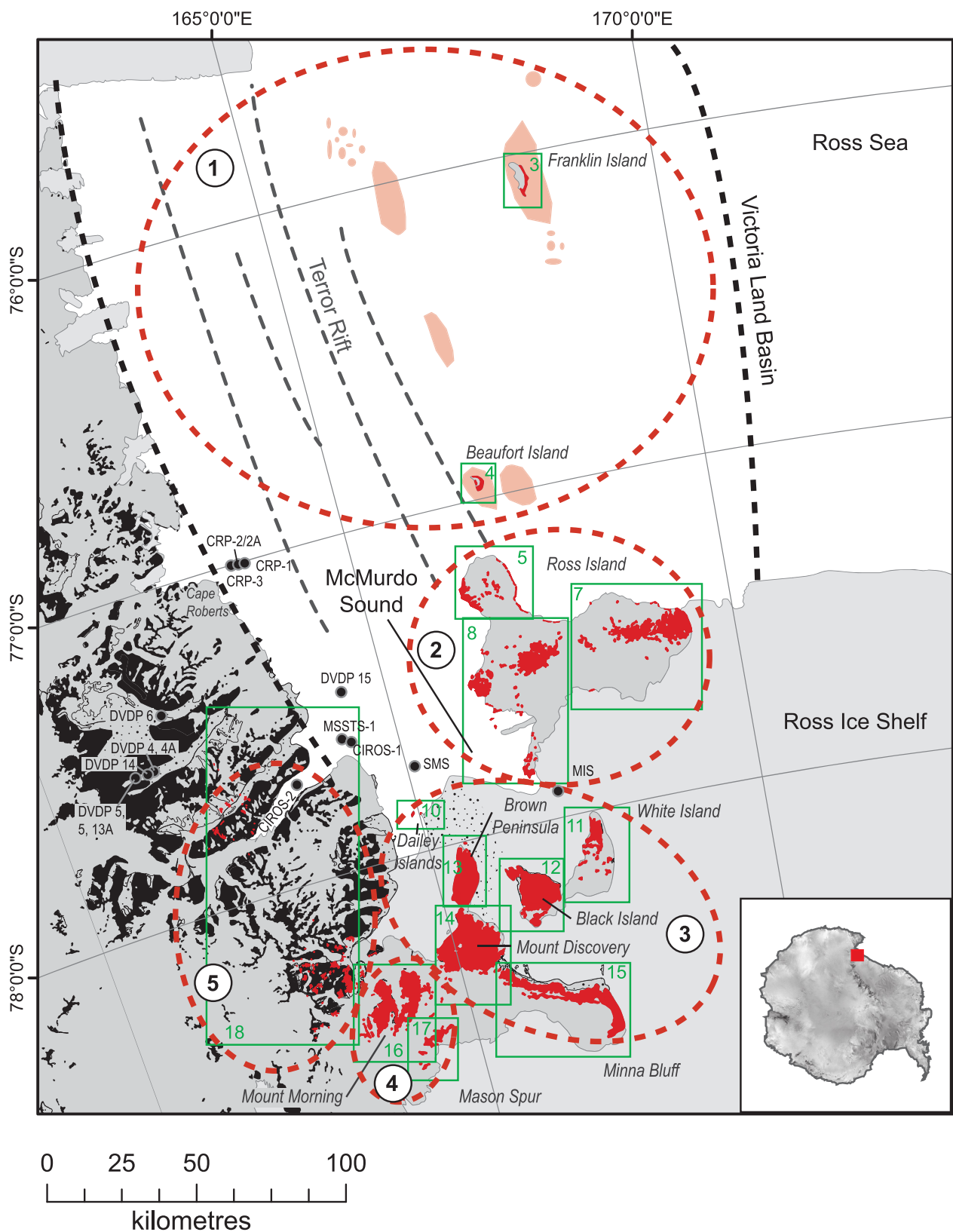


**Fig. 1.** A map of southern Victoria Land showing the extent of the Erebus Volcanic Province, significant offshore drill-hole locations and key topographical features. The inset map shows the location within Antarctica. Erebus Volcanic Province rock outcrop is shown in red (subaerial) or light red (subaqueous; interpreted from dredge samples and geophysical studies: [Lawver \*et al.\* 2012](#)). Other older rock outcrops are shown in black. The stippled pattern indicates supraglacial till. The geological units here follow the classification of [Cox \*et al.\* \(2012\)](#). The Victoria Land Basin is located between the dashed black lines, with the western boundary marking the Transantarctic Mountain Front Fault. The positions of the faults associated with the Terror Rift are shown by thin, grey dashed lines ([Cooper \*et al.\* 1987](#)). Offshore drill-hole locations (filled circles) are shown. The green boxes indicate the location of some figures used elsewhere in this study, with the corresponding figure number shown in green text. The red dashed lines indicate the approximate position of volcanic fields and suites within the Erebus Volcanic Province: 1, Terror Rift Volcanic Field; 2, Ross Island Volcanic Field; 3, Mount Discovery Volcanic Field; 4, Mount Morning Volcanic Field; 5, Southern Local Suite. CIROS, Cenozoic Investigations into the western Ross Sea drill-hole collar locations; CRP, Cape Roberts Project; DVDP, Dry Valley Drilling Project drill-hole collar locations; MSSTS, McMurdo Sound Sediment and Tectonic Study drill-hole collar locations; MIS (McMurdo Ice Shelf) and SMS (Southern McMurdo Sound) drill-hole collar locations from ANDRILL (Antarctic Drilling Project). The scale bar is accurate at 78° S.

## Erebus Volcanic Province: petrology

**Table 1.** Summary of the number of analyses and type from each locality or sample type used in this study of the Erebus Volcanic Province

		Whole-rock chemistry	Isotopes*	Chronology <sup>†</sup>
Terror Rift Volcanic Field	Beaufort Island	3	–	–
	Franklin Island	9	1	3
	Submarine volcanic rocks	17	17	13
	<i>Sub-total</i>	29	18	16
Ross Island Volcanic Field	Cape Crozier	26	5	–
	Holes DVDP 1 and 2	99	11	4
	Hut Point Peninsula	60	17	–
	Mount Bird	33	14	–
	Mount Erebus	107	34	15
	Mount Terror	30	17	–
	<i>Sub-total</i>	355	106	19
Mount Discovery Volcanic Field	Black Island	10	1	–
	Brown Peninsula	8	–	–
	Dailey Islands	1	–	1
	Minna Bluff	39	1	8
	Mount Discovery	49	1	7
	White Island	25	–	4
	<i>Sub-total</i>	132	3	20
Mount Morning Volcanic Field	Mason Spur	110	2	8
	Mount Morning	248	10	22
	<i>Sub-total</i>	358	12	30
Southern Local Suite	–	21	1	–
	<i>Total</i>	895	140	85
Other	Historical Erebus bombs	62	28	28
	Ross Island englacial tephra	37	–	–
	ANDRILL lava	11	–	–
	ANDRILL glass	68	–	24
	<i>Sub-total</i>	178	28	52
	<i>Grand total</i>	1073	168	137

\*Where whole-rock chemistry and isotope analysis have been determined on the same sample.

<sup>†</sup>Chronology where the whole-rock chemistry can be associated with the radiometric age with a high degree of certainty (i.e. from the same sample).

province as a whole are discussed using the [Supplementary material \(ESM1\)](#) dataset. In the discussion, competing petrogenetic hypotheses are evaluated, and the various mantle sources, age of chemical heterogeneity of the mantle sources, asthenospheric v. lithospheric and types of melting are considered. The final sections of the chapter include suggestions regarding pertinent areas for future research, a summary and a concluding statement.

## Geological setting

The earliest, published geological map of the Erebus Volcanic Province rocks is based on notes made by Hartley Ferrar during the 1901–04 British National Antarctic Expedition (Ferrar 1905) and work since then has aimed at adding extra detail, with explanations placed in a modern-science context (Cox *et al.* 2012) (Fig. 2). The region is part of the intracontinental West Antarctic Rift System (Behrendt 1999), with the Transantarctic Mountain Front at the shoulder of the rift. East Antarctica comprises mainly Precambrian cratons (Bentley 1991) compared to West Antarctica, which includes a mosaic of younger crustal blocks (Talarico and Kleinschmidt 2008), with the precise lithological boundary between East and West Antarctica being contentious. The Moho shallows to around 20 km in McMurdo Sound and deepens to around 40 km beneath the Transantarctic Mountains (Bannister *et al.* 2003; An *et al.* 2015). Based on the study of crustal xenoliths, the lower crust beneath the Transantarctic Mountains,

Mount Morning and Mason Spur is mainly calc-alkalic, whereas further east, away from the Transantarctic Mountain Front Fault, the lower crust is more alkali-tholeiitic (Berg *et al.* 1985; Kalamarides *et al.* 1987; Martin *et al.* 2015a). Subduction beneath the region where the Erebus Volcanic Province now sits last occurred at *c.* 0.5 Ga when the palaeo-Pacific Plate subducted westwards beneath the Gondwana margin (Stump 1995).

Some of the most recent tectonic activity in the West Antarctic Rift System has occurred on faults within the Terror Rift (Cooper *et al.* 1987), with regional correlations suggesting that faulting must be younger than 17 Ma (Fielding *et al.* 2006), and some faults cutting the seafloor may be indications of modern activity (Hall *et al.* 2007). Onshore faulting at Mount Morning occurred post-3.9 Ma (Martin and Cooper 2010). During rifting, the Antarctic Plate is thought to have remained effectively stationary since *c.* 60 Ma (Grindley and Oliver 1983; Torsvik *et al.* 2008). Kyle and Cole (1974) first noted a three-fold radial symmetry of vents around Mount Erebus and Mount Discovery, and suggested these could be related to radial fractures at approximately 120° to each other. They postulated that these fractures resulted from crustal doming, whilst Kyle *et al.* (1992) suggested doming at Ross Island is the result of a mantle plume.

Cenozoic volcanism in the province commenced as recently as 18.7 Ma but tephra in cores, inferred to be sourced within the province, indicate that volcanism is likely to have been initiated around 25 Ma (Kyle and Muncy 1989; McIntosh 2000; Martin *et al.* 2010). Mount Erebus is still volcanically active today and, based on chronology and abnormally high heat

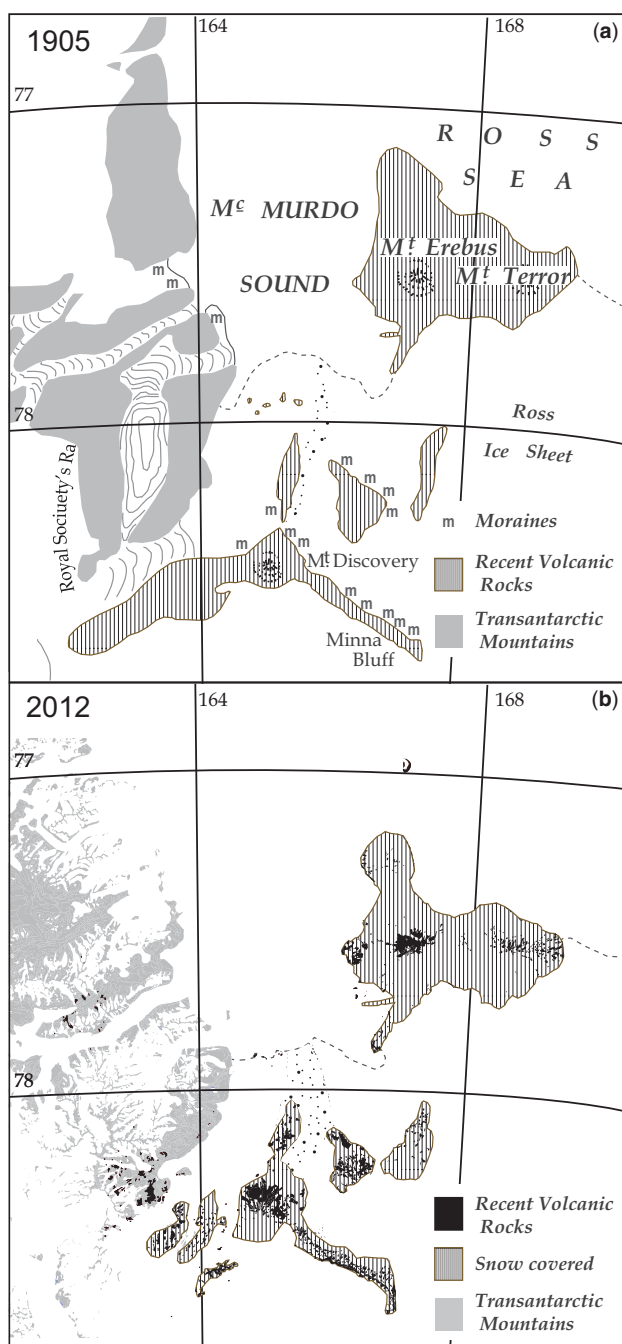


**Fig. 2.** Geological maps of the Erebus Volcanic Province from two separate eras. (a) Possibly the earliest, published geological map of the province, drawn by Ferrar (1905). (b) The current state of knowledge (Cox *et al.* 2012). The shading has been adapted to match the 1905 publication and highlights the quality of the original mapping. Advances in the intervening century have been in understanding petrogenesis of the Erebus Volcanic Province.

flow, several eruptive centres are considered dormant rather than extinct. Volcanic rock compositions are alkalic, and typically range from alkali basalt and basanite to phonolite and trachyte (Fig. 3). Typical, primitive whole-rock compositions are presented in Table 2. The Erebus Volcanic Province is the southernmost of three provinces that comprise the McMurdo Volcanic Group (Kyle 1990a). To the north is the Melbourne Volcanic Province and north of that is the Hallett Volcanic Province. The McMurdo Volcanic Group occurs along a c. 2000 km-long portion of the western shoulder of the West Antarctic Rift System between Cape Adare and Mount

Early. It has long been recognized (e.g. Coombs *et al.* 1986; Panter *et al.* 2006) that McMurdo Volcanic Group rocks, including Erebus Volcanic Province rocks, have a unifying character that is ocean island basalt (OIB)- and HIMU-like (high- $\mu$ : enriched in  $^{206}\text{Pb}$  and  $^{208}\text{Pb}$  and relatively depleted in  $^{87}\text{Sr}/^{86}\text{Sr}$  values). Finn *et al.* (2005) referred to this as a diffuse alkaline magmatic province (DAMP) encompassing West Antarctica, several sub-Antarctic islands, Zealandia, eastern Australia and Papua New Guinea.

### Subdivision of the Erebus Volcanic Province

Harrington (1958b) introduced the term ‘McMurdo Volcanics’ to describe late Cenozoic volcanic rocks in the Western Ross Sea, including those around Ross Island in McMurdo Sound. Kyle (1990a) recommended formal recognition of the McMurdo Volcanic Group. Cole and Ewart (1968) undertook the first detailed mapping of McMurdo Volcanic Group rocks in McMurdo Sound. They defined four stratigraphic formations on Black Island, which they then extrapolated to several volcanic localities in the region, including Ross Island’s Cape Bird (Cole and Ewart 1968), Cape Crozier and the Hut Point Peninsula (Cole *et al.* 1971). These formations consisted of an early basaltic unit overlain by trachyte (now known from chemical data to be phonolite), then a younger basaltic unit overlain by a younger trachyte (phonolite). It is now also known from geochronology that, although the eruptive sequence of alternating basanite and phonolite is very similar throughout the McMurdo Sound area, it was repeated at different times. Consequently, the formations of Cole and Ewart (1968) have not been widely used in the description of the geology. Instead, Kyle and Cole (1974) used tectonic setting and spatial distribution to assign the occurrences of McMurdo Volcanics (Group) to provinces, including the Erebus Volcanic Province. This system has now endured for more than 40 years.

In this chapter, the Cenozoic volcanic rocks in the Erebus Volcanic Province have been further categorized geographically and petrogenetically, using the thickness and composition of the lithosphere through which they have erupted and the relative clinopyroxene–melt equilibration depth from which primitive magmas originated (Table 3; this study). Systematic patterns in trace element and isotopic ratios across the province record these petrogenetic changes. The groupings are (Fig. 1): (1) Terror Rift Volcanic Field, (2) Ross Island Volcanic Field, (3) Mount Discovery Volcanic Field, (4) Mount Morning Volcanic Field and (5) Southern Local Suite. These names, and the method of defining them, have been applied sympathetically with other studies in the McMurdo Volcanic Group reported in this Memoir (Smellie and Rocchi 2021), and with other studies in Victoria Land (Rocchi *et al.* 2002).

### Petrological overview and previous work

This section describes the history of field visits and subsequent petrological and geochemical research undertaken in each volcanic field. The section is divided geographically, and the volcanic centres are described in a level of detail that reflects the complexity of work undertaken there. Subsequently, volcanic rock from marine drill core and englacial tephra are reviewed. This section builds a holistic picture of the province that allows a regional overview approach to be adopted in the geochemistry and discussion sections below. A summary of the minimum age range and mineral assemblage in relatively undifferentiated rocks of the Erebus Volcanic Province are shown in Table 4. Thin-section photographs of relatively

## Erebus Volcanic Province: petrology

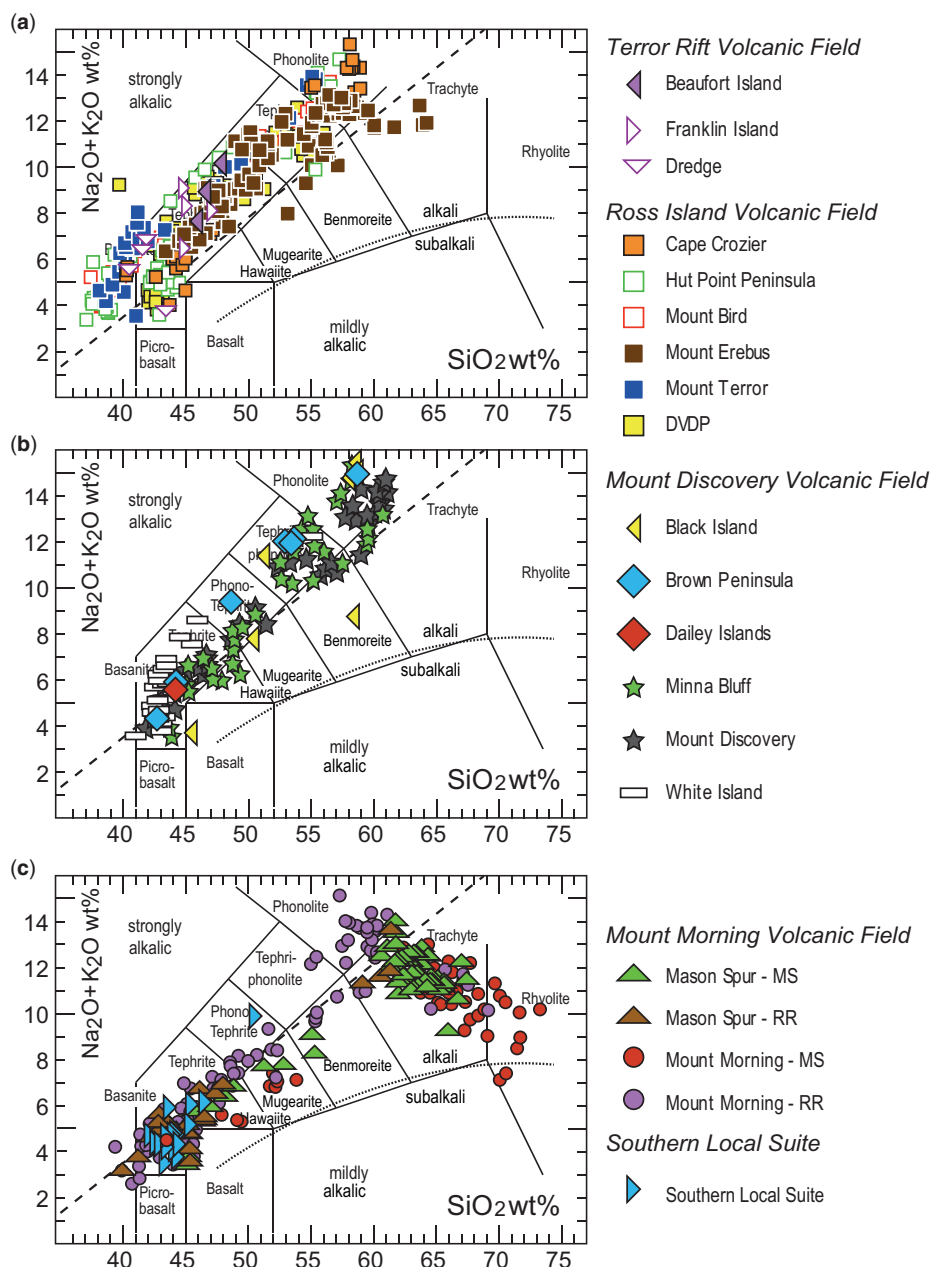


**Fig. 3.** Total alkali v. silica diagram after Le Bas *et al.* (1986). Data ( $n = 895$ ; 100%; anhydrous) are shown for the Erebus Volcanic Province whole-rock compositions from the [Supplementary material \(ESM1\)](#). The alkali–subalkali division (dotted line) follows Kuno (1966), and the mildly alkalic–strongly alkalic division (dashed line) follows Saggerson and Williams (1964). (a) Data for the Terror Rift Volcanic Field and the Ross Island Volcanic Field. (b) Data for the Mount Discovery Volcanic Field. (c) Data for the Mount Morning Volcanic Field and Southern Local Suite. MS, Mason Spur Lineage; RR, Riviera Ridge Lineage.

undifferentiated rock types typical of those found in the Erebus Volcanic Province are shown in Figure 4.

### Terror Rift Volcanic Field

**Franklin Island.** Named by James Ross in 1841 for Sir John Franklin, Lieutenant-Governor of Tasmania and Arctic explorer (Ross 1847), Franklin Island is the eroded remnant of a shield volcano. A map of Franklin Island (Fig. 5) shows volcanic rock outcrops and key topographical features. In all map figures (Fig. 5 *et seq.*), which are adapted from Cox *et al.* (2012), ‘basaltic’ includes basalts, basanites and intermediate mafic compositions, such as hawaiite and mugearite, contours (grey lines) are in metres, and white areas indicate snow and/or ice cover.

At Franklin Island, lava flows and interbedded tuffs are common, and some dykes occur. A sample collected by the Ross party (Ross 1847) was described by Prior (1899). Subsequent visits in the 1900s (Borchgrevink 1901; Scott 1907), the 1960s (Waterhouse 1965), the 1980s (Ellerman and Kyle 1990b) and in 2004 (Rilling *et al.* 2009) collected geological

and other samples. Shipborne investigations near Franklin Island were made in 1958 (Brodie 1959), 2004 (Rilling *et al.* 2009) and 2011 (Lawver *et al.* 2012), with several submarine volcanoes being identified (Rilling *et al.* 2009; Lawver *et al.* 2012). The age of emplacement of Franklin Island volcanic rocks is between  $3.70 \pm 0.05$  and  $3.30 \pm 0.04$  Ma (Armstrong 1978; Rilling *et al.* 2009). The four published whole-rock analyses from Franklin Island are basanites (Fig. 3), and mantle nodules and xenocrysts of olivine and clinopyroxene have been noted from this locality (Ellerman and Kyle 1990b). Olivine  $\pm$  plagioclase phenocrysts occur in a fine-grained groundmass of olivine + clinopyroxene + plagioclase + opaque minerals. Glass vesicularity appears to increase upsection (Ellerman and Kyle 1990b).

**Beaufort Island.** In 1841, Captain J.C. Ross named Beaufort Island after the hydrographer, Captain Francis Beaufort (Ross 1847). The island was visited briefly in 1903 but was only described from remote observations (Ferrar 1907; Debenham 1923; Harrington 1958a) until New Zealand geologists landed in 1965 (Waterhouse 1965) and others in the 1980s (LeMasurier *et al.* 1983), and samples were collected again in the 2000s

**Table 2.** Typical whole-rock compositions of Erebus Volcanic Province

Area	Terror Rift Volcanic Field			Ross Island Volcanic Field					Mount Discovery Volcanic Field						Mount Morning Volcanic Field				Southern Local Suite	
	Location	Beaufort	Franklin	Dredge	Crozier	DVDP	Hut Point	Bird	–	Terror	Black	Brown	Dailey	Minna	Discovery	White	Mason (old)	Mason (young)		Morning (young)
Reference	1	2	3	4	5	6	7	20	9	10	11	12	13	14	15	16	17	18	19	20
Sample No.	1	HC-FRI-2	TRDR02	CC04	2-105.53	3-179.40	R1115	5	R117	12	1	2007	AW82113A	AW84738	OU 74785	OU78634	OU78578	OU78710	OU78559	5
TAS	Tephrite	Basanite	Tephrite	Basanite	Basanite	Basanite	Basanite	Basanite	Basanite	Basanite	Basanite	Basanite	Basanite	Basanite	Basanite	Basanite	Basanite	Basanite	Basanite	Basanite
Mg#	50.36	64.16	57.37	50.67	69.43	52.43	48.48	57.42	55.84	64.19	64.57	63.68	61.82	64.47	69.69	54.18	72.87	34.92	60.65	57.42
DI	42.52	35.07	34.57	26.59	23.88	19.88	19.81	32.43	19.50	23.39	25.19	29.84	33.52	26.88	23.51	37.31	21.33	51.47	27.99	32.43
(wt%)																				
SiO <sub>2</sub>	45.89	44.83	43.18	40.23	42.02	37.62	37.78	43.60	38.51	45.42	42.71	44.13	45.18	43.31	43.22	45.66	45.39	51.51	44.13	43.60
TiO <sub>2</sub>	3.37	2.27	2.98	2.51	4.09	3.71	3.15	3.36	2.85	3.10	4.22	3.26	3.39	3.95	3.27	3.72	2.16	3.02	3.54	3.36
Al <sub>2</sub> O <sub>3</sub>	16.93	14.03	14.55	13.28	13.02	11.92	11.79	14.47	11.69	13.42	13.34	13.71	15.24	14.51	13.06	14.74	12.62	15.45	14.71	14.47
Fe <sub>2</sub> O <sub>3</sub>	2.63	2.79	2.69	3.12	1.92	3.45	3.68	2.22	3.27	1.91	2.06	1.95	1.82	1.93	1.89	2.08	1.74	3.14	2.00	2.22
FeO	8.78	9.31	8.96	15.58	9.60	17.23	18.40	11.10	16.36	9.54	10.32	9.73	9.12	9.65	9.44	10.42	8.72	8.96	9.99	11.10
MnO	0.11	0.22	0.17	0.17	0.18	0.15	0.17	0.21	0.16	0.19	0.21	0.19	0.20	0.19	0.22	0.19	0.22	0.27	0.21	0.21
MgO	5.00	9.35	7.30	8.97	12.23	10.65	9.71	8.40	11.60	9.59	10.55	9.56	8.28	9.83	12.18	6.91	13.14	2.70	8.64	8.40
CaO	9.43	10.13	12.10	9.87	11.41	10.20	10.31	10.12	10.59	12.62	11.38	11.27	10.29	11.15	11.65	9.42	12.01	6.98	11.37	10.12
Na <sub>2</sub> O	5.10	4.74	5.06	4.12	3.19	2.84	2.93	4.36	2.99	2.63	3.71	3.89	3.57	3.32	3.26	3.94	2.46	4.40	3.63	4.36
K <sub>2</sub> O	2.35	1.69	2.02	1.53	1.49	1.48	1.38	1.53	1.25	1.04	0.65	1.69	1.93	1.37	1.15	1.81	1.20	2.41	1.12	1.53
P <sub>2</sub> O <sub>5</sub>	0.41	0.64	0.98	0.62	0.85	0.75	0.69	0.64	0.73	0.55	0.85	0.62	0.96	0.79	0.69	1.06	0.36	1.15	0.67	0.64
Total	100	100	100	100	100	100	100	100	100	100	100	100	100	100	100	100	100	100	100	100
(ppm)																				
Ba	–	–	767	596	277	406	445	410	494	240	290	–	484	513	–	393	204	276	340	410
Be	–	–	–	–	–	–	–	2.7	–	2.2	2.7	–	–	–	–	–	–	–	–	2.7
Ce	–	–	144	112	109	112	107	bdl	102	bdl	bdl	–	127	119	94	96	52	106	91	bdl
Co	–	–	–	50	–	59	57	54	56	45	56	–	–	–	–	59	63	8	64	54
Cr	–	–	–	465	469	449	384	210	673	510	460	–	288	321	–	218	722	30	363	210
Cs	–	–	0.70	0.59	bdl	0.32	0.35	–	0.39	–	–	–	0.35	0.06	0.30	–	–	–	–	–
Cu	–	54	–	–	52	–	–	50	–	85	41	–	33	43	85	–	–	–	–	50
Dy	–	–	6.8	5.5	5.0	6.4	6.6	–	6.3	–	–	–	–	–	–	4.2	3.8	3.0	5.4	–
Er	–	–	3.3	2.7	2.0	2.9	3.0	–	2.8	–	–	–	–	–	–	bdl	1.8	1.5	2.5	–
Eu	–	–	3.4	2.9	2.5	3.1	3.1	–	2.9	–	–	–	–	3.3	3.2	2.7	1.7	1.8	2.4	–
Ga	–	21	–	–	–	–	–	–	–	–	–	–	19	20	15	46	15	223	19	–
Gd	–	–	9.5	7.3	8.4	9.0	8.8	–	8.4	–	–	–	–	–	7.2	5.81	4.5	3.9	6.9	–
Hf	–	–	6.0	5.9	5.4	7.9	6.7	–	6.0	–	–	–	8.5	7.1	5.8	9.2	3.9	2.7	5.2	–
Ho	–	–	1.2	1.0	1.0	1.2	1.2	–	1.1	–	–	–	–	–	–	1.0	0.72	0.56	0.97	–
La	–	–	78	57	68	58	53	54	53	35	52	–	60	55	55	47	26	29	45	54
Lu	–	–	0.40	0.32	–	0.33	0.35	–	0.34	–	–	–	0.41	0.32	0.30	0.82	0.21	0.17	0.29	–
Nb	–	104	108	95	–	81	79	–	75	–	–	–	–	97	87	60	32	24	54	–
Nd	–	–	60	47	56	55	51	–	49	–	–	–	63	55	45	43.4	24	13	42	–
Ni	–	184	70	209	276	245	206	110	293	150	200	–	127	162	259	170	288	13.8	145	110
Pb	–	2	3.8	3.9	4.3	2.8	2.5	4.5	2.7	1.6	2.4	–	3.0	5.0	–	439	3.7	1.9	3.4	4.5
Pr	–	–	16	13	15	14	13	–	12.6	–	–	–	–	–	–	10.1	6.0	6.0	10	–
Rb	–	59	48	53	30	33	35	42	34	36	24	–	39	37	32	36	22	11	29	42
Sc	–	–	–	27	–	36	32	–	34	–	–	–	23	28	–	19	29	14	27	–
Sm	–	–	11	8.7	10	10	10	–	9.5	–	–	–	11	10	9.1	8.7	5.3	bdl	8.6	–
Sr	–	885	999	966	829	861	730	1000	953	640	880	–	1030	1153	861	999	429	107	794	1000
Ta	–	–	6.7	5.7	–	5.3	5.2	–	5.1	–	–	–	5.8	5.5	4.2	2.1	1.7	0.80	3.1	–
Tb	–	–	1.2	1.0	0.90	1.2	1.2	–	1.1	–	–	–	1.2	1.2	0.95	1.2	1.4	1.2	1.5	–
Th	–	9	9.8	7.5	4.6	6.1	5.6	–	5.7	–	–	–	5.9	6.1	5.6	3.4	3.7	1.9	5.2	–
Tm	–	–	0.40	0.37	–	0.38	0.41	–	0.39	–	–	–	–	–	0.32	bdl	0.30	0.71	0.34	–
U	–	–	2.4	2.5	1.0	1.8	1.2	–	1.4	–	–	–	1.70	2.1	1.5	bdl	1.3	2.0	1.7	–
V	–	–	–	251	300	288	271.6	240	275	300	280	–	243	317	275	414	234	23	305	240
Y	–	35	32	27	–	32	30	31	28.7	23	31	–	34	30	27	24	18	10	24	31
Yb	–	–	2.7	2.2	1.6	2.4	2.5	3.2	2.4	2.7	3.4	–	2.6	2.2	2.1	bdl	1.9	1.6	2.2	3.2
Zn	–	105	–	–	82	–	–	153	–	126	110	–	89	84	79	–	–	–	–	153
Zr	–	275	266	273	–	363	308	360	266	260	330	–	401	311	249	231	162	99	222	360
<sup>87</sup> G/ <sup>86</sup> Sr	–	–	0.703 082	0.702 975	0.702 991	0.703 002	0.703 144	–	0.703 032	0.7032	–	–	–	–	–	0.703 350	–	–	–	–
<sup>143</sup> Nd/ <sup>144</sup> Nd	–	–	0.512 971	0.512 949	0.512 929	0.512 922	0.512 891	–	0.512 917	–	–	–	–	–	–	0.512 852	–	–	–	–
<sup>206</sup> Pb/ <sup>204</sup> Pb	–	–	19.434	19.5268	19.496	20.1724	19.7321	19.592	19.5684	–	–	–	–	–	–	–	–	–	19.579	19.592
<sup>207</sup> Pb/ <sup>204</sup> Pb	–	–	15.601	15.6146	15.666	15.6663	15.6253	15.602	15.6197	–	–	–	–	–	–	15.645	–	–	–	15.602
<sup>208</sup> Pb/ <sup>204</sup> Pb	–	–	39.020	39.0721	39.096	39.6660	39.4167	39.285	39.0898	–	–	–	–	–	–	39.268	–	–	–	39.285
Nepheline	17.1	17.7	23.2	18.9	14.1	13.0	13.4	15.9	13.7	6.0	11.9	15.4	9.6	11.0	12.8	8.0	7.8	0.0	11.0	15.9
Diopside	22.7	27.5	34.6	26.3	27.4	20.0	21.4	25.0	21.7	30.1	26.6	29.8	20.2	23.8	28.6	18.5	30.0	9.9	25.5	25.0
Olivine	7.3	15.5	8.0	23.2	19.4	29.1	29.1	16.1	30.1	14.8	17.4	14.9	15.1	16.6	19.7	14.5	21.4	2.2	14.8	16.1

## Erebus Volcanic Province: petrology

**Table 3.** Subdivision of the Erebus Volcanic Province with key eruptive centres and key characteristics, including the nature of the underlying crust and lithosphere, and the estimated depth of clinopyroxene–melt equilibration

Erebus Volcanic Province	Lower crust	Lithosphere	Clinopyroxene–melt equilibration depth
Terror Rift Volcanic Field Franklin Island Beaufort Island Submarine volcanic rocks	Alkalic–Tholeiitic	Thin (<20 km)	Shallow (c. 1 GPa)*
Ross Island Volcanic Field Mount Terror Mount Erebus Mount Bird Hut Point Peninsula	Alkalic–Tholeiitic	Thin (<20 km)	Deep (>2 GPa)
Mount Discovery Volcanic Field Dailey Islands White Island Black Island Brown Peninsula Mount Discovery Minna Bluff	Alkalic–Tholeiitic	Thin (<20 km)	Shallow (c. 1 GPa)
Mount Morning Volcanic Field Mount Morning Mason Spur	Calc-alkalic crust	Thin (<20 km)	Shallow (c. 1 GPa)
Southern Local Suite	Calc-alkalic crust	Thick (>20 km)	Deep (>2 GPa)

\*Not calculated but assumed by comparison with similar data on the normative ternary diagram (Fig. 25).

(Rilling *et al.* 2009). Beaufort Island is the eroded, near-vent remnant of a stratovolcano (Fig. 6). The only ages determined from the island overlap at  $6.80 \pm 0.05$  and  $6.77 \pm 0.03$  Ma (Rilling *et al.* 2009). Less than 5% of Beaufort Island's total

volume lies above current sea-level. Lava flows, volcanic breccias and tuffs are cross-cut by numerous dykes which have hydrothermally altered the wall rock. Three analyses from Ellerman and Kyle (1990a) and two dated samples

**Table 4.** Summary of the mineralogy in relatively undifferentiated rocks from the Erebus Volcanic Province

Erebus Volcanic Province	Potential age range		Phenocrysts	Groundmass
	From	To		
Terror Rift Volcanic Field				
Franklin Island	$3.70 \pm 0.05$	$3.30 \pm 0.04$	Ol + Pl	Ol + Cpx + Pl + Opq
Beaufort Island	$6.80 \pm 0.05$	$6.77 \pm 0.03$	Cpx + Pl + Krs	Cpx + Pl + Krs + Nph $\pm$ Ap
Submarine volcanic rocks	$3.73 \pm 0.05$	0.09	Ol + Cpx	Cpx + Ol + Fe oxides $\pm$ Pl
Ross Island Volcanic Field				
Mount Terror	c. 2.5	$0.82 \pm 0.14$	Ol + Aug	
Mount Erebus	$1.311 \pm 0.016$	$0.040 \pm 0.006$	Ol + Cpx + Fsp + Ap	Ol + Cpx + Nph + Fsp + Opq + Ap
Mount Bird	$4.62 \pm 0.6$	$3.08 \pm 0.15$	Pl + Ol + Aug	Pl + Aug + Hbl + Opq
Hut Point Peninsula	$1.68 \pm 0.06$	$0.33 \pm 0.02$	Ol + Cpx	Ol + Amp + Cpx + Pl + Cr-Spl + titano-Mag + Ilm + Ap + glass
Mount Discovery Volcanic Field				
Dailey Islands	$0.78 \pm 0.04$	$0.76 \pm 0.02$	Ol + Cpx	Cpx + Pl + Ol + Mag
White Island	7.62	0.17	Ol + Di $\pm$ Krs	Aug + Mag + Bt + Pl + Nph
Black Island	$10.9 \pm 0.4$	$1.689 \pm 0.003$	Ol + Aug + Pl + Fe oxides	Pl + Ol + Aug
Brown Peninsula	2.7	2.2	Ol + Cpx	Pl + Opq + glass
Mount Discovery	$5.46 \pm 0.16$	$0.06 \pm 0.006$	Ol + Cpx	Pl + Opq + Cpx + Nph
Minna Bluff	12	4	Ol + Cpx	Pl + Opq + Ap
Mount Morning Volcanic Field				
Mount Morning – MS	25	$13.0 \pm 0.3$	Pl + Di + Ol	Pl + Cpx + Ilm + Ap
Mount Morning – RR	$5.01 \pm 0.04$	$0.06 \pm 0.08$	Pl + Cpx + Ol	Pl + Afs + Ne + Opq + Ol + Ap + Cpx
Mason Spur – MS	$12.9 \pm 0.1$	$11.4 \pm 0.1$	Pl + Di + Ol	Afs + Nph + Pl + Opq + Ap
Mason Spur – RR	$6.13 \pm 0.2$	$0.07 \pm 0.08$	Pl + Cpx + Ol + Krs	Pl + Afs + Nph + Opq + Ol + Cpx + Ap
Southern Local Suite				
	$13.8 \pm 0.20$	$0.08 \pm 0.13$	Ol + Cpx $\pm$ Pl $\pm$ Fe-Ti oxides	Pl + Opq + Nph + Cpx

Mineral abbreviations follow Whitney and Evans (2010). Afs, alkali feldspar; Amp, amphibole; Ap, apatite; Aug, augite; Bt, biotite; Cpx, clinopyroxene; Cr-Spl, chromium spinel; Di, diopside; Fsp, feldspar; Hbl, hornblende; Ilm, ilmenite; Krs, Kaersutite; Mag, magnetite; Nph, nepheline; Ol, olivine; Opq, opaque; Pl, plagioclase. Age ranges are minimum ranges, see text for discussion. Mineralogy is only shown for relatively undifferentiated rock types in the province. MS, Mason Spur Lineage; RR, Rivera Ridge Lineage.

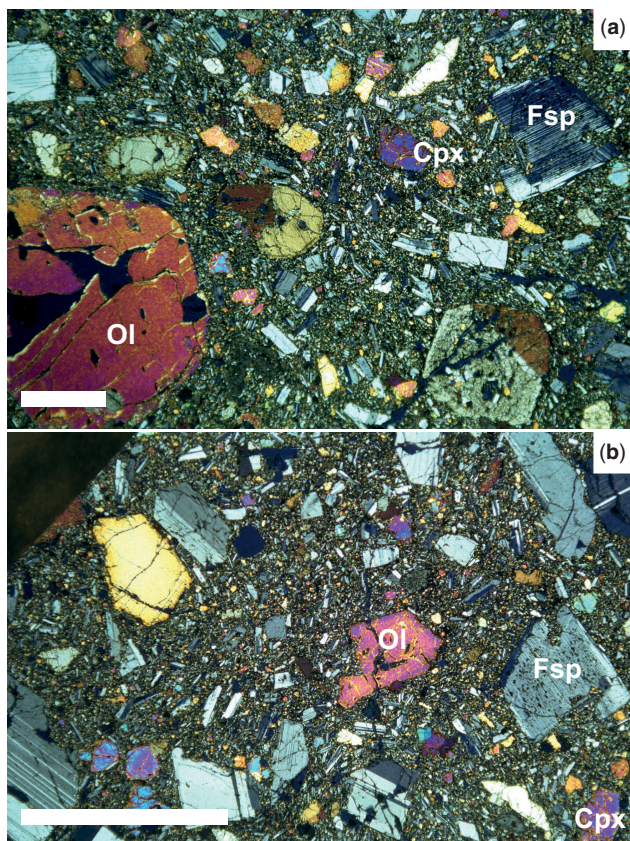


**Fig. 4.** (a) & (b) Petrographical photographs of relatively undifferentiated rock types typical of the Erebus Volcanic Province. The white bar in each photograph is 5 mm long. The photographs were taken in cross-polarized light. Cpx, clinopyroxene; Fsp, feldspar; Ol, olivine. Porphyritic texture in a fine-grained groundmass.

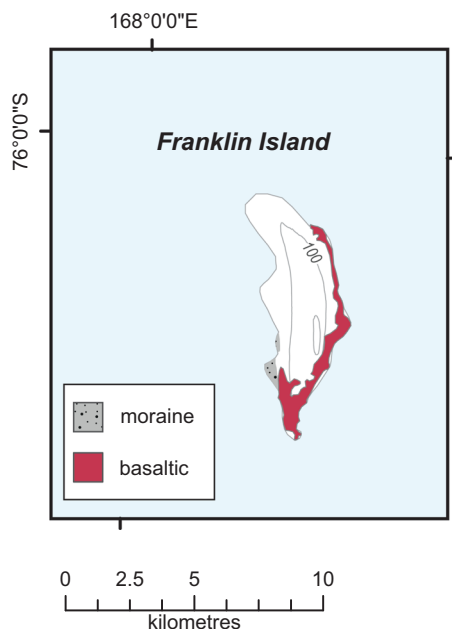


**Fig. 5.** Map of Franklin Island showing volcanic rock outcrops and key topographical features. In all map figures (Fig. 5 et seq.), 'basaltic' includes basalts, basanite and intermediate compositions, such as hawaiite and mugearite. This grouping reflects the scale of the original mapping, and follows Cox *et al.* (2012) for southern Victoria Land or LeMasurier (2013) for Marie Byrd Land. Contours (grey lines) are in metres, and white areas indicate snow and/or ice cover.

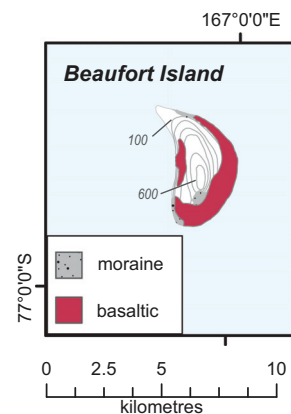


**Fig. 6.** Map of Beaufort Island showing volcanic rock outcrops and key topographical features.

from Rilling *et al.* (2009, fig. 6) are nepheline-normative and strongly alkali, and they define an apparent lineage between tephrite and phonotephrite (Fig. 3). Phenocrysts of titanite + plagioclase + kaersutite are observed with nepheline  $\pm$  apatite in the groundmass (Ellerman and Kyle 1990a). Olivine is conspicuous by its absence. Most rocks are pervasively altered.

*Submarine volcanic rocks in the Victoria Land Basin.* Geophysical studies indicate that submarine volcanism is widespread in the Ross Sea region where it appears to be closely associated with extensional tectonics (Behrendt *et al.* 1991a). The Victoria Land Basin is a broad, sediment-filled half-graben extending for approximately 350 km from Mount Melbourne in the north to Mount Erebus in the south (Cooper *et al.* 1987; Lawver *et al.* 2007). Volcanic rocks with Erebus Volcanic Province affinities have been dredged from the flanks of Franklin Island, in the western Victoria Land Basin, and from the Terror Rift, an extensional trough along the central axis of the basin (Fig. 1).

During a geophysical cruise by the RVIB *Nathaniel B. Palmer* in 2004, samples of volcanic rock were dredged from the north and south flanks of Franklin Island. The samples were basaltic in composition (Fig. 3), and three were dated by the  $^{40}\text{Ar}/^{39}\text{Ar}$  method. Ages ranged from  $3.73 \pm 0.05$  to  $3.28 \pm 0.04$  Ma (Rilling *et al.* 2007). More recently, this suite of dredged samples has been studied by Aviado *et al.* (2015), who documented the petrology and geochemistry of volcanic rocks from seven sea mounts sampled during the 2004 cruise and from subaerial samples from Franklin and Beaufort Islands. The dredged samples are vesicular, weakly porphyritic basanites (Fig. 3) containing phenocrysts of olivine and clinopyroxene in fine-grained groundmasses of clinopyroxene + olivine + iron oxide  $\pm$  plagioclase. Ultramafic xenoliths are present in some samples and the olivine populations include grains interpreted as xenocrysts.

Samples of Erebus Volcanic Province basaltic rock were also dredged from the Terror Rift during the 2010–11 cruise of the RV *Araon*. Lee *et al.* (2015) carried out geochemical analysis and geochronology on samples from four of these dredge sites, and compared these data with those for the nearby Melbourne Volcanic Province. The dredged volcanic rock samples gave  $^{40}\text{Ar}/^{39}\text{Ar}$  ages ranging from  $3.55 \pm 0.25$  to  $2.89 \pm 0.18$  Ma. Four whole-rock samples were analysed for major element, trace element, and Sr, Nd and Pb isotope composition (Lee *et al.* 2015). The analysed samples have basanite and tephri-basanite compositions (Fig. 3).

## Erebus Volcanic Province: petrology

*Ross Island Volcanic Field*

Ross Island comprises the four main eruptive centres of Mount Bird, Mount Terror, Mount Erebus and the Hut Point Peninsula. Mount Terra Nova (named after the ship used by Robert Scott in his 1910–13 British *Terra Nova* Antarctic Expedition) is a ‘parasitic’ vent that sits on the western flanks of Mount Terror and is included here as part of the Mount Terror eruptive centre. The first sighting of Ross Island in January 1841 by Captain Ross was the beginning of an understanding of the volcanic geology of the region. Ross named mounts Erebus and Terror, after his two tiny sailing ships. Ross noted in his journal on 28 January 1841 ‘at 4 p.m. Mount Erebus was observed to emit smoke and flames in unusual quantities ... and some of the officers believed they could see streams of lava pouring down its side’ (Ross 1847, pp. 220–221). At the time, Captain Ross did not identify the volcanoes as part of an island as the Ross Ice Shelf blocked its circumnavigation.

The observations of Captain Ross were followed in the early 1900s by the heroic era of Antarctic exploration. Three British expeditions under the direction of Robert Scott (1901–04 and 1910–13) and Ernest Shackleton (1907–09) made Ross Island their base of operations. All three expeditions included geologists, and the first descriptions of the Ross Island physiography and petrology were made. Notable contributions on the petrology of the volcanic rocks of Ross Island (Ferrar 1907; Prior 1907; Jensen 1916; Smith 1954) were supplemented by descriptions of the physiography, which included many descriptions of the volcanic geology (David and Priestly 1914; Taylor 1922; Debenham 1923).

*Mount Bird.* Although there are several Adelie penguin rookeries on the western flank of Mount Bird, they are not the origin of the name. Captain Ross named features on the northern

extremity of Ross Island after Lieutenant Edward J. Bird who served on the ship HMS *Erebus*. Mount Bird has a classic basaltic shield form with 11° slopes. The summit is 1800 m above sea-level, and the diameter of the volcano at sea-level is 23 km north–south and 18 km east–west, making it weakly ovoid (Fig. 7). The volume of the shield is estimated at 470 km<sup>3</sup> (Esser *et al.* 2004). Rock exposure on the volcano is limited to small scoria cones, a phonolite dome in the summit area, exposures around Lewis Bay to the east and a 10-km-long strip along the western coast in the Cape Bird area (Fig. 7). The timing of eruptions at Mount Bird is poorly constrained from four samples giving ages between 4.62 ± 0.6 and 3.08 ± 0.15 Ma (recalculated to current decay constants for the <sup>40</sup>K system: Armstrong 1978). There are marine cliffs bounding Lewis Bay along the eastern coast of Mount Bird which are mostly unexplored and assumed to be basaltic (Fig. 7), except for one area from which several phonolite rock samples were analysed by Phillips *et al.* (2018).

*Cape Bird.* Smith (1954) reported on several ‘trachyte’ samples from Cape Bird but very little was known of the volcanic geology at Cape Bird until the work of Cole and Ewart (1968). Recent sampling and geochemical analyses reported in this study (P.R. Kyle), and by Rasmussen *et al.* (2017) and Phillips *et al.* (2018), have provided new insights into the petrology and magmatic evolution and source for the Mount Bird eruptive centre. The geology of Cape Bird consists of basanite lava flows erupted from the main Mount Bird cone overlain by basanite scoria cones and phonolite domes (Cole and Ewart 1968). Lava flows of the main Mount Bird cone form a thick sequence of basanite lava flows which are well exposed along the coastal cliffs. The lava flows vary from about 10 m to less than 1 m in thickness, and typically have oxidized scoriaceous tops. Cole and Ewart (1968) recognized three, older, main Mount Bird cone ‘basalt’ rock units. The oldest, a ‘hornblende

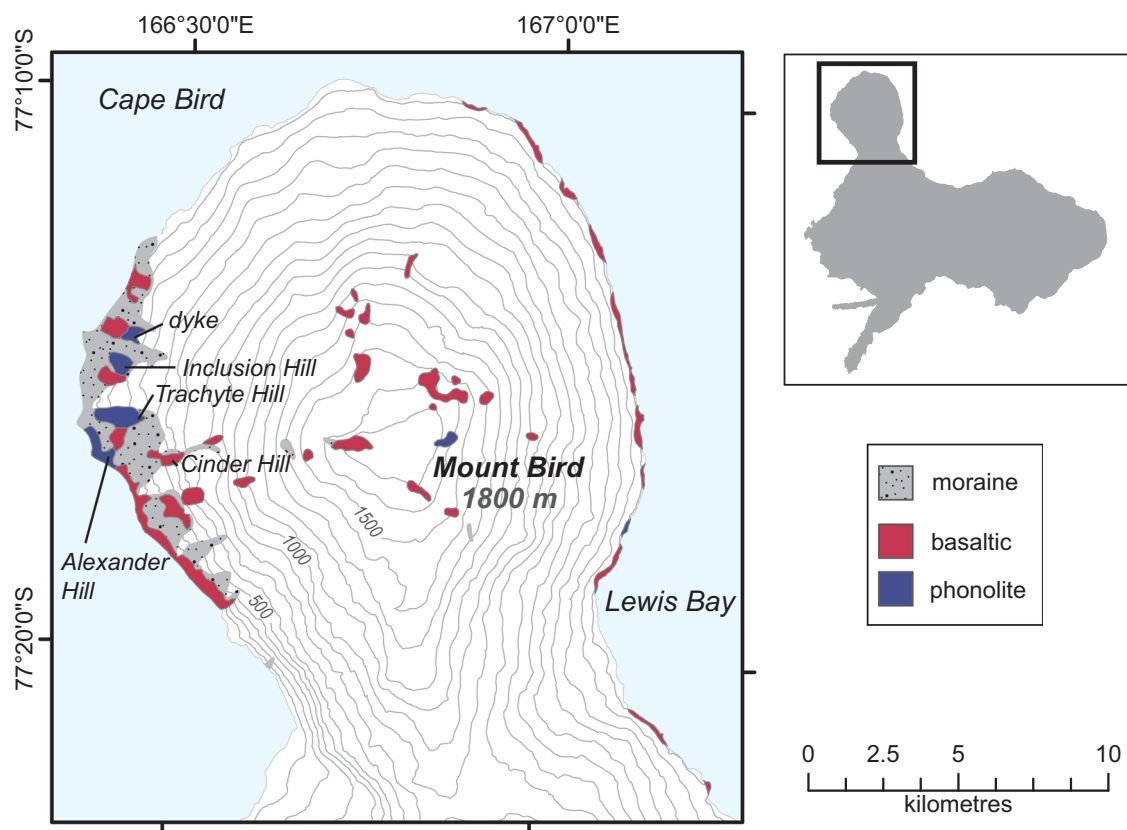


Fig. 7. Map of northwestern Ross Island showing volcanic outcrops and key topographical features, including Mount Bird, Cape Bird and Lewis Bay.

(kaersutite)–augite–plagioclase’ basanite, has normal magnetic polarity (Kyle 1976). It is followed by an olivine–augite basanite. This is, in turn, overlain by a magnetically reverse polarized ‘olivine–augite–plagioclase’ basanite which has a K–Ar age of  $3.8 \pm 0.2$  Ma (Armstrong 1978). Alexander Hill (Fig. 7) consists of the eroded remnants of two complex phonolite–basanite cones and four rock units were recognized by Cole and Ewart (1968). Basanite is interbedded with phonolite and there is no evidence of lava flows with intermediate compositions. A pyroxene phonolite has reversed magnetic polarity (Kyle 1976) and a K–Ar age of  $3.23 \pm 0.09$  Ma (Armstrong 1978). Bright red, scoriaceous, olivine-rich basanite with peridotite xenoliths was erupted at Cinder Hill and this is overlain by black, massive olivine basanite lava flows. Large (no quantitative data are reported) crystals of gem-quality olivine (peridot) are found at Cinder Hill (Wilson *et al.* 1974). At Inclusion Hill, the Cinder Hill igneous rocks are overlain by a phonolite dome. A tephriphonolite dome at Trachyte Hill represents the youngest eruptive event and has a K–Ar age of  $3.08 \pm 0.15$  Ma. A tephriphonolite dyke exposed at the northern end of the Cape Bird exposures is similar in composition to the tephriphonolite at Trachyte Hill.

Lava-flow samples analysed from the Mount Bird eruptive centre have a classic bimodal distribution of compositions comprising mainly basanitic lava flows and scoria cones with later-stage tephriphonolite (Fig. 3) and phonolite domes. There is a Daly gap between 48 and 54 wt% SiO<sub>2</sub> (Fig. 3). Five phonolite vents and a phonolite dyke are known (Fig. 7). Most of the phonolite domes appear to be

late in the eruptive sequence. The recent discovery of a phonolite on the Lewis Bay cliffs (Fig. 7) indicates that phonolite may also have been involved in the main cone-building phase of Mount Bird.

**Mount Terror.** Mount Terror is a 3262 m-high basaltic shield volcano (Wright and Kyle 1990e). It is roughly circular in outline, being 35 km north–south and 40 km east–west, with slopes of about 9° (Fig. 8). It has an estimated eruptive volume of about 1700 km<sup>3</sup> (Esser *et al.* 2004). The volcano is mainly snow- and ice-covered but there is a large triangular shaped area of exposed rocks extending from the summit down slope to the east towards the Cape Crozier area (Fig. 8). The summit area and eastern slope consist of numerous basanitic scoria cones, and rare phonotephrite, tephriphonolite and phonolite (Fig. 3) cones and domes, that overlie the main shield. Several samples were collected by early British expeditions from Cape Crozier and these are described by Smith (1954). Phillips *et al.* (2018) sampled some of the cones on the summit and higher parts of the eastern slopes but no detailed geological mapping exists for other areas except around Cape Crozier.

Eruptions at Cape Crozier have been dated at between at least  $1.75 \pm 0.3$  and  $0.82 \pm 0.14$  Ma (Kyle 1976; Armstrong 1978; Lawrence *et al.* 2009). A single sample from Mount Terra Nova (Fig. 8) yielded an imprecise K–Ar age of  $0.82 \pm 0.5$  Ma (Armstrong *et al.* 1968). The eruption age of the main Mount Terror shield is unknown but it must be older than the small phonolite vents at Cape Crozier.

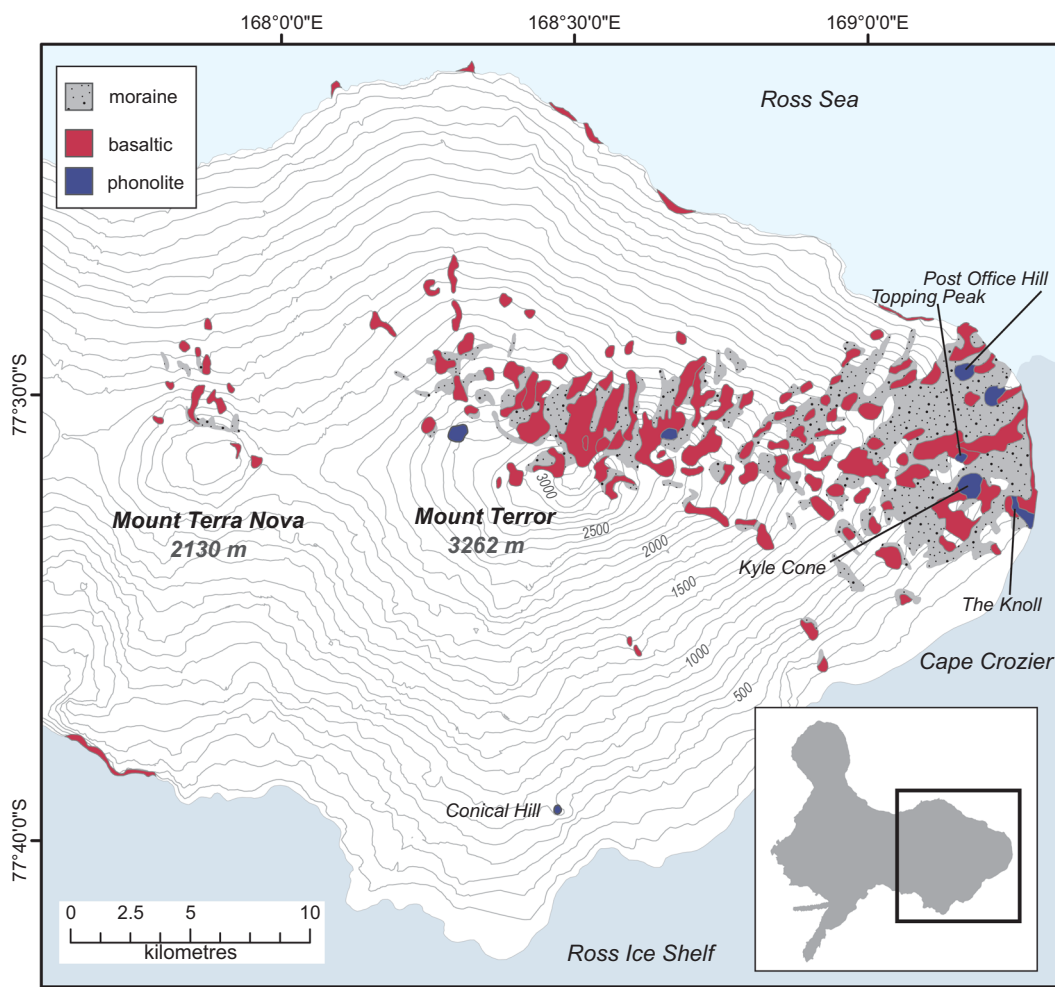


**Fig. 8.** Map of eastern Ross Island showing volcanic rock outcrops and key topographical features, including Mount Terror, Mount Terra Nova and Cape Crozier.

Considering the size of Mount Terror and that it probably took 1 myr to form, we speculatively suggest it started forming somewhere in the 3–2.5 Ma time period. Compositionally, analysed lava flows from the Mount Terror eruptive centre define a predominantly bimodal distribution with mainly basanitic lava flows and scoria cones and later-stage phonolite domes (Figs 3 & 8). Three lava-flow samples analysed by Phillips *et al.* (2018) are intermediate in composition (Fig. 3a).

**Cape Crozier.** The eruptive history of Cape Crozier is representative of the eastern flanks of Mount Terror, and described in detail here and in Figure 8. Cape Crozier extends north–south for over 10 km as an ice-free area along the east margin of Mount Terror (Fig. 8). Cole *et al.* (1971) described the geology of Cape Crozier and provided a reconnaissance geological map. The oldest lava flows, exposed in coastal cliffs north of The Knoll, comprise olivine–augite basanite lava flows with interbedded volcanic breccia and some tuffs. Lava flows at the base of the exposed sequence originated from the flanks of Mount Terror, and these are commonly overlain by younger lava flows and pyroclastic deposits from small vents at Cape Crozier. Rare dykes indicate local vents for some of the lava flows. On the east flank of Topping Peak, erosion has exposed a section of rocks with compositions of basanite and kaersutite phonolite, the latter were fed by at least four irregular dykes. Post Office Hill is a steep-sided endogenous kaersutite phonolite dome. Using colour and phenocryst variations, Cole *et al.* (1971) recognized three main rock types. Chemically, the lava flows are very similar (see the Supplementary material (ESM1)). The Knoll and Kyle Cone are steep-sided endogenous domes composed of aegirine–augite phonolite. At Kyle Cone, a kaersutite basanite lava flow underlies the phonolite dome; whereas, at The Knoll, two lava flows of olivine–augite basanite mantle the phonolite. The Knoll basanite lava flows were erupted from a small circular crater near the summit. Five outcrops with a phonolite composition have been identified previously on Cape Crozier but samples from recently identified and analysed domes near the summit of Mount Terror and Conical Hill are confirmed here as having a phonolite composition (Figs 3 & 8). One scoria cone is an alkali basalt, which is a rarity in the Ross Island Volcanic Field.

**Mount Erebus.** As defined here, the Mount Erebus volcanic centre includes Mount Erebus and the Dellbridge Islands (Tent, Inaccessible, Big Razorback Island and Little Razorback Island) in Erebus Bay (Fig. 9). At 3794 m, Mount Erebus is the highest and largest volcano on Ross Island and dominates the centre of the island. Esser *et al.* (2004) estimated the volume of the Erebus centre to be about 2200 km<sup>3</sup>, making it one of the 20 largest volcanoes in the world. The ‘Main Crater’ at the summit of Mount Erebus is currently active with a persistent active phonolite lava lake, which has existed for over 45 years (Giggenbach *et al.* 1973; Kyle *et al.* 1982; Kyle 1994; Oppenheimer and Kyle 2008).

**Anorthoclase-phyric phonolite** (*‘kenyte’*). Large (up to 10 cm) rhombic crystals of anorthoclase feldspar occur in Mount Erebus phonolite lava flows. David and Priestly (1914, p. 277) noted ‘that the covering of snow became thinner until it almost entirely disappeared, being replaced by a surface formed of crystals of anorthoclase felspar from half an inch to four inches in length’. This rock was originally described as ‘kenyte’ (e.g. Ferrar 1907), an igneous rock found mainly around Mount Kenya, with a variant, ‘Antarctic Kenyte’, also proposed for the nepheline phenocryst-free variant on Ross Island (Smith 1954). It is now more properly referred to as anorthoclase-phyric phonolite (e.g. Kyle 1977;

Cox *et al.* 2012). Its significance relates to mapping of the presence or absence of anorthoclase-phyric phonolite erratics to reconstruct grounded ice-sheet flowlines in McMurdo Sound at the last glacial maximum (Vella 1969; Cole *et al.* 1971; Denton and Marchant 2000; Anderson *et al.* 2017). On Ross Island, *in situ* anorthoclase-phyric phonolite lava is found in flows between Cape Barne and Cape Royds, as well as in recent ejecta and the convecting phonolitic lake of the Mount Erebus summit (Goldich *et al.* 1975; Kyle 1977; Kyle *et al.* 1992). Anorthoclase phenocrysts with the composition Or<sub>16</sub>Ab<sub>63</sub>An<sub>21</sub> (Treves 1967) make up 30–40% of the rock volume (Goldich *et al.* 1975), and occur in a groundmass of plagioclase, anorthoclase, apatite, opaque mineral and nepheline (Goldich *et al.* 1975). Anorthoclase-phyric phonolites here are thought to have evolved from basanite parent material as part of the Erebus Lineage (Kyle *et al.* 1992).

**Dellbridge Islands.** The earliest study of the field geology and physiography of the Dellbridge Islands was discussed by Debenham (1923). The petrology was summarized by Smith (1954), with Moore and Kyle (1987) describing the four small heavily eroded volcanic islands in more detail. Inaccessible Island (Fig. 9), the most northerly in the group, is composed of many irregular lava flows that dip from 10° to 40° to the north. These are well exposed in coastal cliffs along the south side of the island. The oldest exposed rocks are clinopyroxene–feldspar-phyric phonotephrite (see the Supplementary material (ESM1)). These are overlain by palagonitized breccias with pillow lavas, which are, in turn, overlain by feldspar-phyric phonotephrite lava flows. Kaersutite-bearing lava flows of tephriphonolite and phonolite are interbedded in the sequence. Esser *et al.* (2004) dated the groundmass from a phonolite at Inaccessible Island as 539 ± 12 ka. The lower part of Tent Island is composed mainly of pillow lavas, lava flows and breccias of clinopyroxene–feldspar-phyric phonotephrite (see the Supplementary material (ESM1)).

**Mount Erebus lower slopes.** Turks Head and Trygve Point are two distinct promontories on the SW side of Mount Erebus (Fig. 9). They are composed of hyaloclastite, pillow breccia and palagonitic tuffs. Luckman (1974) described the geology and believed the hyaloclastite rocks to be products of both submarine and subglacial eruptions, and they have yielded an <sup>40</sup>Ar/<sup>39</sup>Ar age of 378 ± 28 ka (Esser *et al.* 2004). A dyke which intrudes the same sequence of hyaloclastites at Trygve Point has been dated by the <sup>40</sup>Ar/<sup>39</sup>Ar method as 368 ± 18 ka (Esser *et al.* 2004), indistinguishable from the radiometric date of Turks Head. The hyaloclastite comprises porphyritic andesine-rich phonotephrite. Anorthoclase tephriphonolite lava flows from the main cone-building phase of Mount Erebus have a <sup>40</sup>Ar/<sup>39</sup>Ar age of 243 ± 18 ka and they overlie the hyaloclastite rocks at Turks Head. The geology of Cape Evans (Fig. 9) was described by numerous early workers and summarized by Smith (1954). Two anorthoclase phonolite lava flows, which reach up to 15 m in thickness (Treves 1962), have been dated by the <sup>40</sup>Ar/<sup>39</sup>Ar method at 40 ± 6 ka (Esser *et al.* 2004) and 55 ± 10 ka (Tauxe *et al.* 2004).

Fine-grained basanite and phonotephrite volcanic rocks occur along the south coast of Ross Island at Cape Barne (Figs 3 & 9). They have been dated at 1311 ± 16 ka (<sup>40</sup>Ar/<sup>39</sup>Ar: Esser *et al.* 2004) and they comprise the oldest eruptive products from the Mount Erebus volcanic centre. The Cape Barne rocks have been interpreted as pyroclastic cones (e.g. Armstrong 1978) but more recent work interprets them as lava-fed deltas intruded by coeval dykes (Smellie and Martin 2021). Erosion has removed over half of the western outcrop, exposing an intrusion which now forms the striking ‘Cape Barne Pillar’ (Fig. 9). Above Cape Barne is a

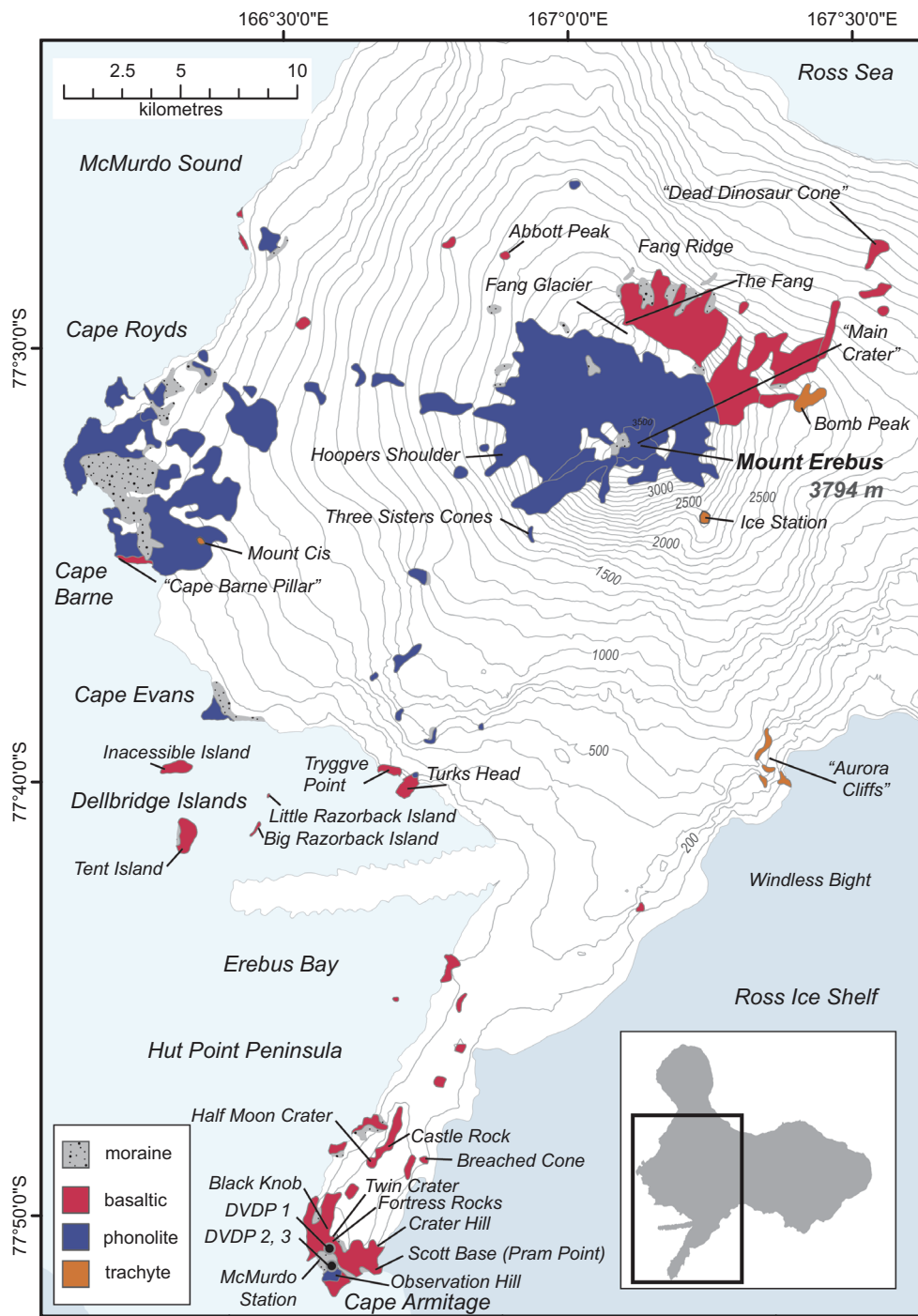


**Fig. 9.** Map of southwestern Ross Island showing volcanic rock outcrops and key topographical features, including Mount Erebus, Cape Royds, Cape Evans, the Dellbridge Islands and the Hut Point Peninsula, and the locations of the Dry Valley Drilling Project drill holes 1–3.

5 m-high trachyte mound named by the early British explorers as Mount Cis (Fig. 9). This small outcrop has received attention because it contains sandstone xenoliths (Thomson 1916) believed to be from the Beacon Supergroup. The xenoliths indicate that downfaulted rocks, like those in the Transantarctic Mountains, underlie Ross Island and McMurdo Sound. Three anorthoclase tephriphonolite lava flows are exposed along the coast at Cape Royds (Fig. 9). Early work (also summarized by Smith 1954) described the geology and rocks at this location. Many small outcrops on the slopes of Mount Erebus above Cape Royds were described by early workers as cones and potential sources of the lava flows. Most of the outcrops are, however, not cones but small moraine debris mounds, and a source for the lava flows at Cape Royds has not been identified. Until further evidence is found it must be assumed that the lava flows along the coast to the west of

Mount Erebus were erupted from vents that are now obscured by the snow and ice cover. Tauxe *et al.* (2004) reported a whole-rock  $^{40}\text{Ar}/^{39}\text{Ar}$  age of  $74 \pm 14$  ka, and Esser *et al.* (2004) reported  $73 \pm 10$  ka dated by the  $^{40}\text{Ar}/^{39}\text{Ar}$  method on anorthoclase crystals for a Cape Royds lava flow.

**Fang Ridge and Mount Erebus summit.** Fang Ridge (the peak, called The Fang, is 3159 m above sea-level) is a prominent feature paralleling the NE slope of Mount Erebus but separated from it by the Fang Glacier (Fig. 9). The north and NE slopes have an average dip of over  $45^\circ$ , and are composed of scree and ribs of rubbly lava flows and pyroclastic rocks. The Fang Glacier side of the ridge has steep, in places vertical, cliffs more than 150 m in height. The lava flows are strongly porphyritic and commonly show well-developed flow banding defined by aligned plagioclase phenocrysts.

The lavas are phonotephrite and tephriphonolite (Fig. 3). Smith (1954) reported the presence of olivine basalt from the lower west end of Fang Ridge but the location of this lava flow has not been found.

The steep (>30°) slopes of Mount Erebus, from 1800 m to the caldera rim at about 3000 m, are made up of numerous (50–100) sinuous, irregular rubbly anorthoclase-phyric phonolitic lava flows. Mount Erebus has five small parasitic vents around its lower flanks. These are Abbott Peak, Hoopers Shoulder, and three endogenous domes that constitute the Three Sisters Cones. All the parasitic vents are composed of black, glassy, porphyritic anorthoclase phonolite which is extremely fresh in appearance. Abbott Peak (1793 m) consists of phonotephrite lava flows that mantle a cone which formed in the main by endogenous growth.

**Hut Point Peninsula.** This peninsula extends for over 20 km in a SSW direction from Mount Erebus (Fig. 9), indicating that it may be related to a major crustal fracture or weakness radiating from Mount Erebus. Unlike the other Ross Island centres, a major volcanic edifice did not evolve at Hut Point Peninsula. The peninsula is mostly snow- and ice-covered, except for the southern end where the American McMurdo Station and New Zealand Scott Base are situated. The southern tip of the peninsula is made up of an echelon line of mainly basanite scoria cones and a single endogenous dome of phonolite (Observation Hill). Esser *et al.* (2004) estimated the eruption volume of the peninsula as 82.5 km<sup>3</sup>, making it the smallest eruptive centre on Ross Island.

The geology of the Hut Point Peninsula is known from collections made by the early British explorers (e.g. Smith 1954), mapping, for example, by Cole *et al.* (1971) and from onshore drilling of three holes as part of the DVDP. During the period 1973–75, 15 holes were drilled in the Dry Valleys and elsewhere as part of the DVDP, an international research programme involving science agencies from the USA, Japan and New Zealand. There is extensive literature relating to the project, with a large number of papers and reports being published in the 1970s and early 1980s. A comprehensive bibliography was compiled by Rebert (1981). Three of the DVDP holes were cored through volcanic rocks of the Erebus Volcanic Province at the Hut Point Peninsula on Ross Island (Fig. 9); the other holes were largely through lake and glacial sediments.

Hole DVDP 1 cored 40 stratigraphic units and reached a depth of 201 m. Holes DVDP 2 and 3 were drilled 3 m apart on the flank of Observation Hill and are essentially identical. Hole DVDP 2 reached a depth of 179 m, and DVDP 3 sampled 15 stratigraphic units and reached a depth of 381 m (Kyle 1981b). The geological evolution of the Hut Point Peninsula can be reconstructed from geological mapping, the DVDP drill cores, palaeomagnetic data and radiometric dating (Kyle 1981b). The peninsula has been magmatically active since possibly as early as 1.68 ± 0.06 Ma, continuing to at least 0.33 ± 0.02 Ma. Lithostratigraphic unit 2.4 in the AND-1B (McMurdo Ice Shelf (MIS): discussed in the 'Sub-surface volcanic rocks of the Erebus Volcanic Province recovered by offshore drilling' subsection later in this section) core is approximately 12 m thick (Pompilio *et al.* 2007) and is a primary basanite pyroclastic fall deposit. Glass from the unit has an <sup>40</sup>Ar/<sup>39</sup>Ar age of 1.68 ± 0.06 Ma (Ross *et al.* 2012a). The Hut Point Peninsula is the closest volcanic centre to the AND-1B (MIS) drill core and we suggest the AND-1B (MIS) tephra represents the earliest eruptive phases of the polygenetic Crater Hill on the Hut Point Peninsula, although a source from White Island or other active eruptive centres in the province cannot be excluded. The oldest dated rocks from the peninsula are basanitic (see the Supplementary

material (ESM1)) hyaloclastite rocks which are 54 and 214-m-thick in DVDP 1 and DVDP 3, respectively. They have been dated by the K/Ar method at 1.34 ± 0.23 Ma in DVDP 1 and 1.32 ± 0.16 Ma in DVDP 3, yielding ages that overlap within error (Kyle 1981b). The hyaloclastite rocks in these drill cores are representative of the submarine pedestal on which the Hut Point Peninsula was erupted (as also seen for Mount Erebus). Lawrence *et al.* (2009) reported an <sup>40</sup>Ar/<sup>39</sup>Ar age of a basaltic rock sample collected at McMurdo Station as 1.33 ± 0.12 Ma, which overlaps in time with the eruptive sequence seen in DVDP 1. The ages yielded from the deepest and oldest samples in DVDP 2 and 3 are older than in Observation Hill surface outcrops, where the K/Ar method has yielded a 1.21 ± 0.04 Ma date (Forbes *et al.* 1974), and the <sup>40</sup>Ar/<sup>39</sup>Ar method on two different samples has yielded a 1.23 ± 0.02 Ma date (Lawrence *et al.* 2009) and a 1.18 ± 0.01 Ma date (Tauxe *et al.* 2004); this later date from Observation Hill (1.18 ± 0.01 Ma) overlaps with a shallower sample in the DVDP 2 core at 62.38 m dated at 1.16 ± 0.03 Ma (Kyle *et al.* 1979b). Volcanic vents at Castle Rock (1.21 ± 0.05 Ma), Half Moon Crater (1.0 ± 0.2 Ma), Cape Armitage (1.03 ± 0.10 Ma) and Breached Cone (0.65 ± 0.05 Ma) were coincident with episodic growth of the peninsula (Kyle *et al.* 1979b; Tauxe *et al.* 2004; Lawrence *et al.* 2009). The last eruption at the peninsula was a fissure eruption that formed a sequence of younger lava flows from Crater Hill (including the distinct lava flow forming Pram Point where Scott Base is situated), Twin Crater, Black Knob and Fortress Rocks. Samples dated by the <sup>40</sup>Ar/<sup>39</sup>Ar method (Tauxe *et al.* 2004; Lawrence *et al.* 2009) for the fissure eruption yield dates of 0.348 ± 0.008 and 0.33 ± 0.02 Ma (Crater Hill) and 0.34 ± 0.07 Ma (Fortress Rocks), and a K/Ar age of 0.44 ± 0.10 Ma (Kyle *et al.* 1979b) for Black Knob.

More than 150 whole-rock analyses of Hut Point Peninsula and DVDP igneous rock samples have been published (Kyle 1976, 1981b; Goldich *et al.* 1981; Stuckless *et al.* 1981) (Fig. 3) with new analyses also provided in this study (see the Supplementary material (ESM1)). Surface volcanic rock compositions on the peninsula and lava-flow compositions in DVDP drill core complete a differentiation trend of basanite, phonotephrite, tephra-phonolite to phonolite (Fig. 3a). Several DVDP samples have lower whole-rock Na<sub>2</sub>O + K<sub>2</sub>O wt% relative to the majority of DVDP and Hut Point Peninsula compositions (Fig. 3a), and include a benmoreite dyke in DVDP 1 (Kyle 1976). The petrology and possible evolution of these low-alkali lava flows and volcanic rocks have not been examined. Kyle (1981b) used electron probe microanalysis (EPM) to determine olivine, clinopyroxene, plagioclase, amphibole, titanomagnetite and ilmenite compositions, as well as those of less common phases such as apatite, sodalite and chromium spinel. Amphibole is mainly kaersutite in composition. The, relatively rare, mineral rhönite occurs in the groundmass of basanites from DVDP 1, 2 and 3 (Kyle and Price 1975). As part of a broader study of Ross Island volcanic rocks, Weiblen *et al.* (1981) analysed clinopyroxene in DVDP core samples where they showed chemical zoning in clinopyroxene phenocrysts may relate to oxidation of magma during ascent or to local reactions. Basanites are porphyritic (15–36% phenocrysts) with phenocrysts of olivine and clinopyroxene in a groundmass comprising olivine or amphibole, clinopyroxene, plagioclase, chrome spinel, titanomagnetite, ilmenite, apatite and glass. Kaersutite is a rare phenocryst phase in basanites. Intermediate rocks are generally less porphyritic (<10% phenocrysts) than basanites, and kaersutite is a more common phenocryst phase. Tephriphonolites and phonotephrites are aphanitic or weakly porphyritic (3–7% phenocrysts) with microphenocrysts of clinopyroxene, kaersutite, plagioclase, iron oxide and apatite.

*Mount Discovery Volcanic Field*

**Dailey Islands.** Named after the 1901–04 British National Antarctic Expedition's carpenter (Scott 1907), the Dailey Islands are a group of five, extensively glaciated, volcanic islands that are made up of highly eroded mafic cinder cones and lava flows (McCraw 1967; Treves 1967; Del Carlo *et al.* 2009) (Fig. 10). The two published eruption ages overlap at  $0.78 \pm 0.04$  and  $0.76 \pm 0.02$  Ma (Tauxe *et al.* 2004; Del Carlo *et al.* 2009). A nepheline-normative basanite (Fig. 3) sample from Juergens Island in the group has phenocrysts of olivine + pyroxene in a holocrystalline groundmass of clinopyroxene + plagioclase + olivine + magnetite (Del Carlo *et al.* 2009). The phenocrysts show disequilibrium textures (Del Carlo *et al.* 2009).

**White Island.** White Island is an extensively glaciated volcanic island ( $20 \times 12$  km) in the western Ross Embayment of southern Victoria Land, Antarctica (Fig. 11). It lies approximately 25 km SE of Scott Base (New Zealand), Ross Island, and rises to a height of 741 m above sea-level at Mount Heine in the north, and 762 m at Mount Nipha in the south (Fig. 11). White Island was first visited by Shackleton, Wilson and Ferrar on 19 February 1902, during Scott's British National Antarctic Expedition, and was named for the mantle of snow which covers it (Scott 1907). Rocks collected by this party were described by Smith (1954). In 1969–70, the northern part of the island was mapped by Cole *et al.* (1971) and the geology described as comprising two overlapping olivine-augite basalt shield volcanoes, with subsequent subsidiary cones being constructed on the northern flank. In a study of Cenozoic volcanic rocks from the Ross Island area, Goldich *et al.* (1975, 1981) and Stuckless *et al.* (1981) presented major element and trace element analyses for two basanites: one from the 'younger' unglaciated sequence on Mount Hayward, and the other from the 'older' sequence north of Mount Heine. However, the outcrops occur in geographically separate areas of White Island (Fig. 11), making correlation of the volcanic successions impossible without the use of geochronology.

Large areas in the northern part of the island are essentially snow- and ice-free, and there are exposures of subdued areas of basaltic lava flows and low-rimmed, NNE-elongated craters cut by east–west-striking dykes and plugs. Basanites are the greatly dominant rock type (Figs 3b & 11) and throughout White Island they are olivine–pyroxene phyric, and commonly contain nodules of spinel and plagioclase lherzolite, wehrlite, clinopyroxenite, gabbro, granulite, and hornblende

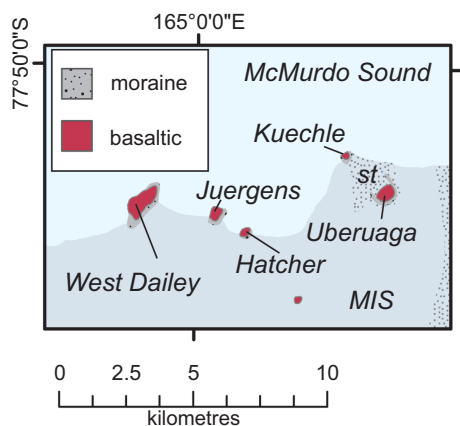


**Fig. 10.** Map of Dailey Islands showing volcanic rock outcrops and key topographical features. The pattern on the McMurdo Ice Shelf (MIS) indicates supraglacial till (st).

with megacrysts of olivine, clinopyroxene, kaersutite, spinel and anorthoclase (Cooper *et al.* 2007). At Camp Crater (Fig. 11), a crater filled with a frozen lake has cliff-forming outcrops of nodule- and megacryst-bearing basanite defining a topographically raised rim. Approximately 200 m to the east, a 40 m-wide crater is defined by an inwardly-dipping sheet of kaersutite-phyric tephriphonolite, the most petrogenetically evolved rock found on White Island. The lower part of the Mount Hayward spatter-clast breccia sequence has a unit of coarse breccia interbedded with cross-bedded lapilli tuffs. Basanite clasts (up to 45 cm) are in places rounded with a glassy rind enclosing a more vesicular core, suggesting a water-chilled pillow-like form.

Four samples of groundmass concentrate from three lava flows and a dyke were dated by Ar/Ar techniques and yielded ages of  $4.86 \pm 0.06$ – $2.11 \pm 0.05$  Ma (Cooper *et al.* 2007), all considerably older than the 0.17 Ma K–Ar age reported by Kyle (1981a) for a basalt collected by Cole *et al.* (1971) from northwestern White Island. An anorthoclase nodule from basanite at Camp Crater contains inclusions of apatite and zircon. Six zircon grains, dated by laser ablation inductively coupled plasma source mass spectrometry (LA-ICPMS) techniques, define a homogeneous population with a mean  $^{206}\text{Pb}/^{238}\text{U}$  age of 7.62 Ma (MSWD 2.11; Cooper *et al.* 2007). A high-resolution aeromagnetic survey of McMurdo Sound (Wilson *et al.* 2007) showed that the White Island volcanic massif extends a further *c.* 25 km north of White Island itself as a submarine volcanic ridge, which is in close proximity to the AND-1B (MIS) core site. and Talarico and Sandroni (2009) and Di Roberto *et al.* (2010) suggested that clasts from both Minna Bluff and White Island are important glacially-transported volcanic

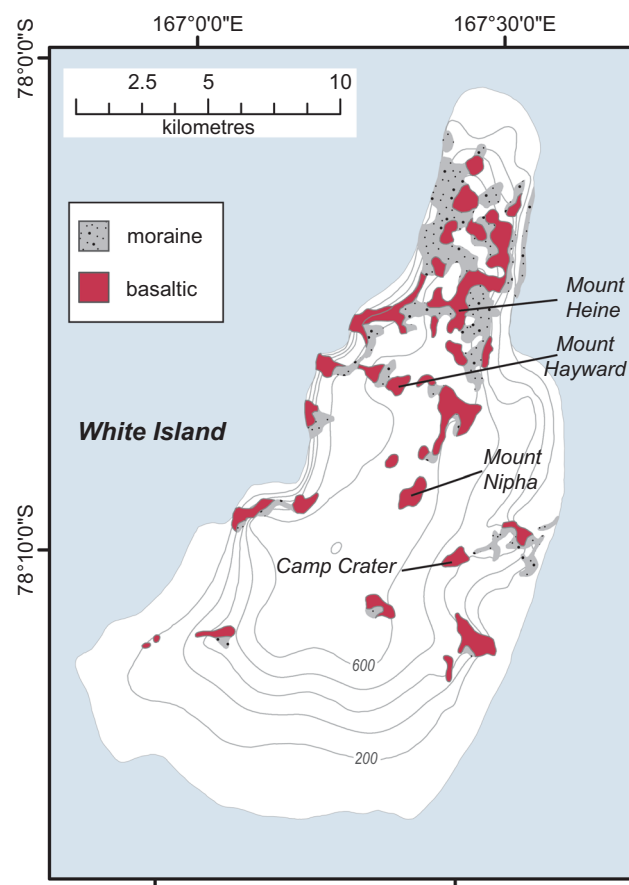


**Fig. 11.** Map of White Island showing volcanic rock outcrops and key topographical features.

## Erebus Volcanic Province: petrology

components of the AND-1B (MIS) core. The White Island volcanic history may well be considerably longer than is indicated by dating of onland samples.

**Black Island.** The island was named during the 1901–04 British National Antarctic Expedition (Scott 1907) because of its mainly snow-free appearance and black volcanic rock. As with the Brown Peninsula, Black Island is believed to have been a stratovolcano (Cole and Ewart 1968), made up predominantly of basanites and basalts (Fig. 12), the latter with varieties characterized by phenocrysts of olivine–augite, plagioclase or hornblende. Trachybasalts and either hornblende- or pyroxene-phyric trachytes make up the more petrologically evolved samples, although Goldich *et al.* (1975) and Timms (2006) described and analysed tephriphonolites and phonolites from the southern part of the island (Figs 3b & 12). Several of the phonolites contain xenocrysts of anorthoclase and 1–20 cm xenoliths of syenite or more plagioclase-rich syenodiorite, interpreted as cumulates. Pyroclastic deposits with clasts ranging in size from 20 cm blocks to fine-grained lapilli and ash are rare.

Although these rock types were assigned formational status by Cole and Ewart (1968), who correlated them with similar lava-flow lithologies on the Brown Peninsula and Cape Bird, different ages indicate that this correlation is invalid (Armstrong 1978). Armstrong (1978) presented the first radiometric (K/Ar) dates from northern and central Black Island, giving ages ranging from  $10.9 \pm 0.4$  and  $3.35 \pm 0.14$  Ma for basalts to a  $3.8 \pm 0.09$  Ma age for trachyte. Timms (2006) obtained  $^{40}\text{Ar}/^{39}\text{Ar}$  laser fusion ages on anorthoclases from

two specimens of phonolite of  $1.689 \pm 0.003$  Ma (MSWD 5.8) and  $1.780 \pm 0.058$  Ma (MSWD 7.0). These might indicate a southward migration of eruptive activity during the life-span of the Black Island eruptive centre.

**Brown Peninsula.** Named by the British National Antarctic Expedition 1901–04 for the colour of its weathered volcanic lava flows and ash deposits, the Brown Peninsula was first visited by R. Koettlitz in 1902 (Scott 1907), with samples collected during this expedition described by Prior (1907). It was again visited during the British *Terra Nova* Antarctic Expedition 1910–13, and samples collected at this time were described by Smith (1954).

Cole and Ewart (1968) mapped alternating basalt–trachyte eruptive sequences at Black Island, Brown Peninsula and Cape Bird in the McMurdo Sound area, and Vella (1969) mapped glacial moraines at Brown Peninsula. The Brown Peninsula (Fig. 13) consists of a series of north–south-aligned basaltic and felsic eruptive centres erupted both before and after glaciation. A single age determination of  $2.7 \pm 0.09$  Ma on the youngest lava flow at Rainbow Ridge (Fig. 13) post-dates glacial erosion (Armstrong 1978). In the Mount Wise area (Fig. 13) three K–Ar age determinations have analytical uncertainties that overlap. The dates indicate that the eruptive events at Mount Wise were only short lived and occurred at about 2.2 Ma (Armstrong 1978).

The basanite rocks contain phenocrysts of olivine and clinopyroxene in a groundmass of plagioclase, opaque oxides and glass (Kyle *et al.* 1979a). The eruptive sequence at the Brown Peninsula consists of at least three basaltic (basanite, hawaiite, mugearite) to felsic (benmoreite, phonolite) eruptive cycles. The oldest dated cycles occur at Rainbow Ridge, where two basaltic–felsic eruptive sequences are found.

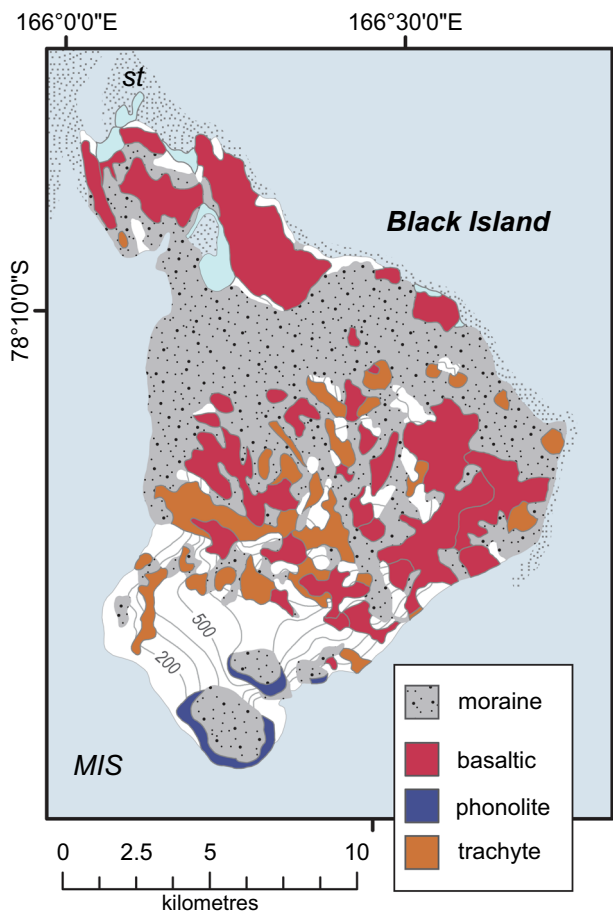


**Fig. 12.** Map of Black Island showing volcanic rock outcrops and key topographical features. The pattern on the McMurdo Ice Shelf (MIS) indicates supraglacial till (st).

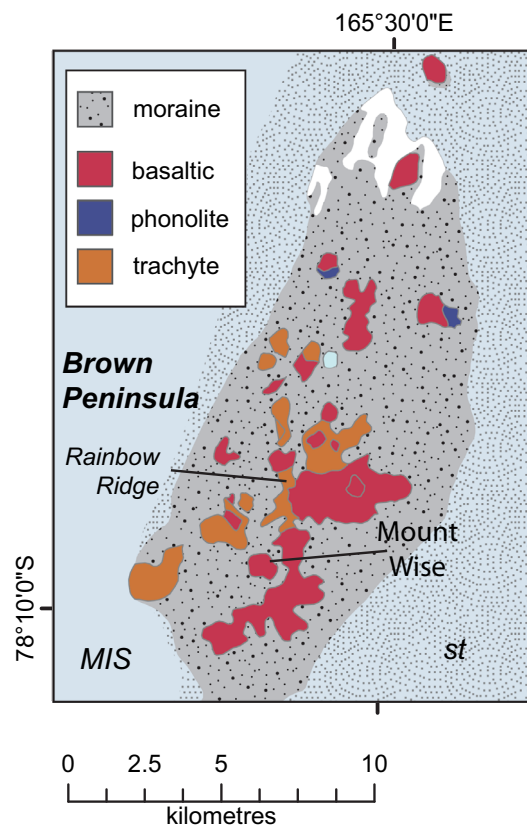


**Fig. 13.** Map of the Brown Peninsula showing volcanic rock outcrops and key topographical features. The pattern on the McMurdo Ice Shelf (MIS) indicates supraglacial till (st).

These are followed by a younger basaltic–felsic–basaltic eruptive sequence at Mount Wise. The total range in rock types is from basanite, through nepheline hawaiite to nepheline mugearite, nepheline benmoreite and phonolite (Adams 1973; Kyle 1976; Kyle *et al.* 1979a). The Brown Peninsula nepheline–hawaiite has been modelled to form from basanite by the fractional crystallization of olivine + spinel + clinopyroxene + plagioclase + titanomagnetite + apatite ± ilmenite ± kaersutite (Kyle *et al.* 1979a). Nepheline–hawaiite to nepheline–benmoreite was modelled by further fractional crystallization of clinopyroxene + kaersutite + titanomagnetite + plagioclase + apatite (Kyle *et al.* 1979a). At the Brown Peninsula, and many other areas in the Erebus Volcanic Province, small cones and lava flows of kaersutite-bearing and/or clinopyroxene-bearing felsic lava flows (nepheline–benmoreite and phonolite) are common. The cones are small, and most involved the eruption of less than 0.5 km<sup>3</sup> of material (Fig. 13).

**Mount Discovery.** In 1902, Robert Scott of the British National Antarctic Expedition (1901–04) noted in his diary the first description of Mount Discovery: ‘and to the south a peculiar conical mountain ... we named the conical mountain after our ship’ (Scott 1907, p. 119). Mount Discovery is a prominent stratovolcano (Global Volcanism Program 2013a) in the Ross Sea (Fig. 14). Rock exposures on Mount Discovery are separated from Mount Morning by the Discovery Glacier, from Minna Bluff by the Minna Saddle and from the Brown Peninsula by Dreary Isthmus (Fig. 14), in a pattern of three-fold radial symmetry (Kyle and Cole 1974).

The volcano was visited once in 1958 by a New Zealand party, with samples collected and described in a doctoral thesis (Kyle 1976). It was visited once again by S.B. Treves between

1960 and 1971 (Goldich *et al.* 1975). Data for samples collected by Treves have formed part of regional, geochemical, isotopic or chronological overviews of the region (Goldich *et al.* 1975; Sun and Hanson 1975; Stuckless and Ericksen 1976; Armstrong 1978) but these compilations usually include data for only one Mount Discovery sample. As part of her PhD work, Wright-Grassham (1987) spent 16 days mapping and collecting samples in the only detailed geological study of the mountain. The results from this work are included in a thesis and three short reports (Wright *et al.* 1984, 1986; Wright and Kyle 1990c).

On Mount Discovery, rock exposures are concentrated on the northern-facing slopes (Fig. 14). Moraine cover is dominant below *c.* 400 m. Above *c.* 1100 m the slope angle steepens to 30°. Lava flows, lava domes and pyroclastic deposits are present, and at least 45, morphologically young, cinder cones have been mapped (Wright-Grassham 1987). Ice-mushrooms (personal observations of A.P. Martin) occur on the summit but fumarolic ice towers have not been observed (Wright-Grassham 1987). Volcanism has been dated at between  $5.46 \pm 0.16$  and  $1.87 \pm 0.43$  Ma (Polyakov *et al.* 1976; Armstrong 1978; Wright-Grassham 1987) but radiometric ages as young as  $0.06 \pm 0.006$  Ma have been reported by Tauxe *et al.* (2004). The mostly undissected morphology indicates that this is a minimum age range for Mount Discovery.

On a total alkali v. silica diagram, nepheline-normative, strongly alkalic (Saggerson and Williams 1964) rocks from Mount Discovery form a lineage between basanite and phonolite, with rare trachyte (Fig. 3b). This lineage can be modelled by the fractional crystallization of olivine + clinopyroxene + plagioclase + titanomagnetite + apatite ± ilmenite ± kaersutite ± nepheline (Wright-Grassham 1987).

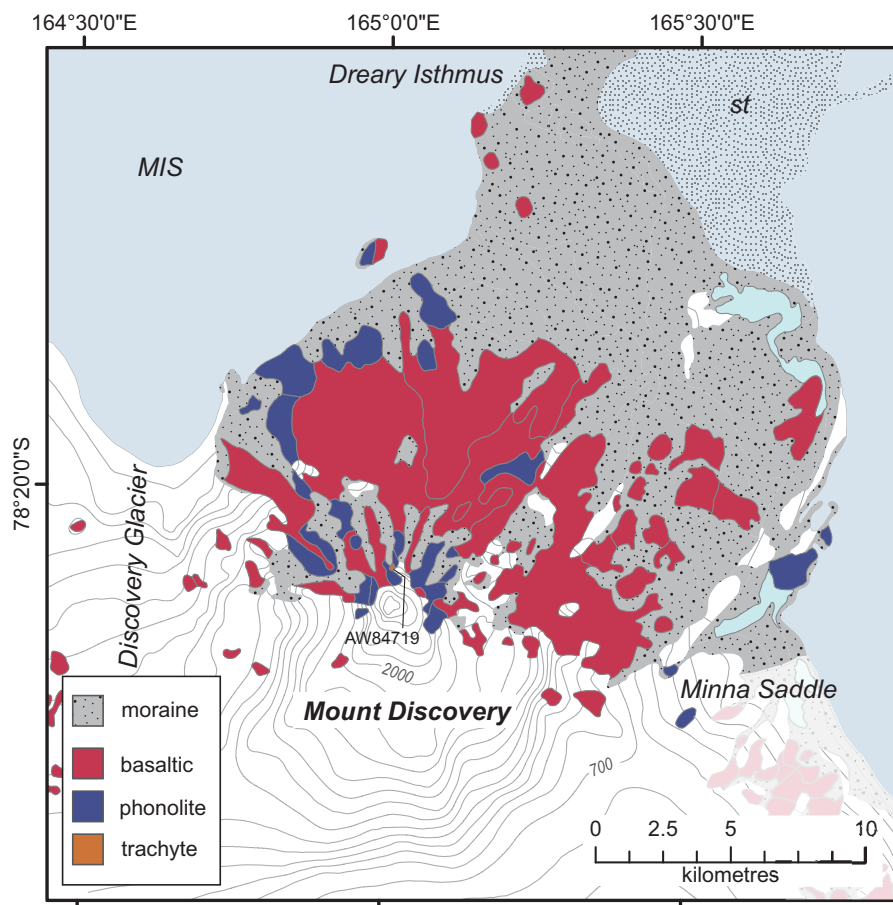


**Fig. 14.** Map of Mount Discovery showing volcanic rock outcrops and key topographical features. The pattern on the McMurdo Ice Shelf (MIS) indicates supraglacial till (st). A rock outcrop with a trachyte composition is linked to sample AW84719 (see the Supplementary material (ESM1))

**Minna Bluff.** Known first as ‘The Bluff’, and later named after the wife of the president of the Royal Geographical Society during the 1901–04 British National Antarctic Expedition (Scott 1907), Minna Bluff is a 45 km-long, southeasterly-trending rock outcrop that ends in a distinct hook (Minna Hook; Fig. 15). Minna Bluff had been visited by S.B. Treeves in the 1960s, with only two of the collected samples being analysed in the 1970s (Goldich *et al.* 1975; Kyle 1976). Wright-Grassham spent 17 days at Minna Bluff in the 1980s, resulting in a thesis and two short publications (Wright *et al.* 1983; Wright-Grassham 1987; Wright and Kyle 1990d). In the 2000s, a further two field seasons of research were undertaken, leading to several theses (Scanlan 2008; Fargo 2009; Antibus 2012; Ross 2014; Redner 2016), abstracts and publications (Fargo *et al.* 2008; Panter *et al.* 2011; Wilch *et al.* 2011a, b; Ross *et al.* 2012b; Antibus *et al.* 2014).

Minna Bluff is made up of coalesced eruptive centres, ranging from small, primitive cinder cones, lava flows and pyroclastic deposits to compositionally evolved domes (Fig. 15). A minimum of four hiatuses separate periods of volcanic activity (Antibus *et al.* 2014). Volcanism occurred between *c.* 12 and 4 Ma (Wright-Grassham 1987; Fargo 2009; Wilch *et al.* 2011a; Antibus *et al.* 2014). Eruptions commenced at Minna Hook (12–8 Ma), with phonolite and tephriphonolite compositions preserved (Wilch *et al.* 2011b) (Fig. 15). Preserved igneous rocks are more mafic and younger (8–4 Ma) to the NW, along Minna Bluff, relative to compositions at Minna Hook.

On a total alkali *v.* silica diagram, analysed rocks form a strongly alkalic, nepheline-normative lineage between basanite and phonolite (Fig. 3b). This lineage can be modelled by the fractional crystallization of olivine + clinopyroxene ± kaersutite for basic compositions and olivine + clinopyroxene + plagioclase + magnetite + apatite for more evolved compositions (Panter *et al.* 2011). Kaersutite and feldspar phenocrysts frequently show disequilibrium textures. Megacrysts are common but mantle xenoliths are rare (Panter *et al.* 2011).

### Mount Morning Volcanic Field

**Mount Morning.** Mount Morning is a poorly dissected shield volcano (Global Volcanism Program 2013b) forming a volcanic island in the Ross Sea (Fig. 16). It was named during the 1901–04 British National Antarctic Expedition (Ferrar 1905; Fletcher and Bell 1907; Scott 1907) after the relief ship *SY Morning*. Much of the ice-free exposure occurs in two lines on the northern flanks of the mountain, the westerly Riviera Ridge and the easterly Hurricane Ridge, separated by the Vereyken Glacier (Fig. 16). A summit caldera is elongated NW–SE, with axes 4.9 and 4.1 km in length (Paulsen and Wilson 2009). The radius of the volcanic edifice is at least 25 km from the summit caldera to furthest exposed outcrop (Fig. 16), making the volume approximately 1785 km<sup>3</sup>, comparable to the volume of Mount Terror. At least 50, morphologically youthful, mafic flank vents occur on the northern slopes (Martin 2009).

Petrological investigations were conducted at a reconnaissance level on Mount Morning in the mid-part of the last century during brief field visits or as part of regional data compilations (e.g. LeMasurier and Wade 1968; Treves 1968, 1977; Kyle and Cole 1974; Goldich *et al.* 1975; Sun and Hanson 1975; Polyakov *et al.* 1976; Armstrong 1978; Stuckless *et al.* 1981; Stuiver and Brazian 1985). In the 1970s and early 1980s, more detailed, thesis-based investigations were carried out (Kyle 1976; Kyle and Muncy 1978, 1983, 1989; Muncy 1979; Wright *et al.* 1986; Wright-Grassham 1987), and again in the 2000s (Sullivan 2006; van Woerden 2006; Paulsen 2008; Martin 2009). Remote sensing of elongated craters, and dating of young volcanic centres, were also carried out in the 2000s (Paulsen 2002; Csatho *et al.* 2005; Paulsen and Wilson 2007, 2009). Palaeomagnetic studies have also been undertaken at Mount Morning (Mankinen and Cox 1988; Tauxe *et al.* 2004).

Mount Morning varies compositionally between basanite-phonolite and basanite-trachyte. The volcanic rocks are porphyritic with phenocrysts 0.5–4 mm in diameter in a fine

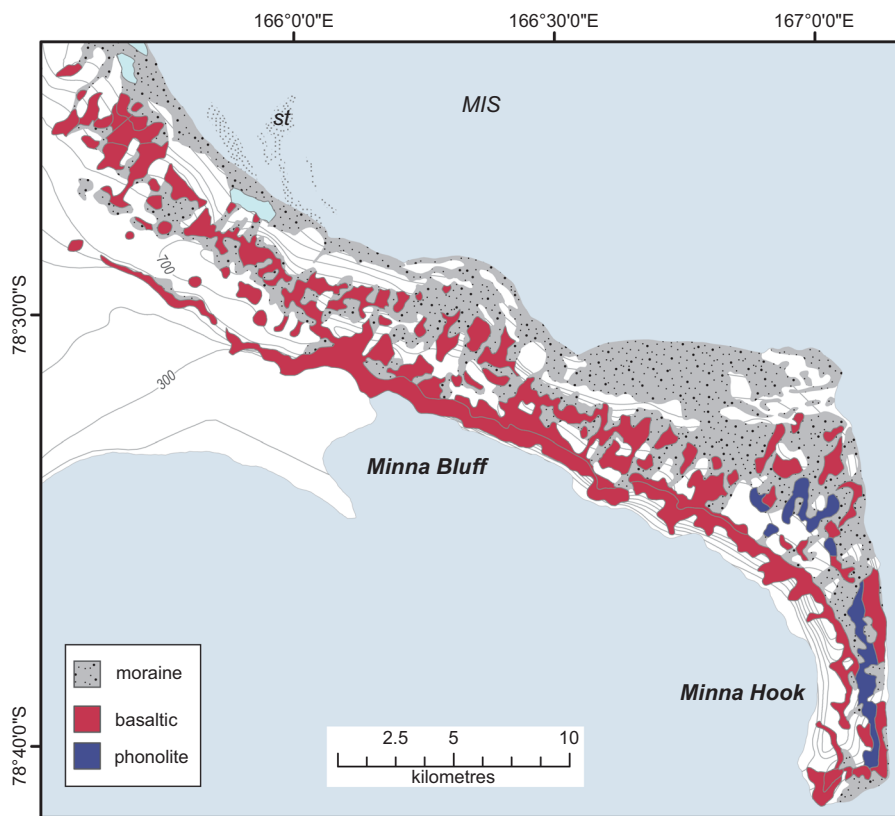


**Fig. 15.** Map of Minna Bluff showing volcanic rock outcrops and key topographical features. The pattern on the McMurdo Ice Shelf (MIS) indicates supraglacial till (st).

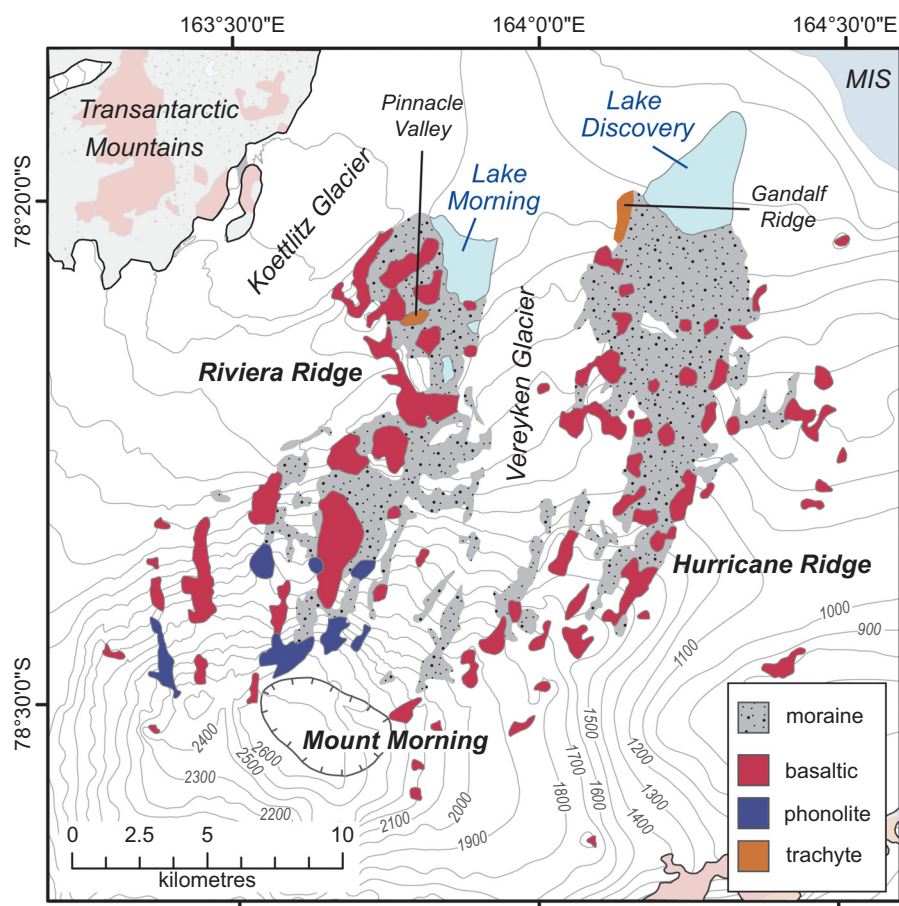


**Fig. 16.** Map of Mount Morning showing volcanic rock outcrops and key topographical features. The summit caldera is shown by the ticked black line. MIS, McMurdo Ice Shelf.

(0.05 mm) to very fine (<0.05 mm) groundmass. Most volcanic rocks are also poorly vesicular to non-vesicular. Detailed petrographical descriptions are available in a number of these (Muncy 1979; Wright-Grassham 1987; Sullivan 2006; van Woerden 2006; Martin 2009), and this information is summarized in Martin *et al.* (2013). Volcanism at Mount Morning has been assigned to two geochemically and chronologically distinct lineages (Kyle 1976; Muncy 1979; Wright-Grassham 1987; Wright and Kyle 1990; Martin 2009), termed by Martin *et al.* (2013) the Mason Spur and Riviera Ridge lineages.

Mason Spur Lineage rocks are preserved at two localities on the lower slopes of Mount Morning (Pinnacle Valley and Gandalf Ridge; Fig. 16). Igneous rocks of this lineage were mostly erupted between  $18.7 \pm 3$  and  $13.0 \pm 0.3$  Ma (Wright-Grassham 1987; Kyle and Muncy 1989; Martin *et al.* 2010). Radiometric dates from volcanic ash layers as old as 24.98 Ma in Cape Roberts drill hole 2/2A (McIntosh 2000) are most probably derived from the Erebus Volcanic Province (Smellie 2002) and logically assigned to the oldest, known, eruptive centre, Mount Morning (Smellie 1998). Pinnacle Valley and Gandalf Ridge might be isolated volcanic centres but a more extensive footprint of Mason Spur Lineage magmatism has been proposed based on the widespread occurrence of Mason Spur Lineage-like trachyte and syenite xenoliths across the exposed, volcanic edifice (Martin *et al.* 2010). The lineage includes both quartz- and nepheline-normative rock types, and all analysed rocks are mildly alkalic (following the Saggerson and Williams 1964 definition). On a total alkali v. silica diagram, most data for analysed rocks lie within an array between tephrite and trachyte (Fig. 3c), and this can be modelled by fractional crystallization involving diopside + nepheline  $\pm$  olivine  $\pm$  magnetite/ilmenite. A second, quartz-normative lineage of mugearite to trachyte/rhyolite can be modelled in terms of fractional crystallization of plagioclase + diopside  $\pm$

magnetite/ilmenite  $\pm$  apatite, with silica oversaturation being related to wall-rock assimilation (Martin *et al.* 2013). Several of the whole-rock compositions are comenditic (Kyle and Muncy 1989; Martin 2009).

Ninety per cent of the outcrop on Mount Morning comprises rocks assigned to the Riviera Ridge Lineage (Fig. 16). These were erupted from at least  $5.05 \pm 0.04$  to  $0.06 \pm 0.08$  Ma (Polyakov *et al.* 1976; Armstrong 1978; Wright-Grassham 1987; Tauxe *et al.* 2004; Paulsen and Wilson 2009; Martin *et al.* 2010). The youngest radiometric age determinations have analytical errors that overlap with the present day, and Martin *et al.* (2010) considered Mount Morning to be dormant rather than extinct. Relative to Mason Spur Lineage rocks, Riviera Ridge Lineage rocks are younger, strongly alkalic and always nepheline-normative. On a total alkali v. silica diagram, analysed samples form an array between basanite and phonolite (Fig. 3c), and this can be modelled by fractional crystallization involving diopside + plagioclase + olivine + magnetite/ilmenite for basic compositions and plagioclase + diopside + aegirine + nepheline + ilmenite/magnetite  $\pm$  apatite  $\pm$  kaersutite for felsic compositions (Martin *et al.* 2013). Mafic rocks of the Riviera Ridge Lineage contain abundant mantle and crustal xenoliths (Kyle *et al.* 1987; Martin *et al.* 2014a, b, 2015a, b).

**Mason Spur.** Mason Spur was named in 1963 after a serving United States Antarctic Research Programme representative, Robert W. Mason. It is a NE-trending, c. 10 km-long linear bluff up to 1300 m above sea-level, with rock exposure in mainly SW- to SE-facing cliffs and along cliff tops (Fig. 17). It was first visited in the 1980s by Wright-Grassham, with petrographical descriptions and chemical and chronological results published in a thesis and short communications

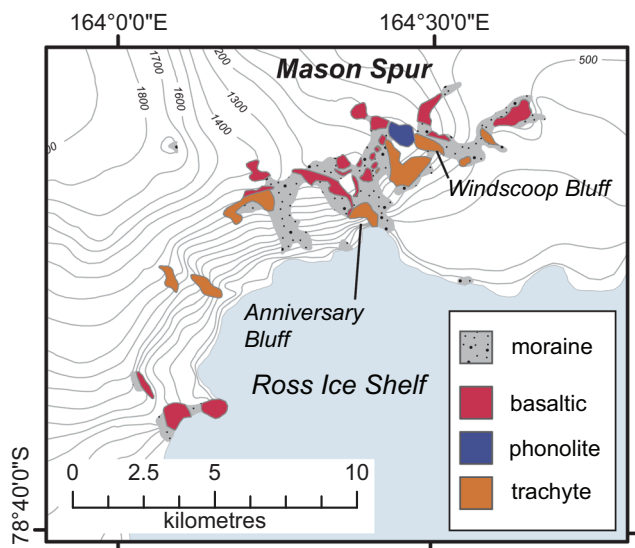


Fig. 17. Map of Mason Spur showing volcanic rock outcrops and key topographical features, adapted from Cox *et al.* (2012) and Martin *et al.* (2018).

(Wright *et al.* 1984, 1986; Wright-Grassham 1987; Wright and Kyle 1990f). It was visited by Martin and others in 2005 and again in 2016, resulting in a thesis and publications (Martin 2009; Martin *et al.* 2010, 2013, 2018). Mason Spur is a separate volcanic centre from Mount Morning (cf. Martin *et al.* 2010), as originally proposed by Wright-Grassham (1987) and shown by recent fieldwork. The two lineages identified at Mount Morning are also present at Mason Spur (Wright-Grassham 1987; Martin 2009).

The lowermost, and volumetrically dominant, volcanic suite, referred to here as the Mason Spur Lineage, is part of a complex intra-caldera sequence of pyroclastic deposits and cross-cutting intrusions. These rocks were emplaced between  $12.9 \pm 0.1$  and  $11.4 \pm 0.1$  Ma (Wright-Grassham 1987; Martin *et al.* 2010). The preserved rocks, which form a lineage with compositions between tephrite and trachyte, range from quartz- to nepheline-normative and all are mildly alkalic (Saggerson and Williams 1964) (Fig. 3c). Fractional crystallization can be modelled by either diopside + nepheline  $\pm$  olivine  $\pm$  magnetite/ilmenite or plagioclase + diopside  $\pm$  magnetite/ilmenite  $\pm$  apatite for nepheline- or quartz-normative lineages, respectively (Martin *et al.* 2013). Aenigmatite and aegirine augite are present in the groundmass of the most evolved trachyte rocks. Overlying the Mason Spur Lineage sequence are younger rocks (6 Ma to near present day) comparable with the Riviera Ridge Lineage of Mount Morning, and consisting of felsic lava domes and mafic scoria cones. The youngest dated material has ages that overlap with present day, and, like Mount Morning, Mason Spur may be dormant (cf. extinct). These rocks form a lineage between basanite and phonolite that is compatible with fractionation of diopside + plagioclase + olivine + magnetite/ilmenite for basic compositions and plagioclase + diopside + aegirine + nepheline + magnetite/ilmenite  $\pm$  apatite  $\pm$  kaersutite for felsic compositions (Martin *et al.* 2013).

#### Southern Local Suite

Throughout southern Victoria Land, in the foothills of the Transantarctic Mountains (Fig. 18), numerous small basaltic scoria cones pepper the landscape and vary in composition from basanite to alkali basalt. More than 50 small centres, up to 1 km across and 300 m high, are found in the foothills

of the Royal Society Range or around the Taylor and Wright valleys, and these vary in age from at least Mid-Miocene to early Pleistocene (Armstrong 1978; Wright 1979a, b, c, d; Wright and Kyle 1990a, b; Tauxe *et al.* 2004; Cox *et al.* 2012), although Holocene ages have been indicated from some unpublished ages obtained by the K–Ar method (Wright and Kyle 1990a). The earliest geological investigations were made here during the heroic era (Ferrar 1907; Prior 1907; Mawson 1916; Smith 1954). Further expeditions were made around the time of the International Geophysical Year programme (the third Polar Year), including the Commonwealth Trans-Antarctic Expedition of 1955–58, resulting in the geological maps of Gunn and Warren (1962). The area was again visited by geologists during the early 1960s (Blank *et al.* 1963; Haskell *et al.* 1965), and by geologists from the Geological Survey of New Zealand in the late 1970s (Wright 1979c, d). Research on the Southern Local Suite rocks has also been undertaken on specific vents, and the xenoliths hosted in the volcanic rocks, at various other times over the past 40 years (e.g. McIver and Gevers 1970; Gamble and Kyle 1987; McGibbon 1991; Wingrove 2005) but a synthesis of the Southern Local Suite has not yet been published.

In the majority of cases, the cones are eroded and the products pyroclastic, with deposits of poorly stratified scoria and agglutinate to rarely preserved hyaloclastite and lava flows (Blank *et al.* 1963; Haskell *et al.* 1965; Skinner *et al.* 1976; Keys *et al.* 1977; Wright 1980; Wright and Kyle 1990a, b). Accordingly, they can be regarded as monogenetic scoria cones, with relatively short life cycles. In this subsection, a number of occurrences are described that can be considered to be generally representative. The rocks are typically porphyritic, with phenocryst assemblages dominated by olivine and clinopyroxene but with plagioclase  $\pm$  Fe–Ti oxides and sometimes Ti-amphibole megacrysts (kaersutite). Xenoliths are common, ranging from lithospheric mantle spinel lherzolite, harzburgite and dunite to lower-crustal granulites and metagabbros (McIver and Gevers 1970; Kirsch 1981; Kyle *et al.* 1987). Foster Crater hosts a unique and unusual phlogopite-bearing pyroxenite that varies from coarse-grained granoblastic to fine-grained mylonitic and porphyroclastic in texture (Gamble *et al.* 1988). Shallow crustal granitoids and meta-sediments, all sintered and partially fused, are also present but less common. The crust throughout this region generally comprises basement of Neoproterozoic–early Cambrian and Ordovician metasedimentary rocks, including quartzites, schists and marbles, intruded by predominantly granitoid plutons of the Granite Harbour Intrusive Complex and unconformably overlain by Permian–Triassic low-grade metasandstone, shales and coal measures of the Beacon Supergroup. These were followed by intrusions and localized lava flows of the Ferrar–Kirkpatrick Large Igneous Province (Cox *et al.* 2012).

*Foster Crater.* This crater is situated on the northern side of the Koettlitz Glacier, about 110 km south of Ross Island. It consists largely of poorly stratified, highly oxidized agglutinate and scoria, with abundant xenoliths ranging from mantle peridotite, lower-crustal gabbros and pyroxenites (Gamble and Kyle 1987; Gamble *et al.* 1988).

*Hooper Crags.* Hooper Crags are isolated outcrops towards the head of the Koettlitz Glacier. The exposures are sparse and appear to be remnants of a lava flow that contains xenoliths of peridotite.

*Pipecleaner Glacier.* Pipecleaner Glacier, Roaring Valley and Radian Glacier are about 10–15 km north of Foster Crater, in a region that was mapped in detail by Worley and others during the Otago University basement study project

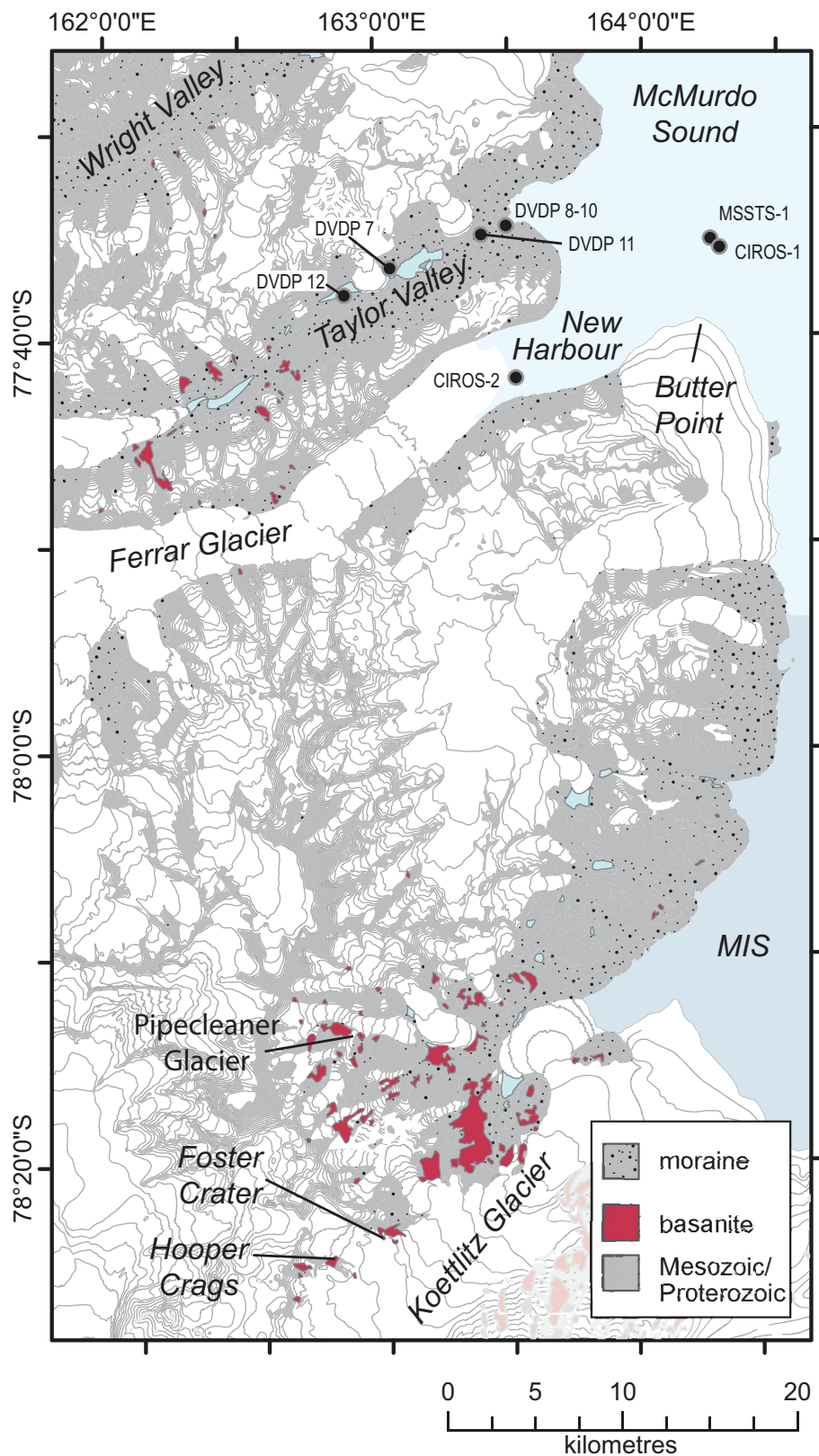


**Fig. 18.** Map of the Southern Local Suite showing volcanic rock outcrops and key topographical features. MIS, McMurdo Ice Shelf. Mesozoic, rock types older than the Erebus Volcanic Province rocks and part of the Transantarctic Mountains.

(Worley 1992; Worley *et al.* 1995). In this area there are a number of basaltic outcrops, mostly comprising pyroclastic material but with rare lava flows, both containing abundant peridotite xenoliths.

*Subsurface volcanic rocks of the Erebus Volcanic Province recovered by onshore drilling.* The DVDP drilled at 14

onshore sites (Figs 1, 9 & 18) between 1973 and 1975. The onshore DVDP (1973) holes 1–3 are discussed in the earlier ‘Hut Point Peninsula’ subsection. In the Wright Valley, DVDP holes 4, 4A, 5, 5A, 13 and 14 were drilled. No Erebus Volcanic Province material is reported in holes 4, 4A, 5 or 5A (Cartwright *et al.* 1974a, b) but basaltic fragments, probably sourced from the Erebus Volcanic Province, are reported in DVDP 13 (Mudrey *et al.* 1975) and DVDP 14 (Chapman-

## Erebus Volcanic Province: petrology

Smith 1975b). In Victoria Valley, hole DVDP 6 penetrated *c.* 10 m of sediment and *c.* 296 m of basement lithologies, with no Erebus Volcanic Material being reported in the sedimentary section (Kurasawa *et al.* 1974).

Holes DVDP 7–12 were drilled in the Taylor Valley. Drill holes DVDP 8 (*c.* 156 m deep) and 10 (*c.* 185 m deep) intersected 185 m of sediment and were sited near the shore of New Harbour (Porter and Beget 1981). Drill hole DVDP 11 (*c.* 330 m deep) was sited 3 km further inland up Taylor Valley. A major lithological change occurs at *c.* 154 m in cores 8 and 10, and at *c.* 185 m in core 11. Above these levels, volcanic clasts of the Erebus Volcanic Province are common but are entirely absent from sections below this interval (Porter and Beget 1981). This lithological change coincides with an unconformity recognized from palaeontological and palaeomagnetic evidence (Porter and Beget 1981). Drill hole DVDP 9 is only *c.* 39 m deep, and was drilled adjacent to holes 8 and 10 near the head of New Harbour. Drill hole DVDP 9 contained *c.* 20–30% clasts of Erebus Volcanic Province affinity (Porter and Beget 1981). Drill hole DVDP 7 reached a depth of only 11 m and was drilled some 7 km inland from the mouth of Taylor Valley (Harris and Mudrey 1974). Drill hole DVDP 12 (185 m depth) drilled 165 m of sediments with volcanic lithic fragments recorded throughout the sedimentary section (Chapman-Smith 1975a), these are most likely to be sourced from Erebus Volcanic Province rocks.

*Subsurface volcanic rocks of the Erebus Volcanic Province recovered by offshore drilling.* Over the past five decades drilling projects have recovered subsurface cores from within the Erebus Volcanic Province and the Ross Sea region (Figs 1 & 19). In chronological order these projects comprise: the McMurdo Sound Sediment and Tectonic Study (MSSTS: 1971); DVDP (1975); Cenozoic Investigations into the western Ross Sea (CIROS: 1980s); the CRP (late 1990s); and

ANDRILL (2000s). Cores were also recovered in 1973 during drilling associated with legs 270–273 of the Deep Sea Drilling Project in the Ross Sea but although mention is made of basaltic and doleritic clasts in the cored sediments these are not described in any detail.

*McMurdo Sound Sediment and Tectonic Study core MSSTS-1.* The stratigraphy and sedimentology of the MSSTS-1 core was described in detail by Barrett and McKelvey (1986). The core was taken 12 km off the Victoria Land coast (Fig. 1) in a water depth of 195 m. Core was recovered to a depth of 227 m, and it comprised a sequence of mudstones and sandstones with intercalated limestone and diamictite units. Examination of the sand fraction of the core indicated that basaltic debris occurs at a depth of 60 m in sediments with an age estimated to be around 21 Ma (Early Miocene) and continues with one short hiatus to the top of the hole. Basaltic pebbles found at a depth of 213 m were described by Gamble *et al.* (1986) who concluded that they were alkalic basalts with petrological affinities to the volcanic rocks of the Erebus Volcanic Province. Two pebbles dated by the K/Ar method gave ages of  $24.3 \pm 2$  and  $13.7 \pm 4$  Ma but palaeomagnetic and palaeontological information indicates a probable age of 30 Ma for the unit in which the pebbles are contained.

*Dry Valley Drilling Project (DVDP).* In 1975, DVDP 15 (Fig. 1) was drilled in 122 m water depth with 52% recovery of a total 61.6 m section cored (penetration depth 65 m: Barrett *et al.* 1976). The top 13 m of the core (unit 1) is fine to coarse sand, with the bottom 13–65 m of the core (unit 2) consisting of fine to medium sand (Barrett and Treves 1981). Petrography shows 65–80% of the sampled intervals are made up of basaltic material derived from the Erebus Volcanic Province (Barrett and Treves 1981). Barrett and Treves (1981) interpreted the recovered sections to be Pliocene–Pleistocene in age.

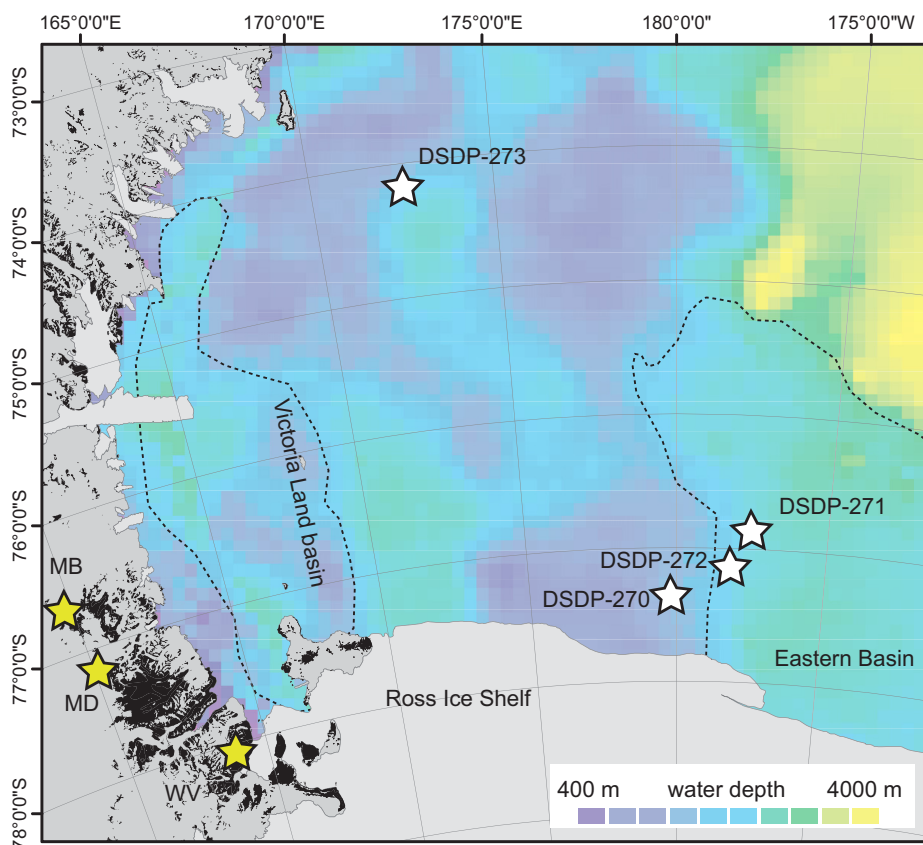


**Fig. 19.** Regional-scale image of Victoria Land showing the location of englacal tephra deposits (yellow stars) and Deep Sea Drilling Project (DSDP) legs 270–273 drill holes (white stars). The approximate position of the Victoria Land Basin is shown. The bathymetry is shown for reference, with warmer colours indicating shallower water depths (*c.* 100–4000 m). The filled black polygons are rock outcrops. MD, Mount De Wit; MB, Manhaul Bay; WV, Ward Valley.

*Cenozoic Investigations into the western Ross Sea (CIROS)*. The 'Cenozoic Investigations into the western Ross Sea' (CIROS) Project drilled two holes in New Harbour (Fig. 18) in McMurdo Sound (Fig. 1) in the southern summer seasons of 1984–85 and 1986–87. CIROS-1 was located 12 km off Butter Point, in *c.* 200 m of water. CIROS-2 was located 1.2 km from the snout of the Ferrar Glacier tongue in 211 m of water. The geology of CIROS-1 is comprehensively described in a New Zealand DSIR Bulletin (Barrett 1989). The hole intersected glacial deposits comprising, in order of abundance, diamictites, sandstones, mudstones, and conglomerates and breccias, with the hole terminating at a depth of 702 m in basement gneiss (Hambrey *et al.* 1989). Fossil, palaeomagnetic and isotopic evidence indicates an age for the sequence of Early Oligocene–Early Miocene with two periods of deposition dated at 36–34.5 Ma and *c.* 30.5–22 Ma, respectively (synthesis of Barrett 1989). Dolerite boulders found in the basal units of the cored sequence are from the Ferrar Supergroup (Grapes *et al.* 1989) and grains of this material also occur in the upper 200 m of the section (George 1989).

Basaltic clasts believed to have derived from the Mount Morning and Mount Discovery eruptive centres in the Erebus Volcanic Province occur throughout the cored section and become more abundant near the top (George 1989). These are porphyritic, fine-grained basalts containing phenocrysts of clinopyroxene, plagioclase, olivine and rare amphibole in groundmass consisting of plagioclase, clinopyroxene, iron oxide and glass. There are no whole-rock geochemical data available for CIROS basaltic grains but George (1989) presented clinopyroxenes analyses from basaltic clasts in sediments recovered from the uppermost part of the section.

CIROS-2 cored through 165.5 m of glacial sediments into basement gneiss. Two sequences were identified in the core: a Pliocene lower sequence dominated by diamictites with intercalated mudstones; and a Pleistocene upper sequence of alternating sandstones and diamictites (Barrett and Hambrey 1992). The clast lithologies have been described by Sandroni and Talarico (2006). The clasts in the Pliocene sequence are predominantly Paleozoic basement granitic rocks but a basal 13 m-thick diamictite is dominated by clasts of Cenozoic Erebus Volcanic Province rocks that are considered to have derived from the Mount Morning and/or Mount Discovery eruptive centres. The abundance of this volcanic clast component declines throughout the sequence into the Pleistocene section. Ferrar gabbro and dolerite clasts are minor components occurring throughout the core. Basalt clasts of Erebus Volcanic Province affinity are fine grained, vesicular and porphyritic with phenocrysts of clinopyroxene, plagioclase, and rare amphibole and alkali feldspar in a fine groundmass of plagioclase, clinopyroxene, titanomagnetite and, in some cases, glass. Plagioclase and clinopyroxene grains were analysed in one basalt sample (Sandroni and Talarico 2006).

*The Cape Roberts Project (CRP)*. The CRP was named after its location near Cape Roberts, in the Ross Sea, 125 km NW of McMurdo Station and Scott Base (Fig. 1). The project was an international joint venture involving researchers from New Zealand, Australia, the UK, Germany, Italy and the USA. Three holes were drilled during the period 1997–99 and collectively they recovered around 1500 m of core, and drilled into strata with maximum ages of between 34 and 17 Ma. Initial reports on all three holes were published as collections of papers in the journal *Terra Antarctica*.

The CRP-1 hole was located 16 km from Cape Roberts in water 150 m deep. The details of stratigraphy, age and lithology were described by Barrett *et al.* (1998). The hole was drilled to a depth of 148 m and the stratigraphy was divided into two sections: an upper unconsolidated Quaternary section

comprising shallow-marine diamictites, sandstones and mudstones dated at 1.8–1.25 Ma ( $^{40}\text{Ar}/^{39}\text{Ar}$  age of  $1.2 \pm 0.1$  Ma at 33 m: McIntosh 1998); and a Miocene section composed of sandstones, siltstones, diamictites and breccias with ages ranging from 22.4 to 17.5 Ma ( $^{40}\text{Ar}/^{39}\text{Ar}$  ages of  $19.73 \pm 0.86$ – $17.15 \pm 0.80$  Ma for the interval 114–61 m: McIntosh 1998).

Throughout the core, the larger clasts are granitic and metamorphic rocks derived from the Paleozoic basement or dolerites of the Ferrar Group but in the sand and finer fractions, particularly in the Quaternary section and the upper part of the Miocene sequence, volcanic material is abundant. This component, which includes volcanic rock fragments, volcanic glass and a wide range of alkalic indicator minerals, is from the Erebus Volcanic Province. In the Quaternary section, lithic grains include tuff and lava fragments, and the mineral grains of volcanic provenance include olivine, clinopyroxene and feldspar. Glass is abundant. Olivine has not been identified in the Miocene section but minerals associated with alkalic volcanism are common. These include titanite, aegirine, kaersutite and aenigmatite. Brown volcanic glass occurs throughout the Miocene section but it becomes much more abundant in the upper 30–40 m.

Holes CRP-2 and CRP-2A were drilled in 1998, 14.2 km from Cape Roberts, in 178 m of water. CRP-2 was cored to 57 m and CRP-2A to 624 m, with the hole transecting a section with an age range estimated at 33–19 Ma (Fielding *et al.* 1999; Wilson *et al.* 2000). Pliocene and Quaternary sediments in the upper part of the cores are unconsolidated diamictite containing clasts of Paleozoic granitic rocks, Ferrar Dolerite, quartz, feldspar and volcanic rock. Volcanic glass is abundant in the silt and sand fraction of the Pleistocene and Quaternary sections of the cores. The pre-Pliocene section comprises fine- to medium-grained sands, silts and muds, diamictite and conglomerate.

Volcanic clasts and mineral grains derived from the Erebus Volcanic Province are common in the cores, particularly in the upper part of the pre-Pliocene section. The clasts range in size up to 5 cm, and rock types include basalt, intermediate alkalic lava flows (hawaiite and mugearite), trachyte and syenite. Of significance are tephra units, interpreted to represent air-fall material deposited through water. The thickest of these was intersected at a depth of 111 m and is 1.22 m thick (Fielding *et al.* 1999). Feldspars from this unit have been dated by the  $^{40}\text{Ar}/^{39}\text{Ar}$  method and they give a mean age of  $21.44 \pm 0.05$  Ma. Grain size in the tephra units varies from <1 up to 10 mm, and are composed of pumice and brown glass with scattered crystals of alkali feldspar, aegirine–augite and sodic amphibole (Fielding *et al.* 1999). A rhyolitic clast from 294 m depth has yielded a sanidine single-crystal  $^{40}\text{Ar}/^{39}\text{Ar}$  laser-fusion radiometric age of  $24.98 \pm 0.08$  Ma (McIntosh 2000).

Drill hole CRP-3, which was drilled in 1999, 12 km from Cape Roberts in 295 m of water was the deepest of the three Cape Roberts project holes. The hole reached a depth of 939 m with the last 116 m being in basement rocks of the Beacon Supergroup. The cored section was through Oligocene diamictites, conglomerates, sandstones and mudstones (Barrett *et al.* 2000). The base of the Cenozoic section, immediately above basement, could be latest Eocene in age (34 Ma). Clasts in the sequence include dolerite, and sedimentary, granitic, metamorphic and volcanic lithologies. Pompilio *et al.* (2001) examined the petrography, mineralogy, and whole-rock and mineral chemistry of volcanic and subvolcanic clasts and concluded that these were derived exclusively from rocks of the Ferrar Supergroup (see also Barrett *et al.* 2000). In contrast to the younger sequences of drill holes CRP-1, CRP-2 and CRP-2A, Erebus Volcanic Province volcanic material does not appear to be present in CRP-3.

*The Antarctic Drilling Project (ANDRILL).* The Antarctic drilling project (ANDRILL) is a multinational, cooperative research programme involving scientists from Brazil, Germany, Japan, Italy, New Zealand, the Republic of Korea, the UK and the USA. The objective of the project is to build on the outcomes of the Cape Roberts Project and to use similar deep drilling technology to core back in time through the Cenozoic and recent geological record beneath Antarctica. The information is intended to be used primarily to understand palaeoclimate and climate change. The first two holes (Fig. 1), designated the McMurdo Ice Shelf (MIS) and Southern McMurdo Sound (SMS) projects, were completed in the 2006–07 and 2007–08 austral summers, respectively.

Hole MIS (AND-1B) was located in Windless Bight, in McMurdo Sound, 10 km from Scott Base and McMurdo Station, in water 870 m deep. The sedimentology and stratigraphy of the core are described in detail by *Krissek et al. (2007)*. Around 1285 m of core were recovered, and this included diamictite, sandstone, mudstone and volcanic ash or tuff. Volcanic material from the Erebus Volcanic Province occurs throughout the cored section, with volcanic clasts representing *c.* 70% of the total clast population (*Pompilio et al. 2007*). Eight volcanic lithostratigraphic units were recognized (*Pompilio et al. 2007*), and clasts and whole-rock samples from these have been dated by the  $^{40}\text{Ar}/^{39}\text{Ar}$  method (*Ross et al. 2012a*). Basalt clasts from *c.* 17 m depth have an age of  $0.310 \pm 0.039$  Ma. Near the top of the section (*c.* 85–86 m depth) is a phonolitic pumice, which has been dated at  $1.014 \pm 0.008$  Ma. This has no known correlatives onshore. Basaltic clasts from a sequence of black volcanic sands at 112–145 m give an age of  $1.633 \pm 0.057$  Ma, and this sequence is interpreted to have derived from subaerial Strombolian- or Hawaiian-style eruptions. A thick volcanic sequence in the middle of the core includes a phonolitic lava flow (646–649 m) with an age of  $4.800 \pm 0.076$  Ma. The lava flow and the associated volcanic sequence are interpreted to have come from a submarine vent. Near the base of the sequence is a unit comprising altered tuffs, and a volcanic clast from this part of the core (1280 m depth) has been dated at  $13.57 \pm 0.13$  Ma.

The petrology and geochemistry of clasts in the MIS (AND-1B) core have been described by *Pompilio et al. (2007)*, who classified volcanic rocks as mafic (basaltic), intermediate or felsic. Basalts have phenocrysts of olivine and clinopyroxene  $\pm$  plagioclase. The phenocryst assemblages in intermediate rocks include plagioclase and clinopyroxene  $\pm$  kaersutite, and in felsic rocks the phenocrysts are K-feldspar  $\pm$  kaersutite  $\pm$  aegirine. In all rocks the groundmass is generally glassy, cryptocrystalline or very fine grained. Glasses in samples from throughout the sequence were analysed by EPM (*Pompilio et al. 2007*), and these have compositions varying from basanite, through phonotephrite and tephriphonolite to phonolite and trachyte (classification of *Le Bas et al. 1986*).

The SMS (AND-2A) hole was located in McMurdo Sound, 13 km from the Dailey Islands, 50 km NW of the Hut Point Peninsula on Ross Island (Fig. 1), in water 384 m deep. About 1139 m of core were recovered and the stratigraphy has been subdivided into 14 lithostratigraphic units (*Fielding et al. 2008*) representing 74 glacial marine sequences (*Fielding et al. 2011*). Lithologies recovered included diamictites, conglomerates, breccias, sandstones, mudstones and diatomites, as well as volcanic rocks including lava flows, pyroclastic material and volcanic sedimentary units (*Fielding et al. 2008*). In nine of the 14 lithostratigraphic units, 50% of the clasts are interpreted to be of volcanic origin. *Di Roberto et al. (2012)* studied 27 volcanoclastic units over virtually the full length of the core (37–1139 m) and classified these as pyroclastic fall, resedimented volcanic and volcanic sedimentary deposits.

*Di Vincenzo et al. (2010)* carried out  $^{40}\text{Ar}/^{39}\text{Ar}$  dating on 17 volcanic samples from the core, and 10 of these analyses gave statistically robust ages. Basanite and phonolite clasts from the top of the core (<10 m) gave apparent ages of  $0.662 \pm 0.042$  and  $0.124 \pm 0.014$  Ma, respectively. Samples from the Middle Miocene section, taken between 128 and 358 m, were mainly mafic compositions and they gave ages of between approximately 16 and 11.5 Ma. Most of the samples dated in the Early Miocene section of the core (depths >358 m) were felsic and they gave ages ranging from approximately 20.1 to 16.0 Ma. These ages are in reasonable agreement with those obtained by *Nyland et al. (2013)* for glasses from the 354–765 m section of the core (19.3–15.1 Ma).

The petrology and geochemistry of volcanic clasts are described by *Panter et al. (2008)*. Mafic compositions have phenocrysts of clinopyroxene + olivine  $\pm$  plagioclase in glassy or fine-grained groundmasses of plagioclase and clinopyroxene. In intermediate rock types, the phenocrysts are plagioclase  $\pm$  clinopyroxene  $\pm$  amphibole and in felsic compositions the phenocryst assemblage is dominated by K-feldspar.

A number of studies have included analyses of SMS (AND-2A) volcanic rocks and glasses. *Panter et al. (2008)* used X-ray fluorescence (XRF) spectrometric analysis to obtain the whole-rock major element compositions of 20 volcanic clasts from lithostratigraphic units in the upper 760 m of the core. They also reported the results of continuous XRF major element scans through sections of the core and they used EPM to determine the compositions of volcanic glass shards in one of the units (lithostratigraphic unit 10: 649–778 m). Whole-rock compositions vary from mafic (basalt and basanite) through intermediate (phonotephrite, tephriphonolite and trachyandesite) to felsic (phonolite, trachyte and rare rhyolite). Glasses in lithostratigraphic unit 10 are predominantly basanitic with a few phonotephrites and basalts (classification of *Le Bas et al. 1986*).

*Del Carlo et al. (2009)* studied the uppermost 37 m of the core (lithostratigraphic unit 1), which contain the highest proportion of volcanic material of any of the units in the section. Mixed, near primary, volcanic clasts predominate in this lithostratigraphic unit with a minor amount of Paleozoic basement material in the clast population. Volcanic material originated in explosive submarine eruptions. Eleven samples were analysed for whole-rock major element composition and seven of these classify as basanites, with one each of basalt, trachybasalt, phonolite and trachyte. Glasses are predominantly basanitic.

Major and trace element analyses were carried out on SMS (AND-2A) glass samples by *Nyland et al. (2013)*. Twenty-four glass samples, spaced through the core and covering the interval between 354 and 765 m, were analysed for major element composition by EPM, and 20 of these were also analysed for trace element composition by LA-ICPMS. The glasses analysed are predominantly basanite, trachybasalt and basalt ( $\text{SiO}_2$  in the range 40–52%) but there are also more evolved compositions.

*Onshore and englacial tephra in the Erebus Volcanic Province.* Tephra has been found across Antarctica in blue ice at the margins of ice sheets, and in englacial settings (*Keys et al. 1977; Harpel et al. 2008; Iverson et al. 2014*), ice cores (*Dunbar and Kurbatov 2011; Dunbar et al. 2017; Narcisi et al. 2017*), in marine sediment cores (*Hillenbrand et al. 2008; Ross et al. 2012a*) and in outcrop (*Keys et al. 1977; Cox et al. 2012*). This subsection discusses onshore and englacial tephra, with marine core tephra discussed in the earlier ‘Subsurface volcanic rocks of the Erebus Volcanic Province recovered by offshore drilling’ subsection. Tephra from sources both

within and external to the Erebus Volcanic Province are found in southern Victoria Land (Cox *et al.* 2012).

In the Transantarctic Mountains, tephra deposits are typically <1 m thick, although an example >1 m thick occurs in Ward Valley (Fig. 19). The latter comprises vesicular glass spherules of tephriphonolitic composition and melanocratic volcanic rock fragments (Cox *et al.* 2012). Other Transantarctic Mountain tephra deposits are either *in situ*, disseminated as ash in colluvium and tills, originally water deposited or redeposited debris flows (Cox *et al.* 2012). In the Transantarctic Mountains the tephra are mostly sourced from eruptive centres in the Erebus Volcanic Province (Hall *et al.* 1993; Marchant *et al.* 1996; Lewis *et al.* 2007, 2008). One sample from Mount De Witt has a phonolitic composition and has been dated at  $39 \pm 6$  ka (Harpel *et al.* 2008) and another from Manhaul Bay is also phonolitic in composition. Both samples are emplaced in the Transantarctic Mountains (Fig. 19) but are inferred to be derived from Mount Erebus (Harpel *et al.* 2008; Iverson *et al.* 2014). Other tephra layers in the Transantarctic Mountains dated by K–Ar and Ar–Ar techniques yield ages between 15.5 and 3.9 Ma (Hall *et al.* 1993; Marchant *et al.* 1996; Lewis *et al.* 2007).

The majority of englacial tephra layers exposed on the flanks of Mount Erebus and Mount Terra Nova have phonolitic compositions indicative of eruption from the Mount Erebus volcano. Anorthoclase crystals in one phonolitic Ross Island tephra at ‘Dead Dinosaur Cone’ (Fig. 9) were dated by the  $^{40}\text{Ar}/^{39}\text{Ar}$  method and yielded a preferred plateau age of  $40 \pm 20$  ka (Iverson *et al.* 2014), which overlaps with the Mount De Witt tephra age. Twenty-nine phonolitic tephra layers have glass compositions similar to the matrix glass of bombs erupted from the current lava lake at Mount Erebus, indicating that the major and trace element composition of the magmatic system has remained unchanged for the past c. 40 kyr (Iverson *et al.* 2014). Some tephra layers from the Mount Terra Nova summit have a range of chemical compositions including trachybasalt and trachytic. These non-phonolitic tephra layers are correlated with eruptive centres in the Transantarctic Mountains or as far afield as Marie Byrd Land (Iverson *et al.* 2014).

### Geochemical overview

**Whole rock.** A comprehensive table of whole-rock geochemical, isotopic and geochronological data for the Erebus Volcanic Province is included in the [Supplementary material \(ESM1\)](#). In addition, selected data for bombs erupted during historical eruptions from Mount Erebus, englacial tephra, and drill-hole clast and glass compositions are included for reference. The originally reported compositional data are provided with the original references and, where different analysis types have been reported from the same sample across multiple publications, these have been linked for ease of comparison. Each whole-rock major element composition has been recalculated to 100% anhydrous, with  $\text{Fe}_2\text{O}_3/\text{FeO}$  ratios recalculated following recommendations by Middlemost (1989). The CIPW wt% normative mineralogy has been calculated, along with differentiation index (normative wt% quartz + orthoclase + albite + nepheline + leucite + kalsilite: Thornton and Tuttle 1960) and whole-rock magnesium number (atomic ratio:  $\text{Mg}/(\text{Mg} + \text{Fe}^{2+}) \times 100$ ). New rock names have been applied following the IUGS classification scheme (Le Maitre *et al.* 2002; Verma and Rivera-Gomez 2013). A summary of the type and location of analyses is shown in Table 1.

Patterns in major and trace element whole-rock data v. wt% MgO are evident: for example, wt% CaO,  $\text{TiO}_2$  and FeO,  $\text{CaO}/\text{Al}_2\text{O}_3$  ratios, and ppm Ni are all positively correlated with MgO abundance (Fig. 20), consistent with control by

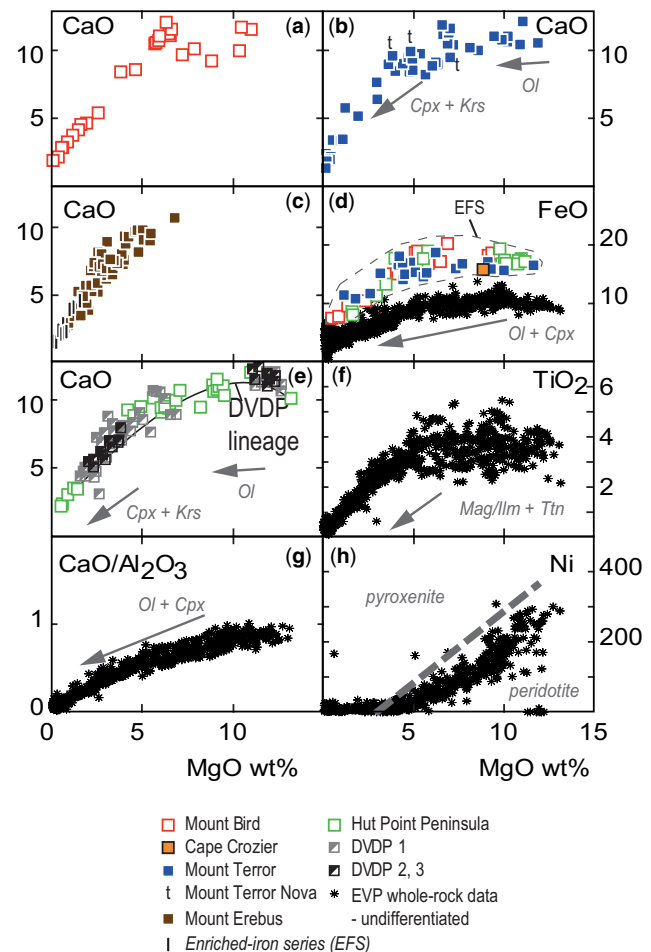


**Fig. 20.** Major element whole-rock data for the Erebus Volcanic Province ( $n = 895$ ) showing wt% MgO v.: (a) wt% CaO Mount Bird data; (b) wt% CaO Mount Terror and Mount Terra Nova data; (c) wt% CaO Mount Erebus data and data from enriched iron series rocks; (d) wt% FeO all Erebus Volcanic Province (asterisks) and enriched iron series data; (e) wt% CaO Hut Point Peninsula outcrop data and Dry Valleys Drilling Project (DVDP) data; (f) wt%  $\text{TiO}_2$  all Erebus Volcanic Province (asterisks) data; (g)  $\text{CaO}/\text{Al}_2\text{O}_3$  all Erebus Volcanic Province (asterisks) data; and (h) Ni (ppm) all Erebus Volcanic Province (asterisks) data. Fractional crystallization control lines (grey arrows) are shown for various minerals. Cpx, clinopyroxene; Mag/Ilm, magnetite or ilmenite; Ol, olivine; Ttn, titanite. The grey dashed curve in (h) separates pyroxenite-derived melts (field above the curves) from peridotite-derived melts (field below the curves) after Sobolev *et al.* (2005). Data (100%; anhydrous) and references are provided in the [Supplementary material \(ESM1\)](#). Iron has been recalculated based on recommendations of Middlemost (1989).

fractional crystallization. For example, on wt% MgO v. CaO plots for mounts Bird, Terror and Erebus, positive correlation is consistent with clinopyroxene and kaersutite fractionation (Fig. 20a–c). On a wt% MgO v. FeO plot, positive correlation is associated with olivine and clinopyroxene fractionation (Fig. 20d). A plot of whole-rock wt% MgO v. CaO abundance (Fig. 20e) can be interpreted to show the magmatic evolution of the Hut Point Peninsula and DVDP igneous rocks. Deeper samples from the DVDP cores are MgO-rich primitive basanites which are probably close to the parental magmas (possibly derived by partial melting of mantle peridotite). Basanites with 7–11 wt% MgO are absent in the DVDP cores but are well represented by the Hut Point Peninsula samples (Fig. 20e). The highly coherent pattern shown in Figure 20e at whole-rock concentrations >5 wt% MgO is consistent with fractional crystallization of olivine + clinopyroxene; whilst at <5 wt%,

## Erebus Volcanic Province: petrology

MgO the pattern is consistent with clinopyroxene + kaersutite fractionation. When combined, analyses of the Hut Point Peninsula and DVDP samples define a petrological lineage from basanite to phonolite, which has been named the DVDP lineage (Figs 3 & 20e). Kyle (1981b) modelled the lineage using fractional crystallization mass-balance models based on EMP analyses of olivine, clinopyroxene, kaersutite, opaque oxides, feldspar and apatite. The models showed excellent agreement with the observed whole-rock chemical compositions of the lava flows, and kaersutite was shown to have an important role in the evolution of the DVDP lineage.

Erebus Volcanic Province rocks are predominantly nepheline normative, although some quartz normative rocks are present (Fig. 21a). Quartz-normative compositions are mostly from Mount Morning, with some quartz-normative samples also reported from Mason Spur and Ross Island, and one example from Black Island. The quartz-normative compositions at Mount Morning are mainly from the older

(>11.4 Ma) Mason Spur Lineage rocks. All the Erebus Volcanic Province quartz-normative samples are highly evolved with differentiation indices typically >60 (Fig. 21a). There is a wide range of differentiation indices in nepheline-normative rocks (Fig. 21a) reflecting an extensive variation in degree of fractionation, as can be seen on whole-rock total alkali v. silica (TAS) diagrams (Fig. 3). On these TAS diagrams, all Erebus Volcanic Province rocks plot as alkalic. The Mount Morning Volcanic Field rocks are mildly alkali-alkalic, plotting around the divisional line of Saggerson and Williams (1964) (Fig. 3c). The volcanic rocks in the Mount Discovery and Ross Island volcanic fields plot mostly in the strongly alkalic field, with volcanic rocks in the latter having higher  $\text{Na}_2\text{O} + \text{K}_2\text{O}$  wt% values at any given  $\text{SiO}_2$  content, relative to either the Mount Discovery or Mount Morning volcanic fields (Fig. 3). On a cumulative probability plot, the volcanic whole-rock data (excluding bombs, tephra and glass compositions: Fig. 21b) indicate that the bulk of the data (c. 69%) is primitive,

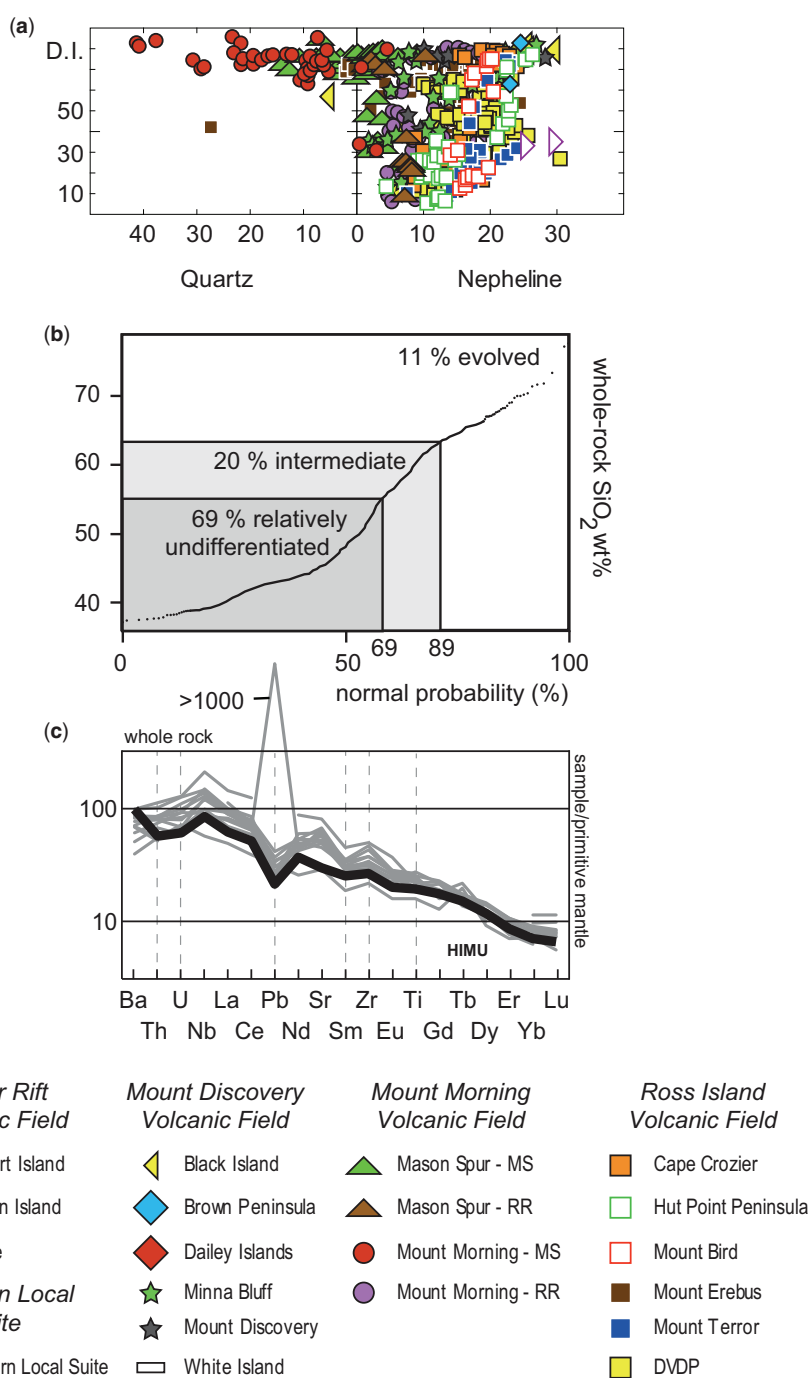


**Fig. 21.** Normative mineralogy and trace element characteristics of Erebus Volcanic Province rocks. (a) A plot of normative quartz or nepheline v. differentiation index (DI: normative wt% quartz + orthoclase + albite + nepheline + leucite + kalsilite: Thornton and Tuttle 1960). (b) A cumulative probability plot of volcanic whole-rock  $\text{SiO}_2$  (wt%) data with subdivisions of relatively undifferentiated (<55 wt%  $\text{SiO}_2$ ), intermediate (55–63 wt%  $\text{SiO}_2$ ) and evolved (>63 wt%  $\text{SiO}_2$ ) included for comparison. (c) Primitive-mantle-normalized extended element plots for selected, relatively undifferentiated, Erebus Volcanic Province whole-rock samples (grey lines). Data from Table 2 have been normalized to the primitive mantle values of McDonough and Sun (1995). The HIMU pattern (black line) is for Mangaia, Austral Islands (sample M-11 of Woodhead 1996). MS, Mason Spur Lineage; RR, Riviera Ridge Lineage.

assuming the primitive cutoff used in this study of 55 wt% SiO<sub>2</sub>. Around 20% of the data is of an intermediate composition and only *c.* 11% of the analysed samples are evolved. The distribution of data (Fig. 21b) is not consistent with claims that the province is bimodal with a paucity of intermediate compositions.

Normalized extended element patterns (Fig. 21c) of primitive volcanic rocks are characterized by enrichments in large ion lithophile elements (LILEs) and high field strength elements (HFSEs), and depletions in Pb relative to primitive

mantle, which is typical of the HIMU mantle reservoir. One exception from Mason Spur has a strongly positive Pb anomaly, which Martin *et al.* (2013) ascribed to a sedimentary-like component in the source. The mantle-normalized patterns feature moderate U/Th and Zr/Sm fractionation but insignificant variation in Ti relative to Eu or Gd (Fig. 21c). Some isotopic systems and trace element ratios in primitive volcanic rocks of the province can be seen to vary with longitude: for example, <sup>87</sup>Sr/<sup>86</sup>Sr, Ba/Rb and Nb/Ta values decrease, and <sup>143</sup>Nd/<sup>144</sup>Nd values increase, from west to east (Fig. 22).

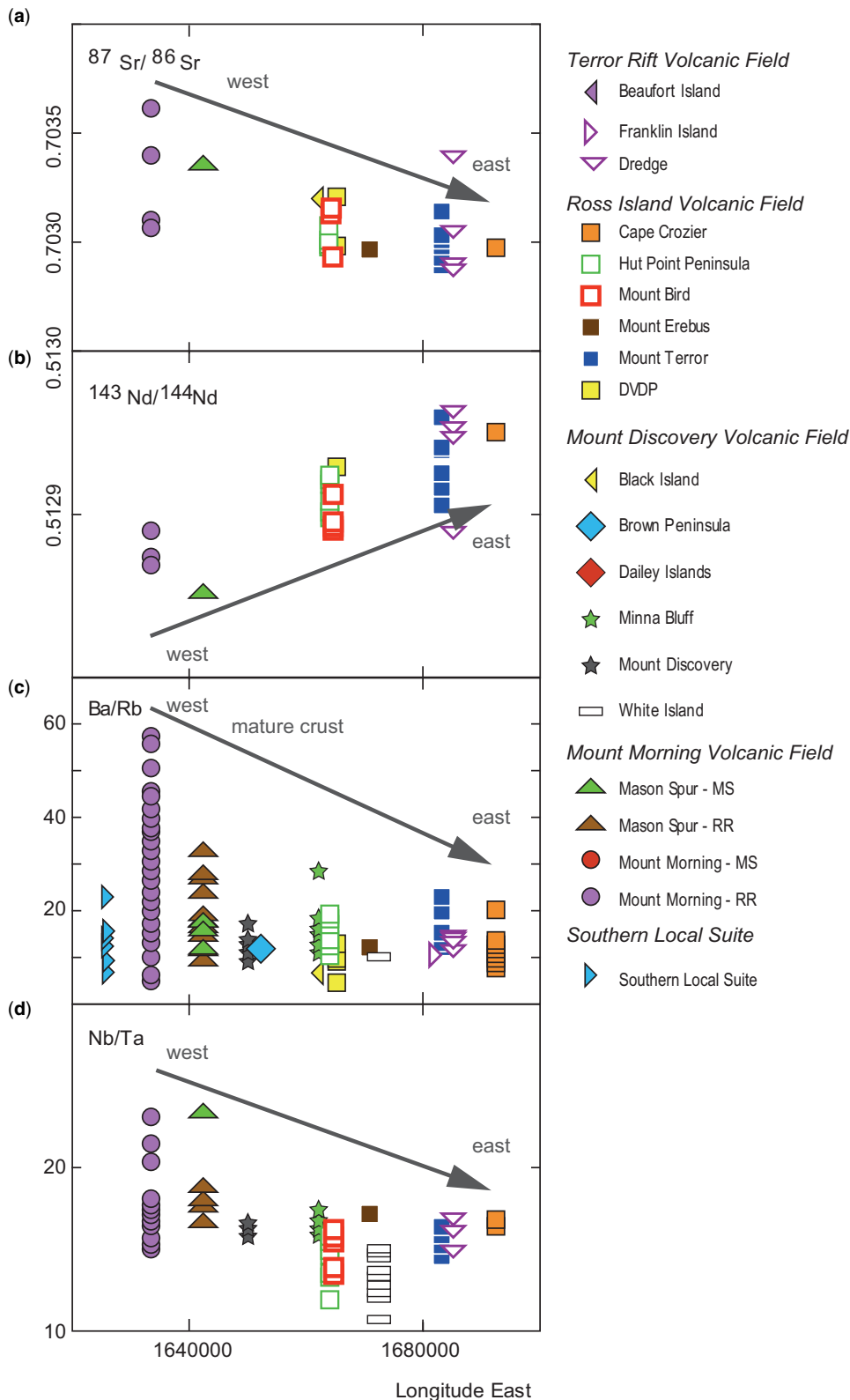


**Fig. 22.** Longitudinal variation of (a) <sup>87</sup>Sr/<sup>86</sup>Sr, (b) <sup>143</sup>Nd/<sup>144</sup>Nd, (c) Ba/Rb and (d) Nb/Ta across the Erebus Volcanic Province for relatively undifferentiated SiO<sub>2</sub> <55 wt%; MgO >6 wt% volcanic rock data included in the Supplementary material (ESM1). MS, Mason Spur Lineage; RR, Riviera Ridge Lineage.

## Erebus Volcanic Province: petrology

Many trace element ratios in primitive volcanic rocks overlap with the field defined for HIMU, with Ba/Nb ratios that extend towards enriched mantle (Fig. 23a). Strontium and Pb isotopic compositions, however, indicate that the source of primitive melts is too low in radiogenic Pb to overlap with the HIMU field as originally defined (Zindler and Hart 1986), although some data still plot towards enriched mantle (Fig. 23b).

**Geothermobarometry.** Clinopyroxene–melt equilibration pressures and temperatures were calculated using published and unpublished clinopyroxene data (see the [Supplementary material \(ESM1\)](#)), paired with whole-rock data for relatively undifferentiated volcanic rocks from the Southern Local Suite, Mount Morning, Minna Bluff and Ross Island. The melt compositions used are for rocks considered to represent magmas parental to more evolved compositions; in the case of Mount Morning, at least, these contain mantle xenoliths. The results using the [Putirka \*et al.\* \(1996\)](#) clinopyroxene–liquid geothermobarometer (Fig. 24) constrain the depths and temperatures at which the pyroxenes equilibrated with melt ([Putirka \*et al.\* 2003](#)). A number of published geothermobarometry equations were tested ([Putirka \*et al.\* 1996, 2003; Putirka 2008](#)), all revealing similar patterns for the province (Fig. 24). Estimates of pressure are broadly correlated with calculated temperatures; the clinopyroxene–melt pairs giving the highest pressures also give the highest temperatures

(Fig. 24). The calculated pressures equate to depths greater than or equal to the measured depth to the Moho in the Erebus Volcanic Province ([Bannister \*et al.\* 2003](#)) (Fig. 24). These pressures are interpreted to indicate that the host magmas bypassed magma-staging areas in the crust and, although the possibility of a pause at the Moho boundary cannot be precluded, the time involved was insufficient to allow significant differentiation. This conclusion is consistent with the occurrence of mantle xenoliths. The clinopyroxene geobarometric data are interpreted to reflect variable source melting depths across the province. The highest pressures are associated with the least chemically evolved volcanic rocks in the Southern Local Suite; the pressures indicate shallower depths of equilibration in the Mount Morning and Mount Discovery volcanic fields, and pressures obtained for Ross Island Volcanic Field clinopyroxenes are higher (Fig. 24).

## Discussion

**Eruptive history and petrogenesis of Mount Erebus.** Mount Erebus is the southernmost active volcano in the world, with an extremely long-lived convective lava lake. This has made it one of the best-studied volcanic centres in Antarctica and for this reason a more detailed overview of it is given here. The geological evolution of Mount Erebus was described by

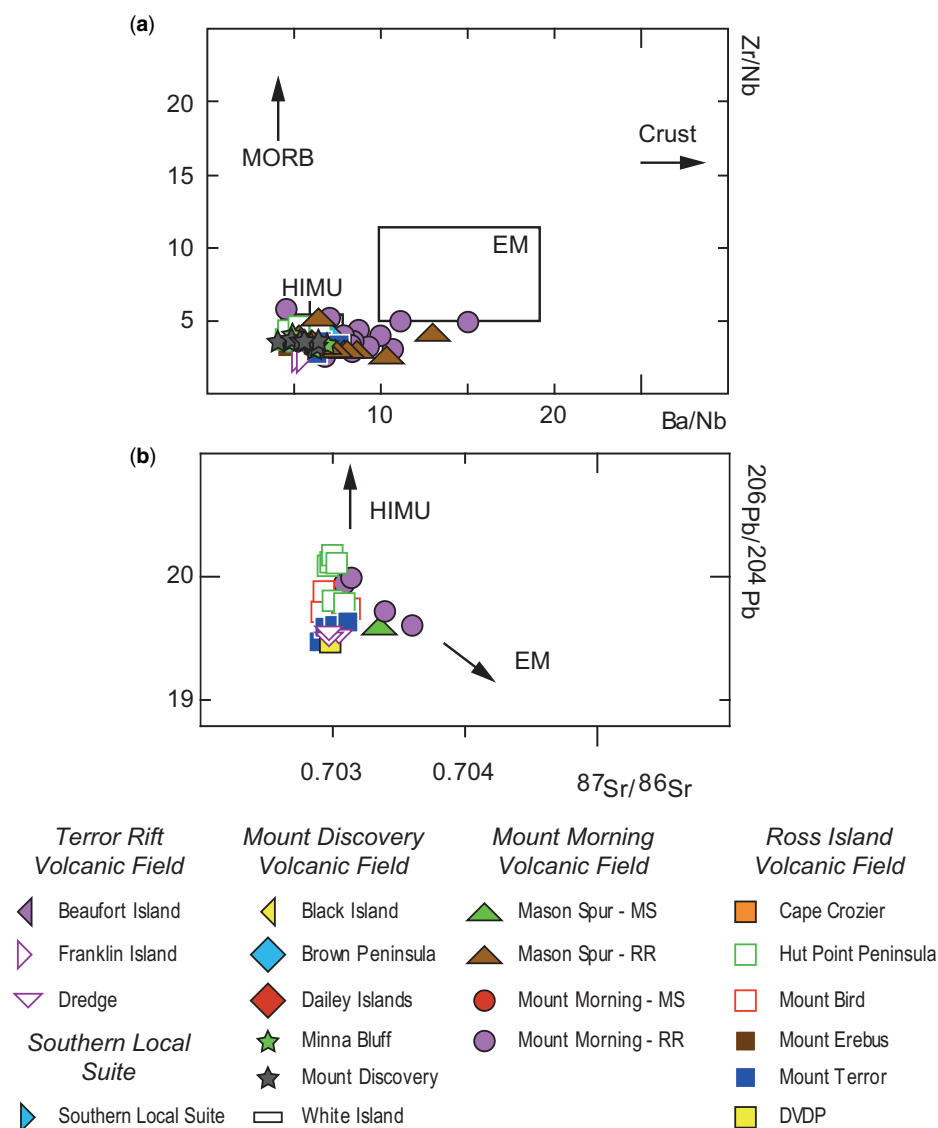


**Fig. 23.** Erebus Volcanic Province trace element and isotopic compositions for relatively undifferentiated ( $\text{SiO}_2 < 55$  wt%;  $\text{MgO} > 6$  wt%) volcanic rocks (data from the [Supplementary material \(ESM1\)](#)) compared with the compositions of selected mantle domains. (a) A Ba/Nb v. Zr/Nb plot. Compositions of HIMU, enriched mantle (EM), mid-ocean ridge basalt (MORB) and continental crust (crust) are from [Weaver \(1991\)](#). (b) A  $^{87}\text{Sr}/^{86}\text{Sr}$  v.  $^{206}\text{Pb}/^{204}\text{Pb}$  plot with the direction for HIMU and EM composition taken from [Zindler and Hart \(1986\)](#). MS, Mason Spur Lineage; RR, Riviera Ridge Lineage.

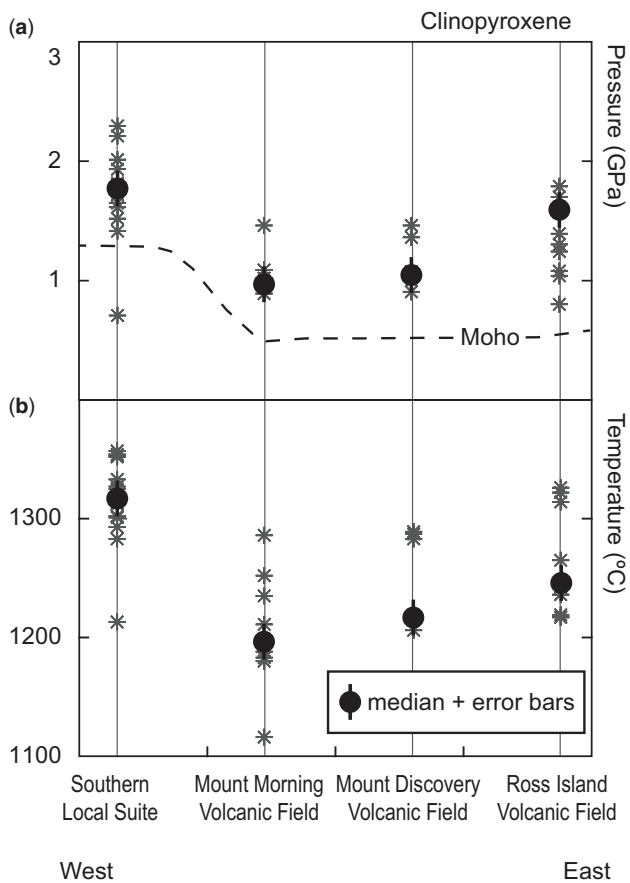


**Fig. 24.** Geothermobarometry results for clinopyroxenes from four volcanic centres in the Erebus Volcanic Province. The equations of Putirka *et al.* (1996) have been applied to data from the Supplementary material (ESM1). From west to east, the four localities are: the Southern Local Suite (Wingrove 2005), Mount Morning (van Woerden 2006), Minna Bluff (Redner 2016) and Ross Island (this study). (a) A plot of barometry results. Median values (circles) and errors estimated at  $\pm 27^\circ\text{C}$  (black bars: Putirka *et al.* 1996) are shown. The Moho (dashed line) is after Bannister *et al.* (2003). (b) A plot of thermometry results. Median values (circles) and errors estimated at  $\pm 0.14$  GPa (black bars: Putirka *et al.* 1996) are shown.

Esser *et al.* (2004) using  $^{40}\text{Ar}/^{39}\text{Ar}$  age determinations from 25 sites around the flanks of Erebus. The ages range from  $1311 \pm 16$  to  $26 \pm 4$  ka, indicating that the growth of the volcano took place over 1 myr. The earliest constructional phase was from 1.3 to 1.0 Ma and is represented by three basanitic cones at Cape Barne (Fig. 9). During this period, a submarine phase of volcanism must have built a hyaloclastite pedestal up from the seafloor. The submarine volcanism was probably contemporaneous with similar basanitic hyaloclastites cored by the DVDP at the Hut Point Peninsula (Kyle 1981a, b). The lower sections of Mount Erebus have a slope of  $<10^\circ$  and they define a profile that is basaltic-shield-like in appearance. Snow and younger lava flows obscure the rocks that comprise most of the shield but the low slope gradient is consistent with these being basaltic.

From 1070 to 718 ka a major proto-Erebus volcano formed and remnants of this are well exposed at Fang Ridge (Fig. 9). The lava flows are mainly phonotephrites and tephriphonolites, and these formed the steep slopes of Fang Ridge which contrast with the lower shield slopes around the base of the mountain. A catastrophic event created a large escarpment which is now Fang Ridge. The origin of the escarpment may have been related to a sector collapse or subsidence due to caldera collapse. The timing of the event is constrained by the stratigraphically youngest lava flow at The Fang, which has

an age of  $718 \pm 66$  ka. There is no dated activity from 718 to 539 ka. From 539 to *c.* 250 ka there were eruptions of phonotephrite, tephriphonolite and rare basanite at and surrounding Abbott Peak, at Inaccessible Island and in the Turks Head area (Fig. 9).

The period from *c.* 250 ka to the present was when the modern Mount Erebus volcanic cone ('Main Crater' and summit area: Fig. 9) was built. The younger tephriphonolite and phonolite lava flows of Mount Erebus are characterized by their porphyritic nature and the presence of large anorthoclase phenocrysts (megacrysts). The oldest anorthoclase-phyric tephriphonolite overlies plagioclase-phyric lava flows at Turks Head and is dated at  $243 \pm 10$  ka, which is identical to the age of similar lava flows further upslope on Mount Erebus. These ages give an indication that eruptions were ultimately centred on the modern Erebus cone. There was a major eruptive episode at 160 ka, and this emplaced trachyte rocks on the eastern flank of Mount Erebus with vents formed at Bomb Peak ( $157 \pm 6$  ka), Ice Station ( $159 \pm 2$  ka) and 'Aurora Cliffs' ( $166 \pm 10$  ka: Esser *et al.* 2004; Kelly *et al.* 2008) (Fig. 9). Ice Station at 2730 m high on the upper eastern slopes of Erebus (Fig. 9) indicates that the modern Mount Erebus volcano was well developed by 160 ka. From 121 to 25 ka, anorthoclase-phyric phonolitic lava flows continued to be erupted as parasitic vents and as thick lava flows on the flanks of Mount Erebus volcano. Simultaneous eruptive activity is likely to have occurred in the summit area of the volcano and there were several caldera-forming events. Between at least  $89 \pm 2$  and  $40 \pm 6$  ka, flank eruptions from unknown vents formed thick anorthoclase tephriphonolite lava flows at Cape Barne, Cape Royds and Cape Evans (Fig. 9). Anorthoclase phonolite parasitic vents were developed at Hooper Shoulder ( $33 \pm 6$  ka) and Three Sisters Cones ( $26 \pm 4$  ka). In summary, Erebus volcano has had a complex eruptive history that spans over 1.3 myr and eruptive activity formed lava flows in the summit area as recently as 4 ka (Parmelee *et al.* 2015). Ongoing Strombolian eruptions have ejected phonolite lava bombs onto the crater rim and their slow accumulation is continuing to build the summit crater.

The petrology and geochemistry of the lava flows on the flanks of Mount Erebus were discussed in detail by Kyle *et al.* (1992), and this work was complemented by experimental studies carried out by Iacovino *et al.* (2016) and isotopic studies by Sims *et al.* (2008). The long eruptive history of Mount Erebus is reflected in the geochemistry. Lava-flow compositions range from basanite to phonolite, and there are numerous benmoreites and a significant number of trachytes (Fig. 3a). Kyle *et al.* (1992) subdivided the Ross Island Volcanic Field lava flows into two main fractional crystallization lineages. On a total alkali v. silica diagram, data for the Erebus Lineage from the Mount Erebus volcanic centre delineate a well-defined and voluminous basanite-phonolite trend (Fig. 3a). This contrasts with Mount Bird and Mount Terror eruptive centres on Ross Island where there is a general lack of lava flows with intermediate compositions (i.e. phonotephrite and tephriphonolite). Also, unlike the Bird and Terror volcanic centres, there are no primitive basanitic rocks exposed in the Mount Erebus volcanic centre (Fig. 20c). Kyle *et al.* (1992) also identified an enriched-iron series of lava flows consisting of benmoreites and trachytes that are relatively lower in total alkali and have higher FeO abundances (Fig. 20d). The Erebus Lineage rocks from the Ross Island Volcanic Field have olivine and clinopyroxene as the main mafic phases, whereas the enriched-iron series lava flows usually contain kaersutite and clinopyroxene. Esser *et al.* (2004) noted that there is a general evolutionary trend with time; the oldest lava flows are basanite, whereas the youngest are phonolites but, overall with time, there is a general evolutionary trend to samples with lower MgO contents.

## Erebus Volcanic Province: petrology

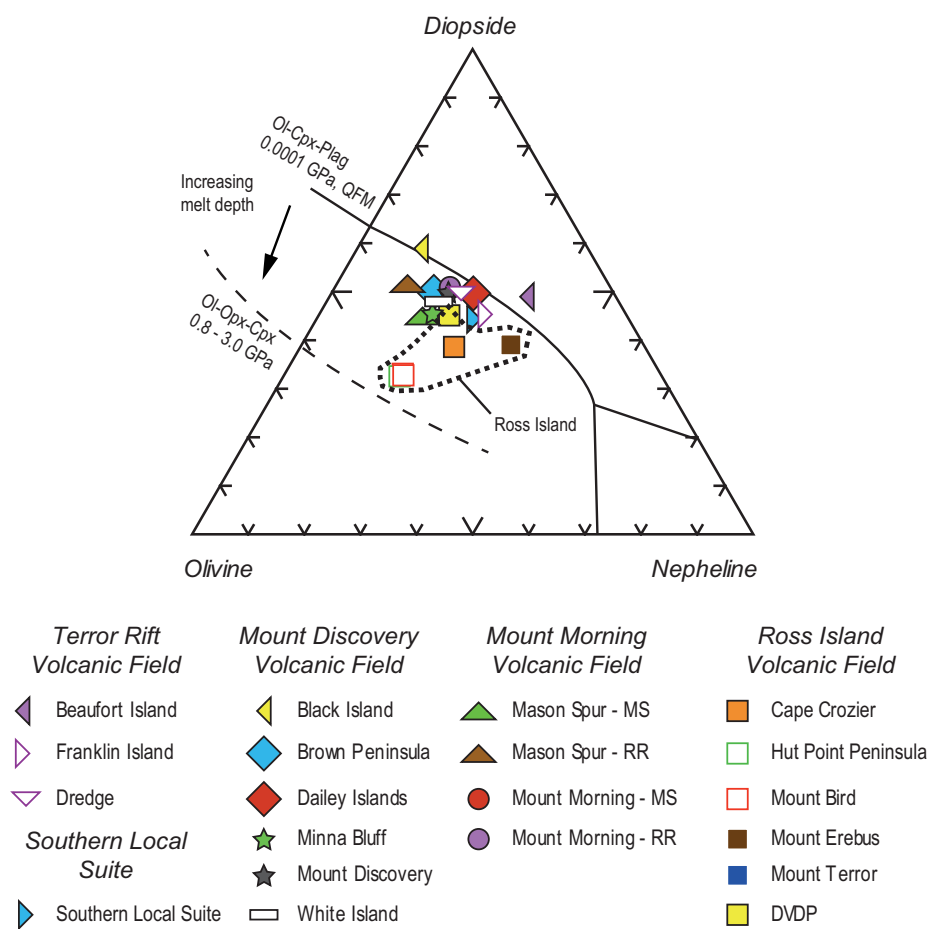


**Fig. 25.** Normative olivine, diopside and nepheline composition of typical relatively undifferentiated volcanic rocks from the Erebus Volcanic Province (Table 2). Also shown are the 0.0001 GPa and limiting 0.8–3.0 GPa cotectics of Sack *et al.* (1987). Cpx, clinopyroxene; DVDP, Dry Valley Drilling Project; HPP, Hut Point Peninsula; Ol, olivine; Opx, orthopyroxene; Plag, plagioclase; LS, Local Suite; MS, Mason Spur Lineage; RR, Riviera Ridge Lineage.

*Assimilation and fractional crystallization processes and lineages.* In the following discussion subsections, a regional approach will be used to discuss the petrogenesis of the Erebus Volcanic Province. This is possible because of the data compiled in this study and is thought preferable to discussing each volcanic field individually. For the province as a whole, total alkali v. silica diagrams (Fig. 3), wt% MgO v. major and trace element plots (Fig. 20), normative nepheline content that varies with differentiation index (Fig. 21a) and normative diopside/olivine ratio (not shown) are all consistent with magmatic evolution controlled by fractional crystallization involving olivine + clinopyroxene + magnetite/ilmenite + titanite. Several studies of the petrology of the province have concluded that Ti-amphibole (kaersutite) and feldspar are important fractionating phases (e.g. Kyle 1981b; Kyle *et al.* 1992; Martin *et al.* 2013). Although relatively rare, quartz-normative volcanic rocks have been found in association with otherwise nepheline normative alkalic suites worldwide (e.g. Price and Chappell 1975; Houghton *et al.* 1992; White *et al.* 2006). In Marie Byrd Land, silica-oversaturated trachytic volcanic rocks at Mount Sidley are hypothesized to have formed via wall-rock assimilation during fractional crystallization (Panter *et al.* 1997), and a similar explanation has been used to explain quartz-normative trachyte rocks at Mount Morning (Martin *et al.* 2013).

Several petrological lineages that record crystal fractionation history have been identified in the Erebus Volcanic Province. These include the DVDP (Kyle 1981b) and Erebus lineages (Kyle *et al.* 1992) identified at Ross Island, and the Mason Spur and Riviera Ridge lineages identified in the Mount Morning Volcanic Field (Martin *et al.* 2013). Kyle *et al.* (1992) also identified the enriched-iron series, members of which have significantly higher whole-rock FeO contents at a given wt% MgO content (Fig. 20d) relative to any other

whole-rock compositions in the province. The identification and description of these lineages is key to understanding petrogenesis of specific magmatic suites. Variations between lineages represent contrasts in the parameters controlling petrogenesis including pressure, temperature and assimilation histories. The differences between volcanic fields and local suites in this province, however, indicate that applying magmatic lineage nomenclature outside any single field or suite may be problematic. Instead, suites in specific areas should be assigned to particular and unique lineages: for example, the Mount Discovery Volcanic Field lineage and the Terror Rift Volcanic Field lineage (both strongly alkalic, nepheline-normative, basanite–phonolite lineages), and the Southern Local Suite lineage (strongly alkalic, nepheline normative, basanite to phonotephrite). With further study, subtle differences between these various lineages may lead to further subdivision and refinements in nomenclature.

*Depth to melting and degree of partial melting.* In the diopside–olivine–nepheline experimental phase diagram of Sack *et al.* (1987), a primitive, whole-rock volcanic composition from Black Island plots on the 0.0001 GPa olivine + clinopyroxene + plagioclase cotectic but other compositions plot away from the 0.0001 GPa cotectic towards higher-pressure cotectics (Fig. 25). In this system, the Ross Island Volcanic Field data plot furthest towards the 0.8–3.0 GPa cotectic, indicating that magmas they represent were generated deeper in the mantle relative to other volcanic rocks in the province. This is supported by clinopyroxene-based geothermobarometry, which indicates that melts beneath Ross Island Volcanic Field partially crystallized at greater depths and higher temperatures than those generated beneath either the Mount Morning or Mount Discovery volcanic fields (Fig. 24). The clinopyroxene

data from the Southern Local Suite indicate a greater depth of partial crystallization than in the Ross Island Volcanic Field, consistent with the greater depth to the Moho in the Transantarctic Mountains but a conclusion that is not supported by the trend in the diopside–olivine–nepheline projection (Fig. 25).

Spinel peridotite xenoliths and plagioclase-bearing spinel peridotite xenoliths were common cargo in the magmas represented by primitive volcanic rocks of the Erebus Volcanic Province (Kyle *et al.* 1987; Martin *et al.* 2014a, b). Garnet is never described in the lower-crustal or mantle xenoliths

collected in igneous rocks of the Erebus Volcanic Province (Berg 1984; Martin *et al.* 2015a) but symplectites of orthopyroxene and spinel, and high-sodium clinopyroxene chemistry in mantle xenoliths, have been interpreted as the products of melting in the garnet–peridotite stability field (Martin *et al.* 2015b). Similar inferences were drawn for some northern Victoria Land xenoliths (e.g. Perinelli *et al.* 2006). Trace element modelling for relatively undifferentiated volcanic whole-rock trace element compositions does not fit well with end-member garnet lherzolite or end-member spinel lherzolite melting (Fig. 26a); instead, a high degree of overlap can be achieved between model melts and relatively undifferentiated rock compositions when partial melting of a mixed spinel and garnet source is modelled. For example, on a ppm Sm v. Sm/Yb plot (Fig. 26a), data for relatively undifferentiated whole-rock samples plot around the 50:50 spinel + garnet lherzolite mixing line (between 0 and 10% partial melt). On a La/Yb v. Gd/Yb plot (Fig. 26b), the majority of the whole-rock data plot on mixing lines between 4% garnet (20% garnet lherzolite: 80% spinel lherzolite) and 8% garnet (40:60) in the source. Also modelled on Figure 26b are degrees of partial melting, with the relatively undifferentiated volcanic rock data modelled at between 1 and 5% partial melting.

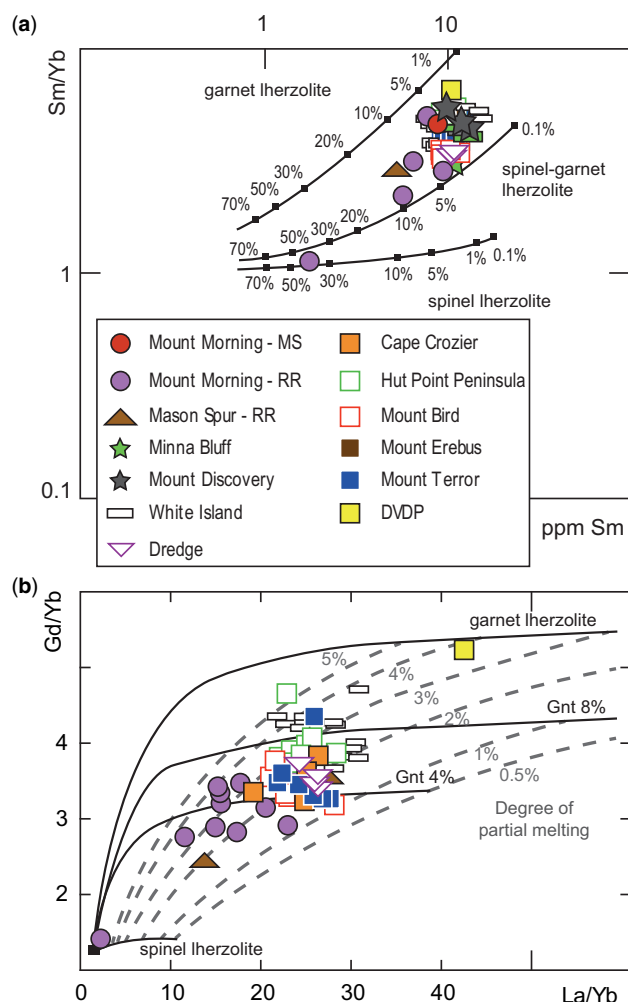


**Fig. 26.** Trace element plots showing relatively undifferentiated ( $\text{SiO}_2 < 55 \text{ wt}\%$ ;  $\text{MgO} > 6 \text{ wt}\%$ ) volcanic rock compositions from the Erebus Volcanic Province with various melt curves plotted for comparison. Data are from the Supplementary material (ESM1). (a) A ppm Sm v. Sm/Yb plot. Melt curves are for non-modal batch melting (Shaw 1970) for spinel lherzolite with (mode: melt mode) olivine<sub>53:6</sub> + orthopyroxene<sub>27:28</sub> + clinopyroxene<sub>17:67</sub> + spinel<sub>3:11</sub> (Kinzler 1997); and garnet lherzolite with olivine<sub>60:16</sub> + orthopyroxene<sub>20:16</sub> + clinopyroxene<sub>10:88</sub> + garnet<sub>10:9</sub> (Walter 1998). The partition coefficients are from McKenzie and O’Nions (1991, 1995), and the diagram follows Aldanmaz *et al.* (2000). (b) A plot of Gd/Yb v. La/Yb. Melt curves of accumulated fractional melting for spinel lherzolite with mode olivine<sub>46</sub> + orthopyroxene<sub>28</sub> + clinopyroxene<sub>18</sub> + spinel<sub>18</sub> and garnet lherzolite with mode olivine<sub>54</sub> + orthopyroxene<sub>17</sub> + clinopyroxene<sub>9</sub> + spinel<sub>20</sub>, and following Workman *et al.* (2004). Orthopyroxene, clinopyroxene and spinel are assumed to react stoichiometrically to form olivine and garnet. Curves representing 4% garnet in the source (garnet:spinel = 20:80) or 8% garnet in the source (garnet:spinel = 40:60) are plotted for comparison. The partition coefficients are from Halliday *et al.* (1995) and the diagram follows Yokoyama *et al.* (2007). MS, Mason Spur Lineage; RR, Riviera Ridge Lineage.

*Variation with longitude.* The wt% Na<sub>2</sub>O + K<sub>2</sub>O values for a given SiO<sub>2</sub> content increase from the Mount Morning Volcanic Field to the Mount Discovery Volcanic Field to the Ross Island Volcanic Field (Fig. 3). This observation is more strongly controlled spatially (variation in longitude) than by age of eruption. This pattern may reflect increased partial melting westwards, with greater partial melting and lower total alkali contents in the Mount Morning Volcanic Field, relative to lower partial melting and higher total alkali abundance in the Ross Island Volcanic Field.

Longitudinal variation in the relatively undifferentiated volcanic rocks of eruptive centres/volcanic fields can also be seen on isotopic (Sr, Nd) and trace element ratio (Ba/Rb, Nb/Ta) plots (Fig. 22). Ratios of Ba/Rb in relatively undifferentiated volcanic rocks are higher in mature lower continental crust, relative to younger lower continental crust and upper continental crust (Stracke *et al.* 2003; Willbold and Stracke 2006). Ratios of Nb/Ta in relatively undifferentiated volcanic rocks can be higher in rocks that have a carbonatite-like component or an eclogite-like component in their sources (e.g. Pfänder *et al.* 2012). Using longitudinal variation of isotopic Sr and Nd (and trace element ratios), Guo *et al.* (2015) argued for a pattern of changing proportions of continental crustal components (including sediment melt and aqueous fluid) in the mantle source of the alkalic magmas they studied. Panter *et al.* (2018) found a pattern of eastward-increasing <sup>143</sup>Nd/<sup>144</sup>Nd and eastward-decreasing <sup>87</sup>Sr/<sup>86</sup>Sr in McMurdo Volcanic Group rocks in the most northerly part of northern Victoria Land, comparable to relationships seen in the Erebus Volcanic Province (Fig. 22), which they considered to be a function of the thickness and age of the mantle lithosphere. The eastward-decreasing radiogenic Sr, and increasing Nd, in the Erebus Volcanic Province relatively undifferentiated volcanic rocks is consistent with a decreasing proportion of crustal component in the primitive magma source (e.g. derived from fluids from an ancient subducted slab; Fig. 22). The eastwardly change in major and trace element abundances and isotopic compositions can be interpreted to indicate a systematically varying pattern of petrogenesis. This may be related to the involvement of an increasing proportion of mature lower continental crust (Ba/Rb), and/or increasing proportion of carbonatite-like or eclogite-like (Nb/Ta) and/or varying proportions of continental crust-like material (radiogenic Sr and Nd) in the mantle source, possibly

## Erebus Volcanic Province: petrology

combined with decreasing partial melting, eastwards (Panter *et al.* 2018).

**Source characteristics.** The trace element and isotope compositions of relatively undifferentiated Erebus Volcanic Province basaltic rocks and xenoliths can only be explained in terms of complex mantle sources, and polybaric and variable partial melting events. Several studies have led to the conclusion that the mantle source for the Erebus Volcanic Province relatively undifferentiated magmas is likely to have comprised depleted mantle modified at various times by the addition of enriched mantle, carbonatitic metasomatism and a HIMU-like component (e.g. see Sims *et al.* 2008; Martin *et al.* 2013; Aviado *et al.* 2015; Martin *et al.* 2015b). It has been suggested that the enriched component may have been compositionally similar to lower continental crust or pelagic sediment and this may have been added during early ancient subduction events (Martin *et al.* 2015b). The trace element and isotopic composition and mineralogy of potential mantle sources is discussed in the following subsections.

**Amphibole, carbonatite and eclogite components.** Melts derived as partial melts from an amphibole-bearing mantle

source have higher Ba/Rb and lower Rb/Sr ratios than those generated by melting a phlogopite-bearing source (Furman and Graham 1999). Trace element ratios in the Erebus Volcanic Province whole-rock samples (Fig. 27a) indicate that amphibole dominates over phlogopite in the mantle source region; a conclusion that is consistent with trace element modelling (Sun and Hanson 1975) and experimental petrology (Iacovino *et al.* 2016) for the province.

Primitive-mantle-normalized extended element plots (Fig. 21c) for the Erebus Volcanic Province relatively undifferentiated rocks are characterized by fractionation of U relative to Th and Zr relative to Sm, and some primitive volcanic rocks have low Zr/Sm ratios relative to average continental crust (Fig. 27b). These features have been argued to indicate a carbonatite-like component in the mantle source (Yaxley *et al.* 1991; Pfänder *et al.* 2012). Carbonated peridotite and carbonated eclogite/pyroxenite in the mantle sources of relatively undifferentiated volcanic rocks have been evoked by some workers to explain the chemical and trace element relationships in the Erebus Volcanic Province (Martin *et al.* 2013; Aviado *et al.* 2015). Cambrian carbonatite dykes have been reported adjacent to the Southern Local Suite (Hall *et al.* 1995), modal carbonate grains have been reported in mantle

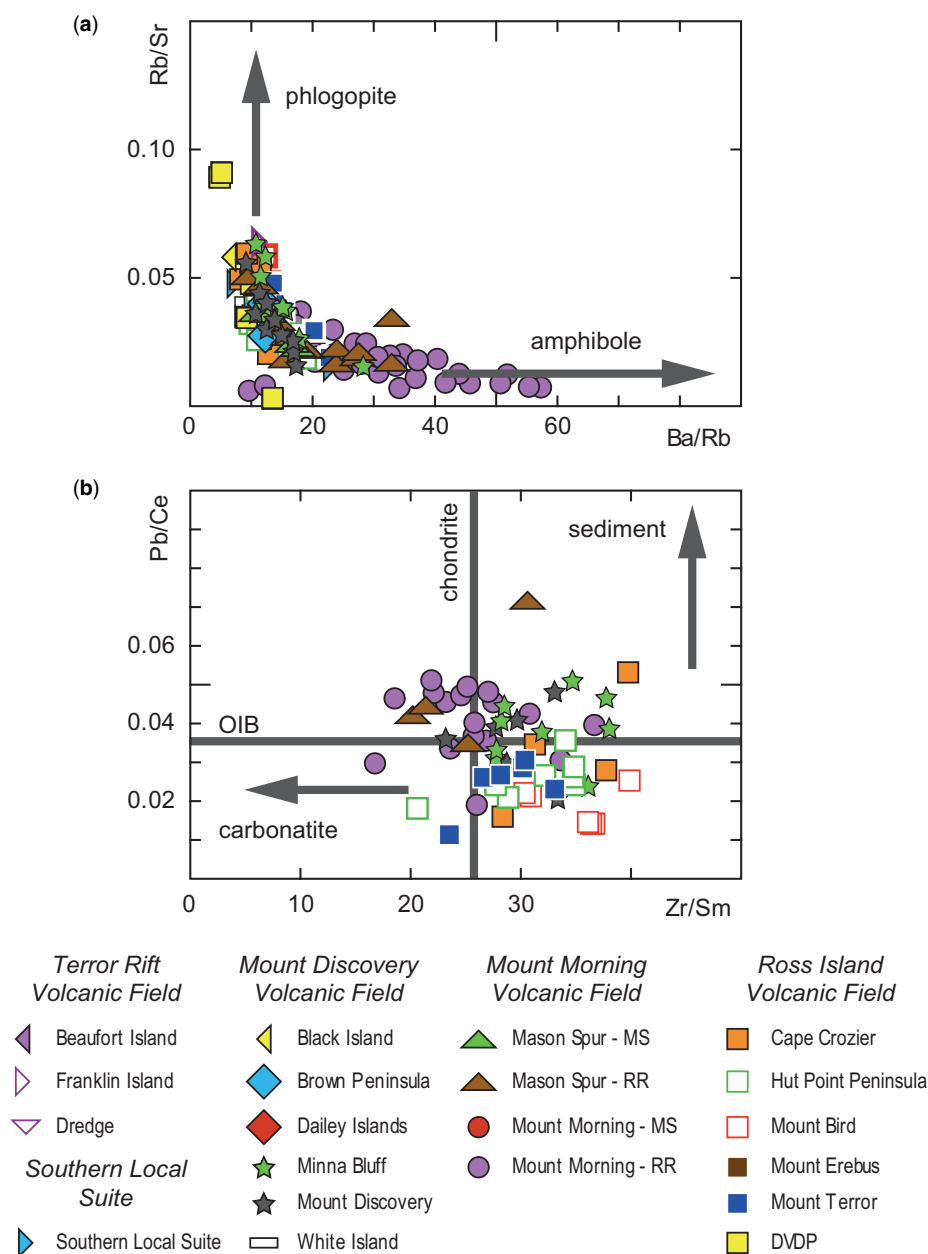


**Fig. 27.** Trace element ratio diagrams showing relatively undifferentiated ( $\text{SiO}_2 < 55 \text{ wt\%}$ ;  $\text{MgO} > 6 \text{ wt\%}$ ) whole-rock compositions for the Erebus Volcanic Province. The data are available in the [Supplementary material \(ESM1\)](#). (a) A Ba/Rb v. Rb/Sr plot showing mantle-source mineralogy that is more strongly amphibole influenced, relative to phlogopite. (b) A Zr/Sm v. Pb/Ce plot showing chondritic Zr/Sm (McDonough and Sun 1995) and typical ocean island basalt (OIB) Pb/Ce (Rudnick and Gao 2003). Values below and above these values are indicative of an influence by carbonatite- or sedimentary-like components, respectively. MS, Mason Spur Lineage; RR, Riviera Ridge Lineage.

xenoliths at Mount Morning (Martin *et al.* 2015b) and Erebus volcano melts have been modelled to be extremely high in CO<sub>2</sub> (Iacovino *et al.* 2016).

Estimated compositions of Terror Rift Volcanic Field primary melt compositions overlap with experimentally determined major element values of carbonated eclogite (Aviado *et al.* 2015) and an eclogite-like component was used to explain pyroxenite whole-rock trace element ratios at Mount Morning (Martin *et al.* 2015b). Ratios La/Nb and Nb/Ta of relatively undifferentiated volcanic rocks from the Erebus Volcanic Province can be used to further test the feasibility

of an eclogite-like component in the mantle source. On a La/Nb v. Nb/Ta diagram (Fig. 28), several relatively undifferentiated volcanic rocks from the province plot towards the refractory eclogite reservoir of Rudnick *et al.* (2000), and this trend can also be seen on a Ti v. Ti/Zr plot (not shown). The possible influence of an eclogite component can be further modelled using La/Yb and Dy/Yb ratios (Fig. 28b). On a La/Yb v. Dy/Yb diagram, the trend defined by relatively undifferentiated volcanic rock data from the province is consistent with <15% mixing between eclogite and depleted mantle, with 10–20% eclogite in the source.

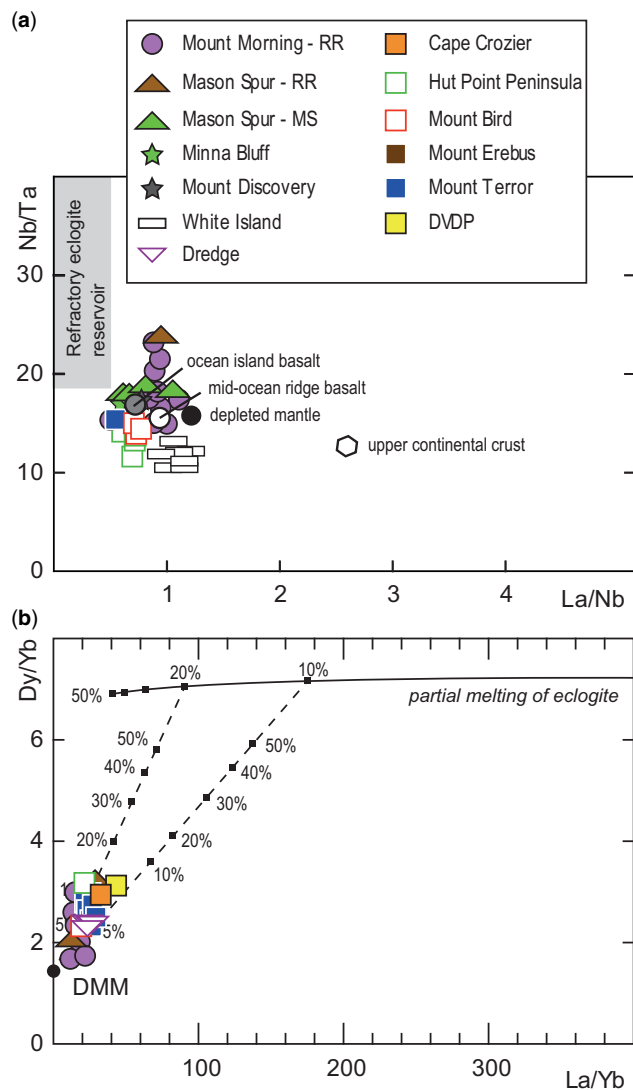


**Fig. 28.** Relatively undifferentiated (SiO<sub>2</sub> <55 wt%; MgO >6 wt%) Erebus Volcanic Province whole-rock compositions plotted on trace element ratio diagrams to show the potential influence of an eclogite-like component in the source. (a) A La/Nb v. Nb/Ta plot showing the refractory eclogite reservoir of Rudnick *et al.* (2000). Average values for upper continental crust (Rudnick and Gao 2014), depleted mantle (Rudnick *et al.* 2000), mid-ocean ridge basalt (Gale *et al.* 2013) and ocean island basalt (Sun and McDonough 1989) are shown for comparison. (b) A La/Yb v. Dy/Yb plot. The data and model parameters are available in the Supplementary material (ESM1). The melt curves follow Guo *et al.* (2015, fig. 23 and references therein). The depleted mid-ocean ridge mantle (DMM) composition is from Workman and Hart (2005), and the horizontal melt curve shows the degree of partial melting of crustal eclogite (numbers in per cent). The subvertical melting curves show the proportions of the eclogite-derived melt in the two-component mixture between DMM and eclogite-derived melt (numbers in per cent). MS, Mason Spur Lineage; RR, Riviera Ridge Lineage.

*Enriched mantle.* Trace element and isotopic data for relatively undifferentiated volcanic rocks from the Erebus Volcanic Province have commonly been interpreted to reflect the involvement of an enriched component in the mantle source (e.g. Sims and Hart 2006; Cooper *et al.* 2007; Martin *et al.* 2013; Aviado *et al.* 2015; Phillips *et al.* 2018) (Fig. 23). There is ambiguity about the nature and origin of this material but whole-rock ratios of Ba/Rb >15 (Fig. 22c) and Ba/Nb >9 (Fig. 23a) are similar to those of mature, lower continental crust. This material may have been added to the mantle during ancient subduction events. Modelling carried out by Martin *et al.* (2015b) was interpreted to show that peridotite xenoliths from Mount Morning can be generated by adding up to 15% enriched mantle (EMI) to a depleted peridotite composition; it was suggested that this enriched component could be ancient lower crust or ancient pelagic sediment. Trace element modelling carried out in other studies has led to similar conclusions with either EMI- or EMII-like components being invoked (e.g. Cooper *et al.* 2007; Aviado *et al.* 2015).

*HIMU.* Trace element ratios and radiogenic isotopes of Erebus Volcanic Province rocks have commonly been interpreted to reflect involvement of a HIMU-like component, although radiogenic Pb isotope ratios are lower than those of pure end-member HIMU (Fig. 23). Furthermore, mantle-normalized extended element patterns have some similarities with HIMU, including enrichments of some LILEs and HFSEs relative to primitive mantle, and depletion of Pb relative to Ce and Nd (Fig. 21c). Using Sr v. Th isotope diagrams, Sims and Hart (2006) have developed a case for the involvement of a HIMU-like component in the mantle source from which Ross Island volcanic rocks were derived. Cooper *et al.* (2007) used trace element ratios in primitive volcanic rocks from White Island to infer a HIMU-like component in the mantle source for these rocks and, using trace element and isotopic data from Mount Morning, Martin *et al.* (2013) also inferred a HIMU-like component at source. Aviado *et al.* (2015) preferred to interpret the trace element and isotopic data from the Terror Rift Volcanic Field to indicate the involvement of a mantle component similar to a FOZO (focal zone – a mantle-plume component) end member rather than HIMU, and they argued that this component reflected mixing between depleted mantle and crust (after Stracke 2012). Using trace element ratios and isotopic compositions for Ross Island Volcanic Field rocks, Phillips *et al.* (2018, fig. 8) modelled mixing between depleted mantle and HIMU with the ratio of the two components varying from 40:60 (depleted mantle:HIMU) to around 90:10. Thus, it is generally accepted that a HIMU-like component exists in the source of Ross Island volcanic rocks, and in some eruptive centres of similar age and composition in the SW Pacific (e.g. Stracke 2012; Scott *et al.* 2013; Gamble *et al.* 2018) and Marie Byrd Land (e.g. Kipf *et al.* 2014). A HIMU-like component is a defining characteristic of the source of Cenozoic, alkalic, primitive volcanic rocks in the SW Pacific linking these rocks into a single diffuse alkaline magmatic province (DAMP: Finn *et al.* 2005).

*Age of mantle source chemistry and asthenosphere v. lithosphere.* For those studying alkalic volcanic provinces, a recurring challenge is the differentiation of lithospheric and asthenospheric sources. On this problem, Herzberg (2011) wrote of the Hawaiian Islands that in mantle peridotite source compositions of volcanic rocks, it is rarely clear whether additional crust-like components are still present as a lithological unit in the source (pyroxenite) or whether only the geochemical signal (fluids or melts) of the recycled crust was imprinted on the source peridotite. To investigate this for the Hawaiian Islands, Sobolev *et al.* (2005) and Herzberg (2011) used major and trace element data to model whether basalt compositions are representative of peridotite- or pyroxenite-derived melts. For example, on a whole-rock wt% MgO v. ppm Ni plot (Fig. 20h) peridotite-derived melts (below the grey dashed curve in Fig. 20h) can be distinguished from pyroxenite-derived melts (above the curve). Most relatively undifferentiated volcanic rocks in the Erebus Volcanic Province have Ni concentrations lower than those expected of pyroxenite-derived melts, indicating that they probably derived from a peridotite mantle source.

The age of the HIMU signature in the source of alkalic rocks continues to be debated. As originally defined, HIMU represented high time-integrated  $^{238}\text{U}/^{204}\text{Pb}$  ratios (Zindler and Hart 1986) with unradiogenic Sr ( $^{87}\text{Sr}/^{86}\text{Sr} < 0.703$ ) relative to radiogenic Pb ( $^{206}\text{Pb}/^{204}\text{Pb} > 20.5$ ). Modelling has shown that the appropriate U–Th–Pb ratios in a source will develop HIMU characteristics following extended storage of around 0.5–3.0 Ga (Hofmann and White 1982; Chauvel *et al.* 1992; Stracke *et al.* 2003). More recently, natural and experimental studies have demonstrated that highly radiogenic  $^{238}\text{U}/^{204}\text{Pb}$  can be preserved relatively quickly (<0.5 Ga) through processes involving carbonatization (e.g. Scott *et al.* 2014; McCoy-West *et al.* 2016; van der Meer *et al.* 2017). This carbonatization may occur in the lithosphere or asthenosphere and therefore the age at which highly radiogenic  $^{238}\text{U}/^{204}\text{Pb}$  formed also informs the debate on asthenospheric v. lithospheric sources for primitive magmas.

In the SW Pacific, this debate has been of particular interest because of the widespread dispersal of Cenozoic volcanic rocks with HIMU-like signatures across Zealandia, eastern Australia, Papua New Guinea and West Antarctica (Coombs *et al.* 1986; Finn *et al.* 2005). In Zealandia, isotopic studies have demonstrated disequilibrium between isotopic systems (Sr, Nd and Pb v. Hf), and constructed age isochrons showing Mesozoic ages for high radiogenic Pb are incongruous with the extended times required for *in situ* development of HIMU *sensu stricto* at some localities (e.g. Scott *et al.* 2014; McCoy-West *et al.* 2016).

The Zealandia example differs from that recorded in the Erebus Volcanic Province. The isotopic systems that were in disequilibrium in Zealandia have equilibrated in primitive volcanic rock samples from Ross Island (Sr, Nd, Pb, Hf), which has been interpreted to indicate high time-integrated HIMU in the mantle source (Sims *et al.* 2008; Phillips *et al.* 2018). However, it has also been highlighted that peridotite and pyroxenite mantle xenoliths from the Erebus Volcanic Province have trace element and isotopic ratios that indicate shared characteristics between their source and the source of relatively undifferentiated volcanic rocks in the province, including HIMU-, enriched-mantle-, carbonatite- and eclogite-like components (Martin 2009; Martin *et al.* 2013, 2014a, b, 2015b; Aviado *et al.* 2015). Furthermore, age determinations on pyroxenite xenoliths, intrusions and carbonatite dykes from southern Victoria Land, and eclogite from northern Victoria Land, are around 0.5 Ga (McGibbon 1991; Hall *et al.* 1995; Di Vincenzo *et al.* 1997; Martin *et al.* 2015a). This age coincides with the timing of subduction of the palaeo-Pacific margin of Gondwana, leading to the suggestion that the lithospheric

mantle was modified by fluids from, or modified by, the subducting plate (Aviado *et al.* 2015; Martin *et al.* 2015b). A complication is that the 0.5 Ga time period also overlaps with the minimum time proposed to allow the *in situ* growth of the high time-integrated HIMU signature (Stracke *et al.* 2003). Sims *et al.* (2008) have pointed out that, because of the long (106 Ga) half-life of  $^{147}\text{Sm}$ , 0.5 Ga is insufficient time to significantly change the radiogenic  $^{143}\text{Nd}/^{144}\text{Nd}$  values of a vein-infused lithosphere. In northern Victoria Land, Panter *et al.* (2018) explained isotopic changes in Nd with longitude as being caused by the progressive reaction between rising alkalic melt and peridotite in the lithospheric mantle. It is, perhaps, significant that, in a classic paper, Sun and Hanson (1975) determined a two-stage model lead age of 1500 Ma for volcanic rocks from Ross Island. They interpreted this as the time since the development of chemical heterogeneity in the mantle source. Furthermore,  $^{143}\text{Nd}/^{144}\text{Nd}$  is shown to vary with longitude across the Erebus Volcanic Province (Fig. 22b), which, as Sims *et al.* (2008) pointed out, is unlikely to be related to *in situ* processes in periods of time <0.5 Ga.

These observations can be explained by either of two possible hypotheses:

- (1) A high time-integrated HIMU signal has developed *in situ* since *c.* 0.5 Ga, with varying radiogenic Nd explained by variable partial melting of the veined lithospheric mantle across the province. The compositions of primitive melts reflect involvement of both lithospheric and asthenospheric sources.
- (2) The mantle source is asthenospheric and ancient (much older than 0.5 Ga). The varying radiogenic Nd is explained by variable *in situ* development.

The evidence discussed here, particularly the 1.5 Ga Pb isochron age of volcanic rocks at Ross Island (Sun and Hanson 1975) and the behaviour of  $\text{TiO}_2$ , FeO, CaO/ $\text{Al}_2\text{O}_3$  and Ni relative to MgO abundance (Fig. 20), are more consistent with melting of an ancient asthenospheric source. This would support a HIMU mantle source *sensu stricto*. Such a hypothesis would be challenged or strengthened if additional age constraints could be placed on the timing of chemical modifications to the mantle source of relatively undifferentiated volcanic rocks in the province.

*Plumes v. decompression melting.* A plume-driven model of melting was originally popular for the Erebus Volcanic Province, and Ross Island in particular (e.g. Behrendt *et al.* 1991b; Kyle *et al.* 1992; Esser *et al.* 2004), with the three-fold radial symmetry of volcanism on Ross Island, and in volcanic centres about Mount Discovery, being argued to reflect plume-related updoming. Opponents to the Cretaceous plume hypothesis point out the absence of regional uplift (Cooper *et al.* 2007; Martin *et al.* 2013), low magma production rates relative to typical rates associated with plumes (Finn *et al.* 2005), and the size and longevity of mantle plumbing required to generate melt simultaneously across >100 km of volcanism in the province (Cooper *et al.* 2007). This model was gradually replaced by the idea of decompression melting promoted by transtensional lithospheric deformation of a mantle metasomatized during a Late Cretaceous amagmatic extensional rift phase (Rocchi *et al.* 2002, 2005). The idea was further developed by Panter *et al.* (2018) for northern Victoria Land, with mantle upwelling possibly related to slab detachment and/or edge-driven mantle flow established at the boundary between the thinned lithosphere of the West Antarctic Rift System and cratonic East Antarctica. Recently, Phillips *et al.* (2018) revived the idea of a Cretaceous mantle plume beneath Ross Island based on three-fold radial symmetry of Ross Island, tomography,  $^3\text{He}/^4\text{He}$  in clinopyroxenes of the DVDP lava flows, isotopic variability between eruptive centres on Ross

Island, and isotopic variability between Ross Island volcanic rock compositions and those in Zealandia.

The cause of contrast in isotopic variability between Zealandia and the Erebus Volcanic Province are, as discussed above, likely to be attributable to differences in the time of *in situ* growth of the HIMU signature in the Erebus Volcanic Province relative to the Mesozoic HIMU-like signature in Zealandia magmatic sources, and it is not diagnostic of a mantle-plume influence. The extensive compilation of data for relatively undifferentiated volcanic rocks of the Erebus Volcanic Province presented here can be used to show that the trace element and isotopic changes seen in the Ross Island Volcanic Field are part of a wider pattern observed across the entire province (e.g. Fig. 22). A plume head, with a >100 km radius centred beneath Ross Island, could explain this element and isotopic variation, as could edge-driven mantle flow. At this width, excess temperatures are modelled to drop significantly (up to four times) at 100 km distance for a plume/edge-driven scenario (Hauri *et al.* 1994, fig. 2b). Median temperatures calculated from clinopyroxene compositions decrease from the Ross Island Volcanic Field, through the Mount Discovery Volcanic Field, to the Mount Morning Volcanic Field, with temperatures rising sharply again in the Southern Local Suite mantle source (Fig. 24). This is contrary to the pattern observed in temperature data calculated for peridotite xenoliths of White Island, Mount Morning and the Southern Local Suite (Martin *et al.* 2014a), which increase eastwards. Whole-rock  $^{87}\text{Sr}/^{86}\text{Sr}$ , Ba/Rb and Nb/Ta ratios all increase westwards across the province (Fig. 22), whereas  $^{143}\text{Nd}/^{144}\text{Nd}$  ratios decrease. High  $^{87}\text{Sr}/^{86}\text{Sr}$  and relatively low  $^{143}\text{Nd}/^{144}\text{Nd}$  are consistent with an increasingly enriched mantle component in the source melt, whereas increasing Ba/Rb and Nb/Ta ratios indicate increasing involvement of an eclogitic crustal component, eastwards. These patterns are consistent with an increasing input of subduction component eastwards in the province, similar to patterns observed in northern Victoria Land (Panter *et al.* 2018) or southern Tibet (Guo *et al.* 2015). This pattern is opposite to what might be expected if the subduction component is related to the 0.5 Ga subduction of the palaeo-Pacific Plate beneath East Antarctica. These variations could reflect a regional gradient caused by changing dynamics in a plume some 100 km in

radius or they could be due to differences in decompression melting associated with uplift and rifting and edge-driven mantle flow. A cross-section down to 350 km-depth across East and West Antarctica in southern Victoria Land, showing shear-wave velocity variations in percentage relative to the Preliminary Reference Earth Model (PREM), corresponds with a sharp discontinuity between cold (fast) mantle beneath the Transantarctic Mountains and cratonic East Antarctica, relative to the warm (slow) anomalies beneath the Ross Sea and West Antarctica (Faccenna *et al.* 2008) (Fig. 29), in agreement with other studies (Watson *et al.* 2006; Martin *et al.* 2014a; An *et al.* 2015; Nield *et al.* 2018; Shen *et al.* 2018). This model (Fig. 29) does not have a deep (>150 km) root beneath the Erebus Volcanic Province, which is more consistent with edge-driven mantle flow than mantle pluming (Faccenna *et al.* 2008; Panter *et al.* 2018), although other workers have presented other mantle images which they interpret as evidence of a mantle plume (e.g. Phillips *et al.* 2018, fig. 9). In summary, regional chemical and isotopic changes are consistent with either edge-driven mantle flow or a Cenozoic plume, and geophysical evidence for both has been presented in the literature.

### Summary and conclusions

Over 100 years of petrographical research on rocks from the Erebus Volcanic Province has contributed to understanding the petrogenesis of alkalic volcanic rocks in Antarctica and globally. Based upon petrogenetic and geographical discrimination, the province can be subdivided into four volcanic fields and one local suite. The mantle source for relatively undifferentiated volcanic rocks of the province is complex and variable with HIMU, enriched mantle, carbonatitic and eclogitic crustal components all being involved to variable extents. Equilibration of radiogenic Sr, Nd, Pb and Hf isotopic systems is best explained in terms of a high time-integrated HIMU *sensu stricto* component in the mantle source, at least beneath the Ross Island Volcanic Field. One model Pb isotope age, and major and trace element modelling of melting of a peridotitic source are most consistent with an asthenospheric mantle source for the depleted mantle and HIMU components. This is in contrast to some Cenozoic volcanism localities in Zealandia, where a HIMU-like component reflects the relatively young (Mesozoic) development of highly radiogenic Pb. Spatial (west–east) variations in Sr, Nd and Pb isotopic compositions and Ba/Rb and Nb/Ta ratios can be interpreted to indicate increasing involvement of an eclogitic crustal component eastwards, which is the opposite pattern to that expected if this component was derived from subduction of the palaeo-Pacific Plate beneath East Antarctica at c. 0.5 Ga. If the Pb isochron ages for Ross Island are applicable across the province, then this increasing eclogitic crustal component would derive from fluids derived from, or modified by, a subducting slab with an age >0.5 Ga: that is, not related to subduction of the palaeo-Pacific Plate at around 0.5 Ga.

The review completed in this study has highlighted areas where additional research could benefit the understanding of alkalic volcanic lineages in continental rift systems. These areas of future research can be summarized as:

- Determining when the chemical heterogeneity was developed in the mantle source at multiple eruptive centres across the province.
- Accurate and precise trace element and isotopic (Sr, Nd, Pb, Hf) measurements performed by a common method across multiple eruptive centres to test isotopic equilibration across the province and to test the eastward migration of trace element ratios further.

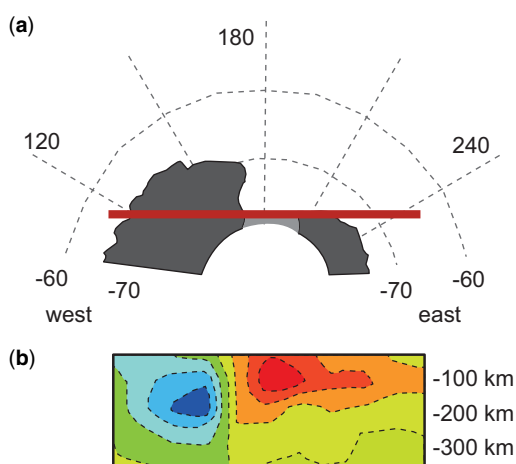


**Fig. 29.** A location diagram (a) and cross-section (b) for Antarctica, the latter showing shear-wave variations in model DM01 (Danesi and Morelli 2001), after Faccenna *et al.* (2008). The cross-section colours represent percentage variations with respect to the anisotropic Preliminary Earth Model (PREM), with the darkest blue colour representing 6% faster than PREM and the darkest red colour representing 5% slower than PREM. The discontinuity between fast (blue) and slow (red) anomalies corresponds with the transition from the Transantarctic Mountains into the Ross Sea.

## Erebus Volcanic Province: petrology

- Analyses that are important but not routinely gathered should be obtained from multiple eruptive centres across the province: for example, halogens (F, Cl, Br, I), CO<sub>2</sub>, isotopes (Os, Re, Hf) and noble gases (He, Ne, Ar, Kr, Xe).
- Key areas are missing, even basic published petrographical information including submarine volcanic centres, Mount Discovery, the Southern Local Suite and some areas around Ross Island (e.g. Lewis Bay). These areas require fieldwork. Furthermore, the area south of the Mount Morning and Discovery volcanic fields is virtually unknown with respect to Cenozoic volcanism. Geophysical investigations should be made to determine whether Cenozoic volcanic rocks are present beneath the Ross Ice Sheet in these areas.
- More work is needed on the plume v. rifting, extension and upwelling melt models to distinguish one from the other.

Despite the long and detailed study of the petrogenesis of volcanic rocks in the Erebus Volcanic Province, many new and exciting research questions remain, and these should, in the future, provide a new generation of Earth scientists with fruitful areas for further research.

**Acknowledgements** We thank Kurt Panter for editorial handling and additional review. Sergio Rocchi, Massimo Pompilio and an anonymous reviewer are thanked for thorough reviews.

**Author contributions** **APM**: conceptualization (lead), data curation (lead), investigation (equal), writing – original draft (lead), writing – review & editing (equal); **AFC**: investigation (equal), writing – original draft (supporting), writing – review & editing (supporting); **RCP**: investigation (equal), writing – original draft (supporting), writing – review & editing (equal); **PRK**: conceptualization (supporting), investigation (equal), writing – original draft (equal), writing – review & editing (supporting); **JAG**: investigation (equal), writing – original draft (supporting), writing – review & editing (supporting).

**Funding** Antarctica New Zealand provided financial and logistical support over several field seasons.

**Data availability** All data generated or analysed during this study are included in this published article (and its supplementary information files).

## References

- Adams, J. 1973. *Petrology and chemistry of an alkaline cone, McMurdo Sound*. BSc (Hon.) thesis, Victoria University of Wellington, Wellington, New Zealand.
- Aldanmaz, E., Pearce, J.A., Thirlwall, M.F. and Mitchell, J.G. 2000. Petrogenetic evolution of late Cenozoic, post-collision volcanism in western Anatolia, Turkey. *Journal of Volcanology and Geothermal Research*, **102**, 67–95, [https://doi.org/10.1016/S0377-0273\(00\)00182-7](https://doi.org/10.1016/S0377-0273(00)00182-7)
- An, M., Wiens, D.A. *et al.* 2015. S-velocity model and inferred Moho topography beneath the Antarctic Plate from Rayleigh waves. *Journal of Geophysical Research: Solid Earth*, **120**, 359–383, <https://doi.org/10.1002/2014JB011332>
- Anderson, J.T.H., Wilson, G.S., Fink, D., Lilly, K., Levy, R.H. and Townsend, D. 2017. Reconciling marine and terrestrial evidence for post LGM ice sheet retreat in southern McMurdo Sound, Antarctica. *Quaternary Science Reviews*, **157**, 1–13, <https://doi.org/10.1016/j.quascirev.2016.12.007>
- Antibus, J.V. 2012. *A Petrographic, Geochemical and Isotopic (Sr, O, H and C) Investigation of Alteration Minerals in Volcaniclastic Rocks at Minna Bluff, Antarctica: Petrogenesis and Implications for Paleoenvironmental Conditions*. MSc thesis, Bowling Green State University, Bowling Green, Ohio, USA.
- Antibus, J.V., Panter, K.S. *et al.* 2014. Alteration of volcanoclastic deposits at Minna Bluff: Geochemical insights on mineralizing environment and climate during the Late Miocene in Antarctica. *Geochemistry, Geophysics, Geosystems*, **15**, 3258–3280, <https://doi.org/10.1002/2014GC005422>
- Armstrong, R.L. 1978. K–Ar dating: Late Cenozoic McMurdo Volcanic Group and dry valley glacial history, Victoria Land, Antarctica. *New Zealand Journal of Geology and Geophysics*, **21**, 685–698, <https://doi.org/10.1080/00288306.1978.10425199>
- Armstrong, R.L., Hamilton, W. and Denton, G.H. 1968. Glaciation in Taylor Valley, Antarctica, older than 2.7 million years. *Science*, **159**, 187–189, <https://doi.org/10.1126/science.159.3811.187>
- Aviador, K.B., Rilling-Hall, S., Bryce, J.G. and Mukasa, S.B. 2015. Submarine and subaerial lavas in the West Antarctic Rift System: Temporal record of shifting magma source components from the lithosphere and asthenosphere. *Geochemistry, Geophysics, Geosystems*, **16**, 4344–4361, <https://doi.org/10.1002/2015GC006076>
- Bannister, S., Yu, J., Leitner, B. and Kennett, B.L.N. 2003. Variations in crustal structure across the transition from West to East Antarctica, Southern Victoria Land. *Geophysical Journal International*, **155**, 870–884, <https://doi.org/10.1111/j.1365-246X.2003.02094.x>
- Barrett, P.J. 1989. *Antarctic Cenozoic History from the CIROS-1 Drillhole, McMurdo Sound*. DSIR Bulletin, **245**.
- Barrett, P.J. and Hambrey, M.J. 1992. Plio-Pleistocene sedimentation in Ferrar Fiord, Antarctica. *Sedimentology*, **39**, 109–123, <https://doi.org/10.1111/j.1365-3091.1992.tb01025.x>
- Barrett, P.J. and McKelvey, B.C. 1986. Stratigraphy. *DSIR Bulletin*, **247**, 9–53.
- Barrett, P.J. and Treves, S.B. 1981. Sedimentology and petrology of core from DVDP 15, Western McMurdo Sound. *American Geophysical Union Antarctic Research Series*, **33**, 281–314.
- Barrett, P.J., Treves, S.B. *et al.* 1976. *Initial Report on DVDP 15, Western McMurdo Sound, Antarctica*. Dry Valleys Drilling Project Bulletin, **7**.
- Barrett, P.J., Fielding, C., Wise, S.W. and the Cape Roberts Science Team. 1998. Initial report on CRP-1, Cape Roberts Project, Antarctica. *Terra Antarctica*, **5**, 187.
- Barrett, P.J., Sarti, M., Wise, S. and the Cape Roberts Science Team. 2000. Studies from the Cape Roberts Project, Ross Sea, Antarctica: Initial report on CRP-3. *Terra Antarctica*, **7**, 209.
- Behrendt, J.C. 1999. Crustal and lithospheric structure of the West Antarctic Rift System from geophysical investigations – a review. *Global and Planetary Change*, **23**, 25–44, [https://doi.org/10.1016/S0921-8181\(99\)00049-1](https://doi.org/10.1016/S0921-8181(99)00049-1)
- Behrendt, J.C., Duerbaum, H.J., Damaske, D., Saltus, R., Bosum, W. and Cooper, A.K. 1991a. Extensive volcanism and related tectonism beneath the western Ross Sea continental shelf, Antarctic. Interpretation of an aeromagnetic survey. In: Thomson, M.R.A., Crame, J.A. and Thomson, J.W. (eds) *Geological Evolution of Antarctica*. Cambridge University Press, New York, 299–304.
- Behrendt, J.C., LeMasurier, W.E., Cooper, A.K., Tessensohn, F., Tréhu, A. and Damaske, D. 1991b. Geophysical studies of the West Antarctic Rift System. *Tectonics*, **10**, 1257–1273, <https://doi.org/10.1029/91tc00868>
- Bentley, C.R. 1991. Configuration and structure of the subglacial crust. In: Tingey, R.J. (ed.) *The Geology of Antarctica*. Clarendon, Oxford, UK, 335–364.
- Berg, J.H. 1984. Crustal inclusions from the Erebus Volcanic Province. *Antarctic Journal of the United States*, **19**, 27.
- Berg, J.H., Hank, R.A. and Kalamarides, R.I. 1985. Petrology and geochemistry of inclusions of lower crustal basic granulites from the Erebus Volcanic Province, Antarctica. *Antarctic Journal of the United States*, **20**, 22–23.
- Blank, H.R., Cooper, R.A., Wheeler, R.H. and Willis, I.A.G. 1963. Geology of the Koettlitz–Blue Glacier region, Southern Victoria Land, Antarctica. *Transactions of the Royal Society of New Zealand*, **2**, 79–102.

- Borchgrevink, C.E. 1901. *First on the Antarctic Continent*. Newnes, London.
- Brodie, J.W. 1959. A shallow shelf around Franklin Island in the Ross Sea, Antarctica. *New Zealand Journal of Geology and Geophysics*, **2**, 108–119, <https://doi.org/10.1080/00288306.1959.10431316>
- Cape Roberts Science Team. 1999. Studies from the Cape Roberts Project: initial report on CRP-2/2A, Ross Sea Antarctica – Summary of results. *Terra Antarctica*, **6**, 156–169.
- Cartwright, K., Treves, S.B. and Torii, T. 1974a. Geology of DVDP 4, Lake Vanda, Wright Valley, Antarctica. *Dry Valleys Drilling Project Bulletin*, **3**, 49–74.
- Cartwright, K., Treves, S.B. and Torii, T. 1974b. Geology of DVDP 5, Don Juan Pond, Wright Valley, Antarctica. *Dry Valleys Drilling Project Bulletin*, **3**, 75–91.
- Chapman-Smith, M. 1975a. Geologic log of DVDP 12, Lake Leon, Taylor Valley. *Dry Valleys Drilling Project Bulletin*, **5**, 61–70.
- Chapman-Smith, M. 1975b. Geologic Log of DVDP 14, North Fork Basin, Wright Valley. *Dry Valleys Drilling Project Bulletin*, **5**, 94–99.
- Chauvel, C., Hofmann, A.W. and Vidal, P. 1992. HIMU-EM: the French Polynesian connection. *Earth and Planetary Science Letters*, **110**, 99–119, [https://doi.org/10.1016/0012-821X\(92\)90042-T](https://doi.org/10.1016/0012-821X(92)90042-T)
- Cole, J.W. and Ewart, A. 1968. Contributions to the volcanic geology of the Black Island, Brown Peninsula, and Cape Bird areas, McMurdo sound, Antarctica. *New Zealand Journal of Geology and Geophysics*, **11**, 793–828, <https://doi.org/10.1080/00288306.1968.10420754>
- Cole, J.W., Kyle, P.R. and Neall, V.E. 1971. Contributions to quaternary geology of Cape Crozier, White Island and Hut Point Peninsula, McMurdo Sound region, Antarctica. *New Zealand Journal of Geology and Geophysics*, **14**, 528–546, <https://doi.org/10.1080/00288306.1971.10421946>
- Coombs, D.S., Cas, R.A., Kawachi, Y., Landis, C.A., McDonough, W.F. and Reay, A. 1986. Cenozoic volcanism in North, East, and Central Otago. *Royal Society of New Zealand Bulletin*, **23**, 278–312.
- Cooper, A.K., Davey, F.J. and Behrendt, J. 1987. Seismic stratigraphy and structure of the Victoria Land basin, western Ross Sea, Antarctica. In: Cooper, A.K. and Davey, F.J. (eds) *The Antarctic Continental Margin: Geology and Geophysics of the Western Ross Sea*. Circum-Pacific Council Energy and Mineral Resources, Houston, TX, 27–65.
- Cooper, A.F., Adam, L.J., Coulter, R.F., Eby, G.N. and McIntosh, W.C. 2007. Geology, geochronology and geochemistry of a basaltic volcano, White Island, Ross Sea, Antarctica. *Journal of Volcanology and Geothermal Research*, **165**, 189–216, <https://doi.org/10.1016/j.jvolgeores.2007.06.003>
- Cox, S.C., Turnbull, I.M., Isaac, M.J., Townsend, D.B. and Smith Lyttle, B. 2012. Geology of southern Victoria Land Antarctica. Institute of Geological and Nuclear Sciences 1:250 000 Geological Map 22. GNS Science, Lower Hutt, New Zealand.
- Csatho, B., Schenk, T. *et al.* 2005. Airborne laser scanning for high-resolution mapping of Antarctica. *Eos, Transactions of the American Geophysical Union*, **86**, 237–238, <https://doi.org/10.1029/2005EO250002>
- Danesi, S. and Morelli, A. 2001. Structure of the upper mantle under the Antarctic Plate from surface wave tomography. *Geophysical Research Letters*, **28**, 4395–4398, <https://doi.org/10.1029/2001GL013431>
- David, T.W.E. and Priestly, R.E. 1914. *Glaciology, Physiography, Stratigraphy and Tectonic Geology of south Victoria Land*. British Antarctic Expedition, 1907–09, Reports on the Scientific Investigations, Geology, **1**. W. Heinemann, London.
- Debenham, F. 1923. *The Physiography of the Ross Archipelago British Antarctic 'Terra Nova' Expedition, 1910–1913*. Harrison, London.
- Del Carlo, P., Panter, K.S., Bassett, K., Bracciali, L., Di Vincenzo, G. and Rocchi, S. 2009. The upper lithostratigraphic unit of ANDRILL AND-2A core (Southern McMurdo Sound, Antarctica): local Pleistocene volcanic sources, paleoenvironmental implications and subsidence in the southern Victoria Land Basin. *Global and Planetary Change*, **69**, 142–161, <https://doi.org/10.1016/j.gloplacha.2009.09.002>
- Denton, G.H. and Marchant, D.R. 2000. The geologic basis for a reconstruction of a grounded ice sheet in McMurdo Sound, Antarctica, at the Last Glacial Maximum. *Geografiska Annaler*, **82A**, 167–211, <https://doi.org/10.1111/j.0435-3676.2000.00121.x>
- Di Roberto, A., Pompilio, M. and Wilch, T.I. 2010. Late Miocene submarine volcanism in ANDRILL AND-1B drill core, Ross Embayment, Antarctica. *Geosphere*, **6**, 524–536, <https://doi.org/10.1130/GES00537.1>
- Di Roberto, A., Del Carlo, P., Rocchi, S. and Panter, K.S. 2012. Early Miocene volcanic activity and paleoenvironment conditions recorded in tephra layers of the AND-2A core (southern McMurdo Sound, Antarctica). *Geosphere*, **8**, 1342–1355, <https://doi.org/10.1130/ges00754.1>
- Di Roberto, A., del Carlo, P. and Pompilio, M. 2021. Marine record of volcanism from drill cores. *Geological Society, London, Memoirs*, **55**, <https://doi.org/10.1144/M55-2018-49>
- Di Vincenzo, G., Palmeri, R., Talarico, F., Andriessen, P.A.M. and Ricci, G.A. 1997. Petrology and geochronology of eclogites from the Lanterman Range, Antarctica. *Journal of Petrology*, **38**, 1391–1417, <https://doi.org/10.1093/ptro/38.10.1391>
- Di Vincenzo, G., Bracciali, L., Del Carlo, P., Panter, K. and Rocchi, S. 2010.  $^{40}\text{Ar}$ – $^{39}\text{Ar}$  dating of volcanogenic products from the AND-2A core (ANDRILL Southern McMurdo Sound Project, Antarctica): correlations with the Erebus Volcanic Province and implications for the age model of the core. *Bulletin of Volcanology*, **72**, 487–505, <https://doi.org/10.1007/s00445-009-0337-z>
- Dunbar, N.W. and Kurbatov, A.V. 2011. Tephrochronology of the Siple Dome ice core, West Antarctica: correlations and sources. *Quaternary Science Reviews*, **30**, 1602–1614, <https://doi.org/10.1016/j.quascirev.2011.03.015>
- Dunbar, N.W., Iverson, N.A. *et al.* 2017. New Zealand supereruption provides time marker for the Last Glacial Maximum in Antarctica. *Scientific Reports*, **7**, 12238, <https://doi.org/10.1038/s41598-017-11758-0>
- Ellerman, P.J. and Kyle, P.R. 1990a. Beaufort Island. *American Geophysical Union Antarctic Research Series*, **48**, 94–96.
- Ellerman, P.J. and Kyle, P.R. 1990b. Franklin Island. *American Geophysical Union Antarctic Research Series*, **48**, 91–93.
- Esser, R.P., Kyle, P.R. and McIntosh, W.C. 2004.  $^{40}\text{Ar}$ – $^{39}\text{Ar}$  dating of the eruptive history of Mount Erebus, Antarctica: volcano evolution. *Bulletin of Volcanology*, **66**, 671–686, <https://doi.org/10.1007/s00445-004-0354-x>
- Faccenna, C., Rossetti, F., Becker, T.W., Danesi, S. and Morelli, A. 2008. Recent extension driven by mantle upwelling beneath the Admiralty Mountains (East Antarctica). *Tectonics*, **27**, TC4015, <https://doi.org/10.1029/2007TC002197>
- Fargo, A. 2009.  $^{40}\text{Ar}$ – $^{39}\text{Ar}$  Geochronological Analysis of Minna Bluff, Antarctica: Evidence for Past Glacial Events within the Ross Embayment. MS thesis, New Mexico Institute of Mining and Technology, Socorro, New Mexico, USA.
- Fargo, A., McIntosh, W., Dunbar, N. and Wilch, T. 2008.  $^{40}\text{Ar}$ – $^{39}\text{Ar}$  geochronology of Minna Bluff, Antarctica: Timing of mid-Miocene glacial erosional events within the Ross Embayment. Abstract presented at the 2008 AGU Fall Meeting, December 15–19, 2008, San Francisco, California, USA.
- Ferrar, H.T. 1905. Notes on the physical geography of the Antarctic. *The Geographical Journal*, **25**, 373–382, <https://doi.org/10.2307/1776138>
- Ferrar, H.T. 1907. Report on the field-geology of the region explored during the 'Discovery' Antarctic expedition, 1901–1904. *Natural History*, **1**, 1–100.
- Fielding, C.R., Thomson, M.R.A. and the Cape Roberts Science Team. 1999. Studies from the Cape Roberts Project, Ross Sea, Antarctica: initial report on CRP-2/2A. *Terra Antarctica*, **6**, 173.
- Fielding, C.R., Henrys, S.A. and Wilson, T.J. 2006. Rift history of the western Victoria Land Basin: a new perspective based on integration of cores with seismic reflection data. In: Futterer, D.K.,

## Erebus Volcanic Province: petrology

- Damaske, D., Kleinschmidt, G., Miller, H. and Tessensohn, F. (eds) *Antarctica: Contributions to Global Earth Sciences*. Springer, Berlin, 307–316.
- Fielding, C.R., Atkins, C.B. *et al.* 2008. Sedimentology and Stratigraphy of the AND-2A Core, ANDRILL Southern McMurdo Sound Project, Antarctica. *Terra Antarctica*, **15**, 77–112.
- Fielding, C.R., Browne, G.H. *et al.* 2011. Sequence stratigraphy of the ANDRILL AND-2A drillcore, Antarctica: a long-term, ice-proximal record of Early to Mid-Miocene climate, sea-level and glacial dynamism. *Palaeogeography, Palaeoclimatology, Palaeoecology*, **305**, 337–351, <https://doi.org/10.1016/j.palaeo.2011.03.026>
- Finn, C.A., Müller, R.D. and Panter, K.S. 2005. A Cenozoic diffuse alkaline magmatic province (DAMP) in the southwest Pacific without rift or plume origin. *Geochemistry, Geophysics, Geosystems*, **6**, Q02005, <https://doi.org/10.1029/2004gc000723>
- Fletcher, L. and Bell, J.F. (eds). 1907. *National Antarctic Expedition 1901–1904. Natural History. Volume I. Geology (Field-geology: Petrography)*. Trustees of the British Museum, London.
- Forbes, R.B., Turner, D.L. and Garden, J.R. 1974. Age of trachyte from Ross Island, Antarctica. *Geology*, **2**, 297–298, [https://doi.org/10.1130/0091-7613\(1974\)2<297:AOTFRI>2.0.CO;2](https://doi.org/10.1130/0091-7613(1974)2<297:AOTFRI>2.0.CO;2)
- Furman, T. and Graham, D. 1999. Erosion of lithospheric mantle beneath the East African Rift system: geochemical evidence from the Kivu volcanic province. *Lithos*, **48**, 237–262, [https://doi.org/10.1016/S0024-4937\(99\)00031-6](https://doi.org/10.1016/S0024-4937(99)00031-6)
- Gale, A., Dalton, C.A., Langmuir, C.H., Su, Y. and Schilling, J.-G. 2013. The mean composition of ocean ridge basalts. *Geochemistry, Geophysics, Geosystems*, **14**, 489–518, <https://doi.org/10.1029/2012GC004334>
- Gamble, J.A. and Kyle, P.R. 1987. The origins of glass and amphibole in spinel–wehrlite xenoliths from Foster Crater, McMurdo Volcanic Group, Antarctica. *Journal of Petrology*, **28**, 755–779, <https://doi.org/10.1093/petrology/28.5.755>
- Gamble, J.A., Barrett, P.J. and Adams, C.J. 1986. Basaltic clasts from Unit 8. *DSIR Bulletin*, **247**, 145–152.
- Gamble, J.A., McGibbon, F., Kyle, P.R., Menzies, M. and Kirsch, I. 1988. Metasomatised xenoliths from Foster Crater, Antarctica: Implications for lithospheric structure and process beneath the Transantarctic Mountain front. *Journal of Petrology*, Special Volume, Issue 1, 109–138, [https://doi.org/10.1093/petrology/Special\\_Volume\\_1.109](https://doi.org/10.1093/petrology/Special_Volume_1.109)
- Gamble, J.A., Adams, C.J., Morris, P.A., Wysoczanski, R.J., Handler, M. and Timm, C. 2018. The geochemistry and petrogenesis of Carnley Volcano, Auckland Islands, SW Pacific. *New Zealand Journal of Geology and Geophysics*, **61**, 480–497, <https://doi.org/10.1080/00288306.2018.1505642>
- George, A. 1989. Sand provenance. *DSIR Bulletin*, **245**, 159–167.
- Giggenbach, W.F., Kyle, P.R. and Lyon, G.L. 1973. Present volcanic activity on Mount Erebus, Ross Island, Antarctica. *Geology*, **1**, 135–136, [https://doi.org/10.1130/0091-7613\(1973\)1<135:PVAOME>2.0.CO;2](https://doi.org/10.1130/0091-7613(1973)1<135:PVAOME>2.0.CO;2)
- Global Volcanism Program. 2013a. Discovery (590835). In: Venzke, E. (ed.) *Volcanoes of the World*, v. 4.6.7. Smithsonian Institution. Downloaded 06 Apr 2018 (<http://volcano.si.edu/volcano.cfm?vn=590835>), <https://doi.org/10.5479/si.GVP.VOTW4-2013>
- Global Volcanism Program. 2013b. Morning (390017). In: Venzke, E. (ed.) *Volcanoes of the World*, v. 4.6.7. Smithsonian Institution. Downloaded 03 Apr 2018 (<http://volcano.si.edu/volcano.cfm?vn=390017>), <https://doi.org/10.5479/si.GVP.VOTW4-2013>
- Goldich, S., Treves, S., Suhr, N. and Stuckless, J. 1975. Geochemistry of the Cenozoic volcanic rocks of Ross Island and vicinity, Antarctica. *The Journal of Geology*, **83**, 415–435, <https://doi.org/10.1086/628120>
- Goldich, S.S., Stuckless, J.S., Suhr, N.H., Bodkin, J.B. and Wamser, R.C. 1981. Some Trace Element Relationships in the Cenozoic Volcanic Rocks from Ross Island and Vicinity, Antarctica. *American Geophysical Union Antarctic Research Series*, **33**, 215–228.
- Grapes, R., Gamble, J. and Palmer, K. 1989. Basal dolerite boulders. *DSIR Bulletin*, **245**, 169–174.
- Grindley, G.W. and Oliver, P.J. 1983. Palaeomagnetism of Cretaceous volcanic rocks from Marie Byrd Land, Antarctica. In: Oliver, R.L., James, P.R. and Jago, J.B. (eds) *Antarctic Earth Science*. Cambridge University Press, Cambridge, UK, 573–578.
- Gunn, B.M. and Warren, G. 1962. *Geology of Victoria Land between the Mawson and Mullock Glaciers, Antarctica*. New Zealand Geological Survey Bulletin, **71**.
- Guo, Z., Wilson, M., Zhang, M., Cheng, Z. and Zhang, L. 2015. Post-collisional ultrapotassic mafic magmatism in South Tibet: Products of partial melting of pyroxenite in the mantle wedge induced by roll-back and delamination of the subducted Indian continental lithosphere slab. *Journal of Petrology*, **56**, 1365–1406, <https://doi.org/10.1093/petrology/egv040>
- Hall, B.L., Denton, G.H., Lux, D.R. and Bockheim, J.G. 1993. Late Tertiary Antarctic paleoclimate and ice-sheet dynamics inferred from surficial deposits in Wright Valley. *Geografiska Annaler. Series A, Physical Geography*, **75**(4), 239–267.
- Hall, C.E., Cooper, A.F. and Parkinson, D.L. 1995. Early Cambrian carbonatite in Antarctica. *Journal of the Geological Society, London*, **152**, 721–728, <https://doi.org/10.1144/gsjgs.152.4.0721>
- Hall, J., Wilson, T. and Henrys, S. 2007. Structure of the central Terror Rift, western Ross Sea, Antarctica. *United States Geological Survey Open-File Report*, **2007-1047**, Short Research Paper 108.
- Halliday, A.N., Lee, D.-C., Tommasini, S., Davies, G.R., Paslick, C.R., Fitton, J.G. and James, D.E. 1995. Incompatible trace elements in OIB and MORB and source enrichment in the sub-oceanic mantle. *Earth and Planetary Science Letters*, **133**, 379–395, [https://doi.org/10.1016/0012-821X\(95\)00097-V](https://doi.org/10.1016/0012-821X(95)00097-V)
- Hambrey, M.J., Barrett, P.J. and Robinson, P.H. 1989. Stratigraphy. *DSIR Bulletin*, **245**, 23–48.
- Harpel, C.J., Kyle, P.R. and Dunbar, N.W. 2008. Englacial tephrostratigraphy of Erebus volcano, Antarctica. *Journal of Volcanology and Geothermal Research*, **177**, 549–568, <https://doi.org/10.1016/j.jvolgeores.2008.06.001>
- Harrington, H.J. 1958a. Beaufort Island, remnant of a Quaternary volcano in the Ross Sea, Antarctica. *New Zealand Journal of Geology and Geophysics*, **1**, 595–603, <https://doi.org/10.1080/00288306.1958.10423167>
- Harrington, H.J. 1958b. Nomenclature of rock units in the Ross Sea Region, Antarctica. *Nature*, **182**, 290, <https://doi.org/10.1038/182290a0>
- Harrington, H.J. 1965. Geology and morphology of Antarctica. *Monographiae Biologicae*, **15**, 1–71, [http://doi-org-443.webvpn.fjmu.edu.cn/10.1007/978-94-015-7204-0\\_1](http://doi-org-443.webvpn.fjmu.edu.cn/10.1007/978-94-015-7204-0_1)
- Harris, H. and Mudrey, M.G. 1974. Core from Lake Fryxell, DVDP 7, and general geology of Lake Fryxell Area, Taylor Valley. *Dry Valleys Drilling Project Bulletin*, **3**, 109–119.
- Haskell, T.R., Kennett, I.P., Prebble, W.M., Smith, G. and Willis, I.A.G. 1965. The geology of the middle and lower Taylor Valley of South Victoria Land, Antarctica. *Transactions of the Royal Society of New Zealand*, **2**, 169–186.
- Hauri, E.H., Whitehead, J.A. and Hart, S.R. 1994. Fluid dynamic and geochemical aspects of entrainment in mantle plumes. *Journal of Geophysical Research: Solid Earth*, **99**, 24 275–24 300, <https://doi.org/10.1029/94JB01257>
- Herzberg, C. 2011. Identification of source lithology in the Hawaiian and Canary Islands: implications for origins. *Journal of Petrology*, **52**, 113–146, <https://doi.org/10.1093/petrology/egq075>
- Hillenbrand, C.D., Moreton, S.G. *et al.* 2008. Volcanic time-markers for Marine Isotopic Stages 6 and 5 in Southern Ocean sediments and Antarctic ice cores: implications for tephra correlations between palaeoclimatic records. *Quaternary Science Reviews*, **27**, 518–540, <https://doi.org/10.1016/j.quascirev.2007.11.009>
- Hofmann, A.W. and White, W.M. 1982. Mantle plumes from ancient oceanic crust. *Earth and Planetary Science Letters*, **57**, 421–436, [https://doi.org/10.1016/0012-821X\(82\)90161-3](https://doi.org/10.1016/0012-821X(82)90161-3)
- Houghton, B.F., Weaver, S.D., Wilson, C.J.N. and Lanphere, M.A. 1992. Evolution of a Quaternary peralkaline volcano: Mayor

- Island, New Zealand. *Journal of Volcanology and Geothermal Research*, **51**, 217–236, [https://doi.org/10.1016/0377-0273\(92\)90124-V](https://doi.org/10.1016/0377-0273(92)90124-V)
- Iacovino, K., Oppenheimer, C., Scaillet, B. and Kyle, P. 2016. Storage and evolution of mafic and intermediate alkaline magmas beneath Ross Island, Antarctica. *Journal of Petrology*, **57**, 93–118, <https://doi.org/10.1093/petrology/egv083>
- Iverson, N.A., Kyle, P.R., Dunbar, N.W., McIntosh, W.C. and Pearce, N.J.G. 2014. Eruptive history and magmatic stability of Erebus volcano, Antarctica: Insights from englacial tephra. *Geochemistry, Geophysics, Geosystems*, **15**, 4180–4202, <https://doi.org/10.1002/2014GC005435>
- Jensen, H.I. 1916. *Report on the Petrology of the Alkaline Rocks of Mount Erebus, Antarctica*. Heinemann, London.
- Kalamarides, R.I., Berg, J.H. and Hank, R.A. 1987. Lateral isotopic discontinuity in the lower crust: an example from Antarctica. *Science*, **237**, 1192–1195, <https://doi.org/10.1126/science.237.4819.1192>
- Kelly, P.J., Kyle, P.R., Dunbar, N.W. and Sims, K.W.W. 2008. Geochemistry and mineralogy of the phonolite lava lake, Erebus volcano, Antarctica: 1972–2004 and comparison with older lavas. *Journal of Volcanology and Geothermal Research*, **177**, 589–605, <https://doi.org/10.1016/j.jvolgeores.2007.11.025>
- Keys, J.R., Anderton, P.W. and Kyle, P.R. 1977. Tephra and debris layers in the Skelton Neve and Kempe Glacier, South Victoria Land, Antarctica. *New Zealand Journal of Geology and Geophysics*, **20**, 971–1002, <https://doi.org/10.1080/00288306.1977.10420692>
- Kinzler, R.J. 1997. Melting of mantle peridotite at pressures approaching the spinel to garnet transition: application to mid-ocean ridge basalt petrogenesis. *Journal of Geophysical Research: Solid Earth*, **102**, 853–874, <https://doi.org/10.1029/96jb00988>
- Kipf, A., Hauff, F. *et al.* 2014. Seamounts off the West Antarctic margin: a case for non-hotspot driven intraplate volcanism. *Gondwana Research*, **25**, 1660–1679, <https://doi.org/10.1016/j.gcr.2013.06.013>
- Kirsch, I.D. 1981. *Evidence for Mantle Metasomatism in Ultramafic Inclusions from Foster Crater, Antarctica*. MSc thesis, Ohio State University, Columbus, Ohio, USA.
- Krissek, L.A., Browne, G. *et al.* 2007. Sedimentology and stratigraphy of the ANDRILL McMurdo Ice Shelf (AND-1B) core. *United States Geological Survey Open-File Report*, **2007-1047**, Extended Abstract 148.
- Kuno, H. 1966. Lateral variation of basalt magma types across continental margins and island arcs. *Bulletin of Volcanology*, **29**, 195–222, <https://doi.org/10.1007/BF02597153>
- Kurasawa, H., Yoshida, Y. and Mudrey, M.G. 1974. Geological log of the Lake Vida core – DVDP 6. *Dry Valleys Drilling Project Bulletin*, **3**, 92–108.
- Kyle, P.R. 1976. *Geology, Mineralogy, and Geochemistry of the Late Cenozoic McMurdo Volcanic Group, Victoria Land, Antarctica*. PhD thesis, Victoria University of Wellington, Wellington, New Zealand.
- Kyle, P.R. 1977. Mineralogy and glass chemistry of recent volcanic ejecta from Mt Erebus, Ross Island, Antarctica. *New Zealand Journal of Geology and Geophysics*, **20**, 1123–1146, <https://doi.org/10.1080/00288306.1977.10420699>
- Kyle, P.R. 1981a. Glacial history of the McMurdo Sound area as indicated by the distribution and nature of McMurdo Volcanic Group Rocks. *American Geophysical Union Antarctic Research Series*, **33**, 403–412.
- Kyle, P.R. 1981b. Mineralogy and geochemistry of a basanite to phonolite sequence at Hut Point Peninsula, Antarctica, based on core from Dry Valley Drilling Project Drillholes 1, 2 and 3. *Journal of Petrology*, **22**, 451–500, <https://doi.org/10.1093/petrology/22.4.451>
- Kyle, P.R. 1990a. McMurdo Volcanic Group, western Ross Embayment: introduction. *American Geophysical Union Antarctic Research Series*, **48**, 18–25.
- Kyle, P.R. 1990b. Erebus Volcanic Province summary. *American Geophysical Union Antarctic Research Series*, **48**, 81–88.
- Kyle, P.R. (ed.). 1994. *Volcanological and Environmental Studies of Mount Erebus*. *American Geophysical Union Antarctic Research Series*, **66**.
- Kyle, P.R. and Cole, J.W. 1974. Structural control of volcanism in the McMurdo Volcanic Group, Antarctica. *Bulletin Volcanologique*, **38**, 16–25, <https://doi.org/10.1007/bf02597798>
- Kyle, P.R. and Muncy, H.L. 1978. Volcanic geology of the lower slopes of Mount Morning. *Antarctic Journal of the United States*, **13**, 34–36.
- Kyle, P.R. and Muncy, H.L. 1983. The geology of the Mid-Miocene McMurdo Volcanic Group at Mount Morning, McMurdo Sound, Antarctica. In: Oliver, R.L., James, P.R. and Jago, J.B. (eds) *Antarctic Earth Science, 4th International Symposium on Antarctic Earth Science*. Australian Academy Science, Adelaide, Australia, 675.
- Kyle, P.R. and Muncy, H.L. 1989. Geology and geochronology of McMurdo Volcanic Group rocks in the vicinity of Lake Morning, McMurdo Sound, Antarctica. *Antarctic Science*, **1**, 345–350, <https://doi.org/10.1017/S0954102089000520>
- Kyle, P.R. and Price, R.C. 1975. Occurrences of rhönite in alkaline lavas of the McMurdo Volcanic Group, Antarctica and Dunedin volcano, New Zealand. *American Mineralogist*, **60**, 722–725.
- Kyle, P.R., Adams, J. and Rankin, P.C. 1979a. Geology and petrology of the McMurdo Volcanic Group at Rainbow Ridge, Brown Peninsula, Antarctica. *Geological Society of America Bulletin*, **90**, 676, [https://doi.org/10.1130/0016-7606\(1979\)90<676:GAPOTM>2.0.CO;2](https://doi.org/10.1130/0016-7606(1979)90<676:GAPOTM>2.0.CO;2)
- Kyle, P.R., Sutter, J.F. and Treves, S.B. 1979b. K/Ar age determinations on drill core from DVDP holes 1 and 2. *Memoirs of the National Institute of Polar Research (Japan)*, **13**, Special Issue, 214–219.
- Kyle, P.R., Dibble, R.R., Giggenbach, W.F. and Keys, J. 1982. Volcanic activity associated with the anorthoclase phonolite lava lake, Mount Erebus, Antarctica. In: Craddock, C. (ed.) *Antarctic Geosciences*. University of Wisconsin Press, Madison, WI, 735–745.
- Kyle, P.R., Wright, A.C. and Kirsch, I. 1987. Ultramafic xenoliths in the late Cenozoic McMurdo Volcanic Group, western Ross Sea embayment, Antarctica. In: Nixon, P.H. (ed.) *Mantle Xenoliths*. John Wiley & Sons, Chichester, UK, 287–293.
- Kyle, P.R., Moore, J.A. and Thirlwall, M.F. 1992. Petrologic Evolution of Anorthoclase Phonolite Lavas at Mount Erebus, Ross Island, Antarctica. *Journal of Petrology*, **33**, 849–875, <https://doi.org/10.1093/petrology/33.4.849>
- Lawrence, K.P., Tauxe, L., Staudigel, H., Constable, C.G., Koppers, A., McIntosh, W. and Johnson, C.L. 2009. Paleomagnetic field properties at high southern latitude. *Geochemistry, Geophysics, Geosystems*, **10**, <https://doi.org/10.1029/2008GC002072>
- Lawver, L.A., Davis, M.B., Wilson, T.J. and Shipboard Scientific Party. 2007. Neotectonic and other features of the Victoria Land Basin, Antarctica, interpreted from multibeam bathymetry data. *United States Geological Survey Open-File Report*, **2007-1047**, Extended Abstract 017.
- Lawver, L., Lee, J., Kim, Y. and Davey, F. 2012. Flat-topped mounds in western Ross Sea: Carbonate mounds or subglacial volcanic features? *Geosphere*, **8**, 645–653, <https://doi.org/10.1130/GES00766.1>
- Le Bas, M., Maitre, M.J., Streckeisen, A. and Zanettin, B. 1986. A chemical classification of volcanic rocks based on the total alkali–silica diagram. *Journal of Petrology*, **27**, 745–750, <https://doi.org/10.1093/petrology/27.3.745>
- Lee, M.J., Lee, J.I., Kim, T.H., Lee, J. and Nagao, K. 2015. Age, geochemistry and Sr–Nd–Pb isotopic compositions of alkali volcanic rocks from Mt. Melbourne and the western Ross Sea, Antarctica. *Geosciences Journal*, **19**, 681–695, <https://doi.org/10.1007/s12303-015-0061-y>
- Le Maitre, R.W., Streckeisen, A. *et al.* 2002. *Igneous Rocks. A Classification and Glossary of Terms: Recommendations of the International Union of Geological Sciences Subcommission of the Systematics of Igneous Rocks*, 2nd edn. Cambridge University Press, Cambridge, UK.

## Erebus Volcanic Province: petrology

- LeMasurier, W. 2013. Shield volcanoes of Marie Byrd Land, West Antarctic rift: oceanic island similarities, continental signature, and tectonic controls. *Bulletin of Volcanology*, **75**, 726, <https://doi.org/10.1007/s00445-013-0726-1>
- LeMasurier, W.E. and Wade, A.F. 1968. Fumarolic activity in Marie Byrd Land, Antarctica. *Science*, **162**, 352, <https://doi.org/10.1126/science.162.3851.352>
- LeMasurier, W.E., McIntosh, M.C., Ellerman, P.J. and Wright, A.C. 1983. USCGS Glacier cruise 1, December 1982–January 1983: Reconnaissance of hyaloclastites in the western Ross Sea Region. *Antarctic Journal of the United States*, **18**, 60–61.
- Lewis, A., Marchant, D., Ashworth, A., Hemming, S. and Machlus, M. 2007. Major middle Miocene global climate change: Evidence from East Antarctica and the Transantarctic Mountains. *Geological Society of America Bulletin*, **119**, 1449–1461, [https://doi.org/10.1130/0016-7606\(2007\)119\[1449:MMMGCC\]2.0.CO;2](https://doi.org/10.1130/0016-7606(2007)119[1449:MMMGCC]2.0.CO;2)
- Lewis, A.R., Marchant, D.R. *et al.* 2008. Mid-Miocene cooling and the extinction of tundra in continental Antarctica. *Proceedings of the National Academy of Sciences of the United States of America*, **105**, 10 676–10 680, <https://doi.org/10.1073/pnas.0802501105>
- Luckman, P. 1974. *Products of submarine and subglacial volcanism in the McMurdo Sound region, Ross Island, Antarctica*. BSc (Hon.), Victoria University of Wellington, Wellington, New Zealand.
- Mankinen, E.A. and Cox, A. 1988. Paleomagnetic investigation of some volcanic rocks from the McMurdo Volcanic Province, Antarctica. *Journal of Geophysical Research*, **93**, 11 599–11 612, <https://doi.org/10.1029/JB093iB10p11599>
- Marchant, D.R., Denton, G.H., Swisher, I.I.C.C. and Potter, J.N. 1996. Late Cenozoic Antarctic paleoclimate reconstructed from volcanic ashes in the Dry Valleys region of southern Victoria Land. *Geological Society of America Bulletin*, **108**, 181–194, [https://doi.org/10.1130/0016-7606\(1996\)108<0181:LCAPRF>2.3.CO;2](https://doi.org/10.1130/0016-7606(1996)108<0181:LCAPRF>2.3.CO;2)
- Martin, A.P. 2009. *Mount Morning, Antarctica: Geochemistry, Geochronology, Petrology, Volcanology, and Oxygen Fugacity of the Rifted Antarctic Lithosphere*. PhD thesis, University of Otago, Dunedin, New Zealand.
- Martin, A.P. and Cooper, A.F. 2010. Post 3.9 Ma fault activity within the West Antarctic rift system: onshore evidence from Gandalf Ridge, Mount Morning eruptive centre, southern Victoria Land, Antarctica. *Antarctic Science*, **22**, 513–521, <https://doi.org/10.1017/S095410201000026X>
- Martin, A.P., Cooper, A.F. and Dunlap, W.J. 2010. Geochronology of Mount Morning, Antarctica: Two-phase evolution of a long-lived trachyte–basanite–phonolite eruptive center. *Bulletin of Volcanology*, **72**, 357–371, <https://doi.org/10.1007/s00445-009-0319-1>
- Martin, A.P., Cooper, A.F. and Price, R.C. 2013. Petrogenesis of Cenozoic, alkalic volcanic lineages at Mount Morning, West Antarctica and their entrained lithospheric mantle xenoliths: lithospheric v. asthenospheric mantle sources. *Geochimica et Cosmochimica Acta*, **122**, 127–152, <https://doi.org/10.1016/j.gca.2013.08.025>
- Martin, A.P., Cooper, A.F. and Price, R.C. 2014a. Increased mantle heat flow with on-going rifting of the West Antarctic rift system inferred from characterisation of plagioclase peridotite in the shallow Antarctic mantle. *Lithos*, **190–191**, 173–190, <https://doi.org/10.1016/j.lithos.2013.12.012>
- Martin, A.P., Price, R.C. and Cooper, A.F. 2014b. Constraints on the composition, source and petrogenesis of plagioclase-bearing mantle peridotite. *Earth-Science Reviews*, **138**, 89–101, <https://doi.org/10.1016/j.earscirev.2014.08.006>
- Martin, A.P., Cooper, A.F., Price, R.C., Turnbull, R.E. and Roberts, N.M.W. 2015a. The petrology, geochronology and significance of Granite Harbour Intrusive Complex xenoliths and outcrop sampled in western McMurdo Sound, Southern Victoria Land, Antarctica. *New Zealand Journal of Geology and Geophysics*, **58**, 33–51, <https://doi.org/10.1080/00288306.2014.982660>
- Martin, A.P., Price, R.C., Cooper, A.F. and McCammon, C.A. 2015b. Petrogenesis of the rifted Southern Victoria Land lithospheric mantle, Antarctica, inferred from petrography, geochemistry, thermobarometry and oxybarometry of peridotite and pyroxenite xenoliths from the Mount Morning eruptive centre. *Journal of Petrology*, **56**, 193–226, <https://doi.org/10.1093/petrology/egu075>
- Martin, A.P., Smellie, J.L., Cooper, A.F. and Townsend, D.B. 2018. Formation of a spatter-rich pyroclastic density current deposit in a Neogene sequence of trachytic–mafic igneous rocks at Mason Spur, Erebus volcanic province, Antarctica. *Bulletin of Volcanology*, **80**, 13, <https://doi.org/10.1007/s00445-017-1188-7>
- Mawson, D. 1916. Petrology of rock collections from the mainland of South Victoria Land. British Antarctic Expedition 1907–09. Reports and scientific investigations. *Geology*, **II**, 161–168.
- McCoy-West, A.J., Bennett, V.C. and Amelin, Y. 2016. Rapid Cenozoic ingrowth of isotopic signatures simulating ‘HIMU’ in ancient lithospheric mantle: distinguishing source from process. *Geochimica et Cosmochimica Acta*, **187**, 79–101, <https://doi.org/10.1016/j.gca.2016.05.013>
- McCraw, J.D. 1962. Volcanic Detritus in Taylor valley, Victoria Land, Antarctica. *New Zealand Journal of Geology and Geophysics*, **5**, 740–745, <https://doi.org/10.1080/00288306.1962.10417635>
- McCraw, J.D. 1967. Soils of Taylor Dry Valley, Victoria Land, Antarctica, with notes on soils from other localities in Victoria Land. *New Zealand Journal of Geology and Geophysics*, **10**, 498–539, <https://doi.org/10.1080/00288306.1967.10426754>
- McDonough, W.F. and Sun, S.-S. 1995. The composition of the Earth. *Chemical Geology*, **120**, 223–253, [https://doi.org/10.1016/0009-2541\(94\)00140-4](https://doi.org/10.1016/0009-2541(94)00140-4)
- McGibbon, F.M. 1991. Geochemistry and petrology of ultramafic xenoliths of the Erebus Volcanic Province. In: Thomson, M.R.A., Crame, J.A. and Thomson, J.W. (eds) *Geological Evolution of Antarctica*. Cambridge University Press, Cambridge, UK, 317–321.
- McIntosh, W.C. 1998.  $^{40}\text{Ar}/^{39}\text{Ar}$  geochronology of volcanic clasts and pumice in CRP\_1 core, Cape Roberts, Antarctica. *Terra Antarctica*, **5**, 683–690.
- McIntosh, W.C. 2000.  $^{40}\text{Ar}/^{39}\text{Ar}$  geochronology of tephra and volcanic clasts in CRP-2A, Victoria Land Basin, Antarctica. *Terra Antarctica*, **7**, 621–630.
- McIver, J.R. and Gevers, T.W. 1970. Volcanic vents below the Royal Society Range, Central Victoria Land, Antarctica. *Transactions of the Geological Society of South Africa*, **73**, 65–88.
- McKenzie, D.A.N. and O’Nions, R.K. 1991. Partial melt distributions from inversion of rare earth element concentrations. *Journal of Petrology*, **32**, 1021–1091, <https://doi.org/10.1093/petrology/32.5.1021>
- McKenzie, D.A.N. and O’Nions, R.K. 1995. The source regions of ocean island basalts. *Journal of Petrology*, **36**, 133–159, <https://doi.org/10.1093/petrology/36.1.133>
- Middlemost, E.A.K. 1989. Iron oxidation ratios, norms and the classification of volcanic rocks. *Chemical Geology*, **77**, 19–26, [https://doi.org/10.1016/0009-2541\(89\)90011-9](https://doi.org/10.1016/0009-2541(89)90011-9)
- Moore, J. and Kyle, P. 1987. Volcanic geology of Mount Erebus, Ross Island, Antarctica. *Proceedings of the NIPR Symposium on Antarctic Geosciences*, **1**, 48–65.
- Moussallam, Y., Oppenheimer, C., Scaillet, B. and Kyle, P.R. 2013. Experimental phase-equilibrium constraints on the phonolite magmatic system of Erebus volcano, Antarctica. *Journal of Petrology*, **54**, 1285–1307, <https://doi.org/10.1093/petrology/egt012>
- Moussallam, Y., Oppenheimer, C. *et al.* 2015. Megacrystals track magma convection between reservoir and surface. *Earth and Planetary Science Letters*, **413**, 1–12, <https://doi.org/10.1016/j.epsl.2014.12.022>
- Mudrey, M.G., Torii, T. and Harris, H. 1975. Geology of DVDP 13 – Don Juan Pond, Wright Valley, Antarctica. *Dry Valleys Drilling Project Bulletin*, **5**, 78–93.

- Muncy, H.L. 1979. *Geologic History and Petrogenesis of Alkaline Volcanic Rocks, Mount Morning, Antarctica*. MSc thesis, Ohio State University, Columbus, Ohio, USA.
- Naish, T., Powell, R. *et al.* 2009. Obliquity-paced Pliocene West Antarctic ice sheet oscillations. *Nature*, **458**, 322, <https://doi.org/10.1038/nature07867>, <https://www.nature.com/articles/nature07867#supplementary-information>
- Narcisi, B., Petit, J.R. and Langone, A. 2017. Last glacial tephra layers in the Talos Dome ice core (peripheral East Antarctic Plateau), with implications for chronostratigraphic correlations and regional volcanic history. *Quaternary Science Reviews*, **165**, 111–126, <https://doi.org/10.1016/j.quascirev.2017.04.025>
- Nield, G.A., Whitehouse, P.L., van der Wal, W., Blank, B., O'Donnell, J.P. and Stuart, G.W. 2018. The impact of lateral variations in lithospheric thickness on glacial isostatic adjustment in West Antarctica. *Geophysical Journal International*, **214**, 811–824, <https://doi.org/10.1093/gji/ggy158>
- Nyland, R.E., Panter, K.S. *et al.* 2013. Volcanic activity and its link to glaciation cycles: Single-grain age and geochemistry of Early to Middle Miocene volcanic glass from ANDRILL AND-2A core, Antarctica. *Journal of Volcanology and Geothermal Research*, **250**, 106–128, <https://doi.org/10.1016/j.jvolgeores.2012.11.008>
- Oppenheimer, C. and Kyle, P.R. 2008. Probing the magma plumbing of Erebus volcano, Antarctica, by open-path FTIR spectroscopy of gas emissions. *Journal of Volcanology and Geothermal Research*, **177**, 743–754, <https://doi.org/10.1016/j.jvolgeores.2007.08.022>
- Panter, K.S., Kyle, P.R. and Smellie, J.L. 1997. Petrogenesis of a phonolite–trachyte succession at Mount Sidley, Marie Byrd Land, Antarctica. *Journal of Petrology*, **38**, 1225–1253, <https://doi.org/10.1093/ptro/38.9.1225>
- Panter, K.S., Blusztajn, J., Hart, S.R., Kyle, P.R., Esser, R. and McIntosh, W.C. 2006. The origin of HIMU in the SW Pacific: Evidence from intraplate volcanism in southern New Zealand and subantarctic islands. *Journal of Petrology*, **47**, 1673–1704, <https://doi.org/10.1093/ptrology/eg1024>
- Panter, K., Talarico, F. *et al.* 2008. Petrologic and geochemical composition of the AND-2A core, ANDRILL Southern McMurdo Sound Project, Antarctica. *Terra Antarctica*, **15**, 147–192.
- Panter, K., Dunbar, N.W., Scanlan, M., Wilch, T., Fargo, A. and McIntosh, W. 2011. Petrogenesis of alkaline magmas at Minna Bluff, Antarctica: evidence for multi-stage differentiation and complex mixing processes. Abstract V31F-2590 presented at the AGU 2011 Fall Meeting, December 5–9, 2011, San Francisco, California, USA.
- Panter, K.S., Castillo, P. *et al.* 2018. Melt origin across a rifted continental margin: a case for subduction-related metasomatic agents in the lithospheric source of alkaline basalt, northwest Ross Sea, Antarctica. *Journal of Petrology*, **59**, 517–558, <https://doi.org/10.1093/ptrology/egy036>
- Parnelee, D.E.F., Kyle, P.R., Kurz, M.D., Marrero, S.M. and Phillips, F.M. 2015. A new Holocene eruptive history of Erebus volcano, Antarctica using cosmogenic <sup>3</sup>He and <sup>36</sup>Cl exposure ages. *Quaternary Geochronology*, **30**, 114–131, <https://doi.org/10.1016/j.quageo.2015.09.001>
- Paulsen, H.-K. 2008. *A Lithological Cross Section through Mount Morning, Antarctica: A Story Told from Xenolithic Assemblages in a Pyroclastic Deposit*. MSc thesis, University of Otago, Dunedin, New Zealand.
- Paulsen, T. 2002. Volcanic cone alignments and the intraplate stress field in the Mount Morning region, South Victoria Land, Antarctica. *Geological Society of America Abstracts with Programs*, **34**, 437.
- Paulsen, T.S. and Wilson, T.J. 2007. Elongate summit calderas as Neogene paleostress indicators in Antarctica. *United States Geological Survey Open-File Report*, **2007-1047**, Short Research Paper 072, <https://doi.org/10.3133/ofr20071047SRP072>
- Paulsen, T.S. and Wilson, T.J. 2009. Structure and age of volcanic fissures on Mount Morning: a new constraint on Neogene to contemporary stress in the West Antarctic Rift, southern Victoria Land, Antarctica. *Geological Society of America Bulletin*, **121**, 1071–1088, <https://doi.org/10.1130/b26333.1>
- Perinelli, C., Armienti, P. and Dallai, L. 2006. Geochemical and O-isotope constraints on the evolution of lithospheric mantle in the Ross Sea rift area (Antarctica). *Contributions to Mineralogy and Petrology*, **151**, 245–266, <https://doi.org/10.1007/s00410-006-0065-8>
- Pfänder, J.A., Jung, S., Munker, C., Stracke, A. and Mezger, K. 2012. A possible high Nb/Ta reservoir in the continental lithospheric mantle and consequences on the global Nb budget – Evidence from continental basalts from Central Germany. *Geochimica et Cosmochimica Acta*, **77**, 232–251, <https://doi.org/10.1016/j.gca.2011.11.017>
- Phillips, E.H., Sims, K.W.W. *et al.* 2018. The nature and evolution of mantle upwelling at Ross Island, Antarctica, with implications for the source of HIMU lavas. *Earth and Planetary Science Letters*, **498**, 38–53, <https://doi.org/10.1016/j.epsl.2018.05.049>
- Polyakov, M.M., Krylov, A.Y. and Mazina, T.I. 1976. New data on radiogeochronology of Antarctic Cenozoic vulcanites (in Russian). *Informatsionnyi Biulleten Sovetskoi Antarktich*, **93**, 19–26.
- Pompilio, M., Armienti, P. and Tamponi, M. 2001. Petrography, mineral composition and geochemistry of volcanic and subvolcanic rocks of CRP-3, Victoria Land Basin, Antarctica. *Terra Antarctica*, **8**, 463–480.
- Pompilio, M., Dunbar, N. *et al.* 2007. Petrology and Geochemistry of the AND-1B Core, ANDRILL McMurdo Ice Shelf Project, Antarctica. *Terra Antarctica*, **14**, 255–288.
- Porter, S.C. and Beget, J.E. 1981. Provenance and depositional environments of Late Cenozoic sediments in permafrost cores from lower Taylor Valley, Antarctica. *American Geophysical Union Antarctic Research Series*, **33**, 351–364.
- Price, R.C. and Chappell, B.W. 1975. Fractional crystallisation and the petrology of Dunedin volcano. *Contributions to Mineralogy and Petrology*, **53**, 157–182, <https://doi.org/10.1007/bf00372602>
- Prior, G.T. 1899. Petrographical notes on the rock specimens collected in Antarctic regions during the voyage of H.M.S. Erebus and Terror under Sir James Clark Ross in 1839–43. *Mineralogical Magazine*, **12**, 69–91.
- Prior, G.T. 1902. Report on the rock specimens collected by the *Southern Cross* Antarctic Expedition. In: Lankester, E.R. and Bell, J. (eds) *Report on the Collections of Natural History made in the Antarctic Regions During the Voyage of the 'Southern Cross'*. British Museum (Natural History), London, 321–332.
- Prior, G.T. 1907. Report on the rock specimens collected during the 'Discovery' Antarctic Expedition, 1901–1904. *Natural History*, **1**, 101–160.
- Putirka, K., Johnson, M., Kinzler, R., Longhi, J. and Walker, D. 1996. Thermobarometry of mafic igneous rocks based on clinopyroxene–liquid equilibria, 0–30 kbar. *Contributions to Mineralogy and Petrology*, **123**, 92–108, <https://doi.org/10.1007/s004100050145>
- Putirka, K.D. 2008. Thermometers and barometers for volcanic systems. *Reviews in Mineralogy and Geochemistry*, **69**, 61–120, <https://doi.org/10.2138/rmg.2008.69.3>
- Putirka, K.D., Mikaelian, H., Ryerson, F. and Shaw, H. 2003. New clinopyroxene–liquid thermobarometers for mafic, evolved, and volatile-bearing lava compositions, with applications to lavas from Tibet and the Snake River Plain, Idaho. *American Mineralogist*, **88**, 1542–1554, <https://doi.org/10.2138/am-2003-1017>
- Rasmussen, D.J., Kyle, P.R., Wallace, P.J., Sims, K.W., Gaetani, G.A. and Phillips, E.H. 2017. Understanding degassing and transport of CO<sub>2</sub>-rich alkalic magmas at Ross Island, Antarctica using olivine-hosted melt inclusions. *Journal of Petrology*, **58**, 841–861, <https://doi.org/10.1093/ptrology/egx036>
- Rebert, R. 1981. Bibliography of the Dry Valley Drilling Project. *American Geophysical Union Antarctic Research Series*, **33**, 453–465.

## Erebus Volcanic Province: petrology

- Redner, E.R. 2016. *Magma Mixing and Evolution at Minna Bluff, Antarctica Revealed by Amphibole and Clinopyroxene Analyses*. MSc thesis, Bowling Green State University, Bowling Green, Ohio, USA.
- Rilling, S.E., Mukasa, S.B., Wilson, T.J. and Lawver, L. 2007.  $^{40}\text{Ar}$ - $^{39}\text{Ar}$  Age constraints on volcanism and tectonism in the Terror Rift of the Ross Sea, Antarctica. *United States Geological Survey Open-File Report*, **2007-1047**, Short Research Paper 092, <https://pubs.usgs.gov/of/2007/1047/srp/srp092/>
- Rilling, S., Mukasa, S., Wilson, T., Lawver, L. and Hall, C. 2009. New determinations of  $^{40}\text{Ar}$ / $^{39}\text{Ar}$  isotopic ages and flow volumes for Cenozoic volcanism in the Terror Rift, Ross Sea, Antarctica. *Journal of Geophysical Research: Solid Earth*, **114**, B12207, <https://doi.org/10.1029/2009JB006303>
- Rocchi, S., Armienti, P., D'Orazio, M., Tonarini, S., Wijbrans, J.R. and Di Vincenzo, G. 2002. Cenozoic magmatism in the western Ross Embayment: role of mantle plume v. plate dynamics in the development of the West Antarctic Rift System. *Journal of Geophysical Research: Solid Earth*, **107**, 2195, <https://doi.org/10.1029/2001jb000515>
- Rocchi, S., Armienti, P. and Di Vincenzo, G. 2005. No plume, no rift magmatism in the West Antarctic Rift. *Geological Society of America Special Papers*, **388**, 435–447, <https://doi.org/10.1130/0-8137-2388-4.435>
- Ross, J. 1847. *A Voyage of Discovery and Research in the Southern and Antarctic Regions, during the Years 1839–43*. John Murray, London.
- Ross, J. 2014. *Ar–Ar Geochronology of Southern McMurdo Sound, Antarctica and The Development of Pychron: an Ar–Ar Data Acquisition and Processing Package*. New Mexico Institute of Mining and Technology, Socorro, NM.
- Ross, J.I., McIntosh, W.C. and Dunbar, N.W. 2012a. Development of a precise and accurate age–depth model based on  $^{40}\text{Ar}$ / $^{39}\text{Ar}$  dating of volcanic material in the ANDRILL (1B) drill core, Southern McMurdo Sound, Antarctica. *Global and Planetary Change*, **96–97**, 118–130, <https://doi.org/10.1016/j.gloplacha.2012.05.005>
- Ross, J.I., McIntosh, W.C. and Wilch, T.I. 2012b. Detailed Ar–Ar geochronology of volcanism at Minna Bluff, Antarctica: Two-phased growth and influence on Ross Ice Shelf. Abstract presented at the AGU Fall Meeting, December 3–7, 2012. San Francisco, California, USA.
- Rudnick, R.L. and Gao, S. 2003. Composition of the continental crust. In: Rudnick, R.L. (ed.) *Treatise on Geochemistry, Volume 3: The Crust*. Pergamon, Oxford, UK, 1–64.
- Rudnick, R.L. and Gao, S. 2014. Composition of the continental crust. In: Holland, H.D. and Turekian, K.K. (eds) *Treatise on Geochemistry*. 2nd edn. Elsevier, Oxford, UK, 1–51.
- Rudnick, R.L., Barth, M., Horn, I. and McDonough, W.F. 2000. Rutile-bearing refractory eclogites: missing link between continents and depleted mantle. *Science*, **287**, 278–281, <https://doi.org/10.1126/science.287.5451.278>
- Sack, R.O., Walker, D. and Carmichael, I.S.E. 1987. Experimental petrology of alkalic lavas: constraints on cotectics of multiple saturation in natural basic liquids. *Contributions to Mineralogy and Petrology*, **96**, 1–23, <https://doi.org/10.1007/bf00375521>
- Saggerson, E.P. and Williams, L.A.J. 1964. Ngurumanite from southern Kenya and its bearing on the origin of rocks in the northern Tanganyika Alkaline District. *Journal of Petrology*, **5**, 40–81, <https://doi.org/10.1093/petrology/5.1.40>
- Sandroni, S. and Talarico, F.M. 2006. Analysis of clast lithologies from CIROS-2 core, New Harbour, Antarctica – Implications for ice flow directions during Plio-Pleistocene time. *Palaeogeography, Palaeoclimatology, Palaeoecology*, **231**, 215–232, <https://doi.org/10.1016/j.palaeo.2005.07.031>
- Scanlan, M.K. 2008. *Petrology of Inclusion-Rich Lavas at Minna Bluff, McMurdo Sound, Antarctica: Implications for Magma Origin, Differentiation, and Eruption Dynamics*. MSc thesis, Bowling Green State University, Bowling Green, Ohio, USA.
- Scott, J.M., Turnbull, I.M., Auer, A. and Palin, J.M. 2013. The sub-Antarctic Antipodes Volcano: a <0.5 Ma HIMU-like Surtseyan volcanic outpost on the edge of the Campbell Plateau, New Zealand. *New Zealand Journal of Geology and Geophysics*, **56**, 134–153, <https://doi.org/10.1080/00288306.2013.802246>
- Scott, J.M., Waight, T.E., van der Meer, Q.H.A., Palin, J.M., Cooper, A.F. and Münker, C. 2014. Metasomatized ancient lithospheric mantle beneath the young Zealandia microcontinent and its role in HIMU-like intraplate magmatism. *Geochemistry, Geophysics, Geosystems*, **15**, 3477–3501, <https://doi.org/10.1002/2014gc005300>
- Scott, R.F. 1907. *The Voyage of the Discovery*. Charles Scribner, New York.
- Shaw, D.M. 1970. Trace element fractionation during anatexis. *Geochimica et Cosmochimica Acta*, **34**, 237–243, [https://doi.org/10.1016/0016-7037\(70\)90009-8](https://doi.org/10.1016/0016-7037(70)90009-8)
- Shen, W., Wiens, D.A. et al. 2018. Seismic evidence for lithospheric foundering beneath the southern Transantarctic Mountains, Antarctica. *Geology*, **46**, 71–74, <https://doi.org/10.1130/G39555.1>
- Sims, K.W.W. and Hart, S.R. 2006. Comparison of Th, Sr, Nd and Pb isotopes in oceanic basalts: implications for mantle heterogeneity and magma genesis. *Earth and Planetary Science Letters*, **245**, 743–761, <https://doi.org/10.1016/j.epsl.2006.02.030>
- Sims, K.W.W., Blichert-Toft, J. et al. 2008. A Sr, Nd, Hf, and Pb isotope perspective on the genesis and long-term evolution of alkaline magmas from Erebus volcano, Antarctica. *Journal of Volcanology and Geothermal Research*, **177**, 606–618, <https://doi.org/10.1016/j.jvolgeores.2007.08.006>
- Sims, K.W.W., Pichat, S. et al. 2013. On the time scales of magma genesis, melt evolution, crystal growth rates and magma degassing in the Erebus volcano magmatic system using the  $^{238}\text{U}$ ,  $^{235}\text{U}$  and  $^{232}\text{Th}$  decay series. *Journal of Petrology*, **54**, 235–271, <https://doi.org/10.1093/petrology/egs068>
- Skinner, D.N.B., Waterhouse, B.C., Brehaut, G.M. and Sullivan, K. 1976. *New Zealand Geological Survey Antarctic Expedition 1975–76, Skelton–Koettlitz Glaciers*. New Zealand Geological Survey Report, **DS58**.
- Smellie, J.L. 1998. Sand grain detrital modes in CRP-1: provenance variations and influence of Miocene eruptions on the marine record in the McMurdo Sound region. *Terra Antarctica*, **5**, 579–587.
- Smellie, J.L. 2002. Erosional history of the Transantarctic Mountains deduced from sand grain detrital modes in CRP-2/2A, Victoria Land Basin, Antarctica. *Terra Antarctica*, **7**, 545–552.
- Smellie, J.L. and Martin, A.P. 2021. Erebus Volcanic Province: volcanology. *Geological Society, London, Memoirs*, **55**, <https://doi.org/10.1144/M55-2018-62>
- Smellie, J.L. and Rocchi, S. 2021. Northern Victoria Land: volcanology. *Geological Society, London, Memoirs*, **55**, <https://doi.org/10.1144/M55-2018-60>
- Smith, W.C. 1954. The volcanic rocks of the Ross archipelago, British 'Terra Nova' Expedition', 1910. In: *Antarctic ('Terra Nova') Expedition, British, 1910: Geology Volume 2: Natural History Report*. British Museum, London, 1–107.
- Sobolev, A.V., Hofmann, A.W., Sobolev, S.V. and Nikogosian, I.K. 2005. An olivine-free mantle source of Hawaiian shield basalts. *Nature*, **434**, 590, <https://doi.org/10.1038/nature03411>, <https://www.nature.com/articles/nature03411#supplementary-information>
- Sprung, P., Schuth, S., Münker, C. and Hoke, L. 2007. Intraplate volcanism in New Zealand: the role of fossil plume material and variable lithospheric properties. *Contributions to Mineralogy and Petrology*, **153**, 669–687, <https://doi.org/10.1007/s00410-006-0169-1>
- Stracke, A. 2012. Earth's heterogeneous mantle: a product of convection-driven interaction between crust and mantle. *Chemical Geology*, **330–331**, 274–299, <https://doi.org/10.1016/j.chemgeo.2012.08.007>
- Stracke, A., Bizimis, M. and Salters, V.J.M. 2003. Recycling oceanic crust: quantitative constraints. *Geochemistry, Geophysics, Geosystems*, **4**, 8003, <https://doi.org/10.1029/2001gc000223>
- Stuckless, J.S. and Ericksen, R.L. 1976. Strontium isotopic geochemistry of the volcanic rocks and associated megacrysts and inclusions from Ross Island and vicinity, Antarctica. *Contributions to*

- Mineralogy and Petrology*, **58**, 111–126, <https://doi.org/10.1007/BF00382180>
- Stuckless, J.S., Miesch, A.T., Goldich, S.S. and Weiblen, P.W. 1981. A Q-mode factor model for the petrogenesis of the Volcanic Rocks from Ross Island and Vicinity, Antarctica. *American Geophysical Union Antarctic Research Series*, **33**, 257–280.
- Stuiver, M. and Braziunas, T. 1985. Compilation of isotopic dates from Antarctica. *Radiocarbon*, **27**, 117–304, <https://doi.org/10.1017/S0033822200007037>
- Stump, E. 1995. *The Ross Orogen of the Transantarctic Mountains*. Cambridge University Press, New York.
- Sullivan, R.J. 2006. *The Geology and Geochemistry of Seal Crater, Hurricane Ridge, Mount Morning, Antarctica*. BSc (Hon.) thesis, University of Otago, Dunedin, New Zealand.
- Sun, S.S. and Hanson, G.N. 1975. Origin of Ross Island basanitoids and limitations upon the heterogeneity of mantle sources for alkali basalts and nephelinites. *Contributions to Mineralogy and Petrology*, **52**, 77–106, <https://doi.org/10.1007/BF00395006>
- Sun, S.-s. and McDonough, W.F. 1989. Chemical and isotopic systematics of oceanic basalts: implications for mantle composition and processes. *Geological Society, London, Special Publications*, **42**, 313–345, <https://doi.org/10.1144/GSL.SP.1989.042.01.19>
- Talarico, F.M. and Kleinschmidt, G. 2008. The antarctic continent in gondwanaland: A tectonic review and potential research targets for future investigations. In: Fabio, F. and Martin, S. (eds) *Antarctic Climate Evolution*. Elsevier, Amsterdam, 257–308.
- Talarico, F.M. and Sandroni, S. 2009. Provenance signatures of the Antarctic Ice Sheets in the Ross Embayment during the Late Miocene to Early Pliocene: The ANDRILL AND-1B core record. *Global and Planetary Change*, **69**, 103–123, <https://doi.org/10.1016/j.gloplacha.2009.04.007>
- Tauxe, L., Gans, P. and Mankinen, E.A. 2004. Paleomagnetism and  $^{40}\text{Ar}/^{39}\text{Ar}$  ages from volcanics extruded during the Matuyama and Brunhes Chrons near McMurdo Sound, Antarctica. *Geochemistry, Geophysics, Geosystems*, **5**, Q06H12, <https://doi.org/10.1029/2003GC000656>
- Taylor, T.G. 1922. *The Physiography of the McMurdo Sound and Granite Harbour Region. British Antarctic Terra Nova Expedition, 1910–1913*. Harrison and Sons Ltd, London.
- Thomson, J.A. 1916. Report on the inclusions of the volcanic rocks of the Ross Archipelago (with Appendix by F. Cohen). In: *Report of the British Antarctic Expedition 1907–1909: Geology Report*. British Museum, London, 129–151.
- Thornton, C.P. and Tuttle, O.F. 1960. Chemistry of igneous rocks – [Part] 1, Differentiation index. *American Journal of Science*, **258**, 664–684, <https://doi.org/10.2475/ajs.258.9.664>
- Timms, C.J. 2006. *Reconstruction of a Grounded Ice Sheet in McMurdo Sound – Evidence from Southern Black Island*. MSc thesis, University of Otago, Dunedin, New Zealand.
- Torsvik, T.H., Müller, R.D., Van der Voo, R., Steinberger, B. and Gaina, C. 2008. Global plate motion frames: Toward a unified model. *Reviews of Geophysics*, **46**, <https://doi.org/10.1029/2007RG000227>
- Treves, S.B. 1962. The geology of Cape Evans and Cape Royds, Ross Island, Antarctica. *American Geophysical Union Antarctic Research Series*, **33**, 40–46.
- Treves, S.B. 1967. Volcanic rocks from the Ross Island, Marguerite Bay and Mt. Weaver areas, Antarctica. *Japanese Antarctic Research Expedition Scientific Reports*, Special Issue 1, 136–149.
- Treves, S.B. 1968. Volcanic rocks of the Ross Island area. *Antarctic Journal of the United States*, **3**, 108–109.
- Treves, S.B. 1977. Geology of some volcanic rocks from the Ross Island, Mount Morning, and southern Victoria Land areas. *Antarctic Journal of the United States*, **12**, 104–105.
- van der Meer, Q.H.A., Waight, T.E., Scott, J.M. and Münker, C. 2017. Variable sources for Cretaceous to recent HIMU and HIMU-like intraplate magmatism in New Zealand. *Earth and Planetary Science Letters*, **469**, 27–41, <https://doi.org/10.1016/j.epsl.2017.03.037>
- van Woerden, T.H. 2006. *Volcanic Geology and Physical Volcanology of Mount Morning, Antarctica*. Masters thesis, University of Waikato, Hamilton, New Zealand.
- Vella, P. 1969. Surficial geological sequence, Black Island and Brown Peninsula, McMurdo Sound, Antarctica. *New Zealand Journal of Geology and Geophysics*, **12**, 761–770, <https://doi.org/10.1080/00288306.1969.10431110>
- Verma, S.P. and Rivera-Gomez, M.A. 2013. Computer programs for the classification and nomenclature of igneous rocks. *Episodes*, **36**, 115–124, <https://doi.org/10.18814/epiugs/2013/v36i2/005>
- Walter, M.J. 1998. Melting of garnet peridotite and the origin of komatiite and depleted lithosphere. *Journal of Petrology*, **39**, 29–60, <https://doi.org/10.1093/petroj/39.1.29>
- Waterhouse, B.C. 1965. *Western Ross Sea–Balleny Islands Expedition: January–March, 1965*. New Zealand Geological Survey.
- Watson, T., Nyblade, A. *et al.* 2006. P and S velocity structure of the upper mantle beneath the Transantarctic Mountains, East Antarctic craton, and Ross Sea from travel time tomography. *Geochemistry, Geophysics, Geosystems*, **7**, Q07005, <https://doi.org/10.1029/2005gc001238>
- Weaver, B.L. 1991. Trace element evidence for the origin of oceanic island basalts. *Geology*, **19**, 123–126, [https://doi.org/10.1130/0091-7613\(1991\)019<0123:teefot>2.3.co;2](https://doi.org/10.1130/0091-7613(1991)019<0123:teefot>2.3.co;2)
- Weiblen, P.J., Stuckless, J.S., Hunter, W.C., Schulz, K.J. and Mundry, M.G. 1981. Correlation of clinopyroxene compositions with environment of formation based on data from Ross Island volcanic rocks. *American Geophysical Union Antarctic Research Series*, **33**, 229–246.
- White, J.C., Benker, S.C., Ren, M., Urbanczyk, K.M. and Corrick, D.W. 2006. Petrogenesis and tectonic setting of the peralkaline Pine Canyon caldera, Trans-Pecos Texas, USA. *Lithos*, **91**, 74–94, <https://doi.org/10.1016/j.lithos.2006.03.015>
- Whitney, D.L. and Evans, B.W. 2010. Abbreviations for names of rock forming minerals. *American Mineralogist*, **95**, 185–187, <https://doi.org/10.2138/am.2010.3371>
- Wilch, T.I., McIntosh, W. *et al.* 2011a. Two-stage growth of the Late Miocene Minna Bluff Volcanic Complex, Ross Embayment, Antarctica: implications for ice-sheet and volcanic histories. Abstract #V31F-2591 presented at the AGU Fall Meeting, December 5–9, 2011, San Francisco, California, USA.
- Wilch, T.I., Panter, K.S. *et al.* 2011b. Miocene evolution of the Minna Bluff Volcanic Complex, Ross Embayment, Antarctica. Abstract PS5.10 2591 presented at the 11th International Symposium on Antarctic Earth Science, 10–16 July 2011, Edinburgh, UK.
- Willbold, M. and Stracke, A. 2006. Trace element composition of mantle end-members: implications for recycling of oceanic and upper and lower continental crust. *Geochemistry, Geophysics, Geosystems*, **7**, Q04004, <https://doi.org/10.1029/2005gc001005>
- Wilson, A.T., Hندی, C.H. and Taylor, A.M. 1974. Peridot on Ross Island, Antarctica. *Australian Gemologist*, **12**, 124–125.
- Wilson, G., Damaske, D., Möller, H.-D., Tinto, K. and Jordan, T. 2007. The geological evolution of southern McMurdo Sound – new evidence from a high-resolution aeromagnetic survey. *Geophysical Journal International*, **170**, 93–100, <https://doi.org/10.1111/j.1365-246X.2007.03395.x>
- Wilson, G.S., Bohaty, S.M. *et al.* 2000. Chronostratigraphy of CRP-2/2A, Victoria Land Basin, Antarctica. *Terra Antarctica*, **7**, 647–654.
- Wingrove, D. 2005. *Early mixing in the evolution of alkaline magmas: chemical and oxygen isotope evidence from phenocrysts, Royal Society Range, Antarctica*. MSc thesis, Bowling Green State University, Bowling Green, Ohio, USA.
- Woodhead, J.D. 1996. Extreme HIMU in an oceanic setting: the geochemistry of Mangaia Island (Polynesia), and temporal evolution of the Cook–Austral hotspot. *Journal of Volcanology and Geothermal Research*, **72**, 1–19, [https://doi.org/10.1016/0377-0273\(96\)00002-9](https://doi.org/10.1016/0377-0273(96)00002-9)
- Workman, R.K. and Hart, S.R. 2005. Major and trace element composition of the depleted MORB mantle (DMM). *Earth and Planetary Science Letters*, **231**, 53–72, <https://doi.org/10.1016/j.epsl.2004.12.005>

## Erebus Volcanic Province: petrology

- Workman, R.K., Hart, S.R. *et al.* 2004. Recycled metasomatized lithosphere as the origin of the Enriched Mantle II (EM2) end-member: evidence from the Samoan Volcanic Chain. *Geochemistry, Geophysics, Geosystems*, **5**, Q04008, <https://doi.org/10.1029/2003gc000623>
- Worley, B.A. 1992. *Dismal Geology; A Study of Magmatic and Sub-solidus Processes in a Carbonated Alkaline Intrusion, Southern Victoria Land, Antarctica*. MSc thesis, University of Otago, Dunedin, New Zealand.
- Worley, B.A., Cooper, A.F. and Hall, C.E. 1995. Petrogenesis of carbonate-bearing nepheline syenites and carbonatites from Southern Victoria Land, Antarctica: origin of carbon and the effects of calcite-graphite equilibrium. *Lithos*, **35**, 183–199, [https://doi.org/10.1016/0024-4937\(94\)00050-C](https://doi.org/10.1016/0024-4937(94)00050-C)
- Wright, A.C. 1979a. *McMurdo Volcanics at Foster Crater, Southern Foothills of the Royal Society Range, Central Victoria Land, Antarctica*. New Zealand Geological Survey Internal Report.
- Wright, A.C. 1979b. *McMurdo Volcanics northwest of Koettlitz Glacier, Antarctica*. New Zealand Geological Survey Internal Report.
- Wright, A.C. 1979c. *McMurdo Volcanics on Chancellor Ridge, Southern Foothills of the Royal Society Range, Central Victoria Land, Antarctica*. New Zealand Geological Survey Internal Report.
- Wright, A.C. 1979d. A reconnaissance study of the McMurdo Volcanics northwest of Koettlitz Glacier. *New Zealand Antarctic Record*, **1**, 10–15.
- Wright, A.C. 1980. Landforms of McMurdo Volcanic Group, Southern Foothills of Royal Society Range, Antarctica. *New Zealand Journal of Geology and Geophysics*, **23**, 605–613, <https://doi.org/10.1080/00288306.1980.10424132>
- Wright, A.C. and Kyle, P.R. 1990a. Royal Society Range. *American Geophysical Union Antarctic Research Series*, **48**, 131–133.
- Wright, A.C. and Kyle, P.R. 1990b. Taylor and Wright Valleys. *American Geophysical Union Antarctic Research Series*, **48**, 134–135.
- Wright, A.C. and Kyle, P.R. 1990c. Mount Discovery. *American Geophysical Union Antarctic Research Series*, **48**, 120–123.
- Wright, A.C. and Kyle, P.R. 1990d. Minna Bluff. *American Geophysical Union Antarctic Research Series*, **48**, 117–119.
- Wright, A.C. and Kyle, P.R. 1990e. Mount Terror. *American Geophysical Union Antarctic Research Series*, **48**, 99–102.
- Wright, A.C. and Kyle, P.R. 1990f. Mason Spur. *American Geophysical Union Antarctic Research Series*, **48**, 128–130.
- Wright, A.C. and Kyle, P.R. 1990g. Mount Morning. *American Geophysical Union Antarctic Research Series*, **48**, 124–126.
- Wright, A.C., McIntosh, W.C. and Ellerman, P. 1983. Volcanic geology of Turks Head, Tryggve Point, and Minna Bluff, southern Victoria Land. *Antarctic Journal of the United States*, **18**, 35–36.
- Wright, A.C., Kyle, P.R., McIntosh, W.C. and Klich, I. 1984. Geological field investigations of volcanic rocks at Mount Discovery and Mason Spur, McMurdo Sound. *Antarctic Journal of the United States*, **19**, 20–21.
- Wright, A.C., Kyle, P.R., More, J.A. and Meeker, K. 1986. Geological investigations of volcanic rocks at Mount Discovery, Mount Morning, and Mason Spur, McMurdo Sound. *Antarctic Journal of the United States*, **21**, 55.
- Wright-Grassham, A.C. 1987. *Volcanic Geology, Mineralogy, and Petrogenesis of the Discovery Volcanic Subprovince, Southern Victoria Land, Antarctica*. PhD thesis, New Mexico Institute of Mining and Technology, Socorro, New Mexico, USA.
- Yaxley, G.M., Crawford, A.J. and Green, D.H. 1991. Evidence for carbonatite metasomatism in spinel peridotite xenoliths from western Victoria, Australia. *Earth and Planetary Science Letters*, **107**, 305–317, [https://doi.org/10.1016/0012-821X\(91\)90078-V](https://doi.org/10.1016/0012-821X(91)90078-V)
- Yokoyama, T., Aka, F.T., Kusakabe, M. and Nakamura, E. 2007. Plume–lithosphere interaction beneath Mt. Cameroon volcano, West Africa: Constraints from  $^{238}\text{U}$ – $^{230}\text{Th}$ – $^{226}\text{Ra}$  and Sr–Nd–Pb isotope systematics. *Geochimica et Cosmochimica Acta*, **71**, 1835–1854, <https://doi.org/10.1016/j.gca.2007.01.010>
- Zindler, A. and Hart, S. 1986. Chemical Geodynamics. *Annual Review of Earth and Planetary Sciences*, **14**, 493–571, <https://doi.org/10.1146/annurev.earth.14.050186.002425>